Plant carboxylesterases involved in pesticide hydrolysis

Gershater, Markus Christian

PLANT CARBOXYLESTERASES INVOLVED IN PESTICIDE HYDROLYSIS

Markus Christian Gershater

PhD Thesis

2006

School of Biological and Biomedical Sciences

Durham University

ABSTRACT

Many herbicides are applied in the form of carboxylic esters to increase their hydrophobicity and hence aid their passage through the waxy cuticle. Hydrolysis *in planta* of these pro-herbicide esters releases the active acid or alcohol and the rate of this cleavage can be a factor in determining herbicide selectivity.

Protein extracts from 13 crop and weed species were assayed for carboxylesterase activity toward multiple xenobiotic and pesticide ester substrates, including 2,4-D-methyl, aryloxyphenoxypropionate esters and *p*-nitrophenyl esters. A diversity of activities was exhibited by the different species, with *Arabidopsis thaliana* extracts showing high hydrolytic activity toward several xenobiotic esters, particularly 2,4-D-methyl.

The major 2,4-D-methyl hydrolysing enzyme in arabidopsis cell cultures was purified through three rounds of chromatography, then selectively labelled with a biotinylated fluorophosphonate probe (FP-biotin). Following streptavidin affinity purification, the labelled protein was identified by proteomics as the previously uncharacterised serine hydrolase AtCXE12. Recombinant AtCXE12 was subsequently confirmed to effectively hydrolyse 2,4-D-methyl.

A T-DNA insertion knockout line that did not express AtCXE12 was identified and characterised. Protein from the knockout plants did not contain AtCXE12 and was found to have a reduced rate of 2,4-D-methyl hydrolysis compared to wild-type plant extracts. This translated into a higher tolerance of 2,4-D-methyl in young *atcxe12* plants, due to a lower rate of bioactivation of the pro-herbicide.

The fluorophosphonate-based chemical probe was subsequently used to identify other major serine hydrolases in arabidopsis. AtCXE12 and three previously uncharacterised hydrolases were identified, each belonging to a distinct enzyme family.

LIST OF FIGURES

LIST OF TABLES

ABBREVIATIONS

AAE: ajmaline acetylesterase

BFAE: brefeldin A esterase

cDNA: complementary deoxyribonucleic acid

CEH: carboxylic ester hydrolase

CXE: carboxylesterase

dATP: 2'-deoxyadenosine 5'-triphosphate

dCTP: 2'-deoxycytidine 5'-triphosphate

dGTP: 2'-deoxyguanosine 5'-triphosphate

Dicots: dicotyledonous species

DNA: deoxyribonucleic acid

dTTP: 2'-deoxythymidine 5'-triphosphate

DTT: dithiothreitol

EDTA: ethylenediaminetetraacetic acid

FP-biotin: fluorophosphono-biotin

Hnl: hydroxynitrile lyase

IEF: isoelectric focussing

LAE: Lanatoside 15'-*O*-acetylesterase

MALDI: matrix assisted laser desorption ionisation

Monocots: monocotyledonous species

mRNA: messenger ribonucleic acid

OP: organophosphate

PAGE: polyacrylamide gel electrophoresis

PCR: polymerase chain reaction

PNAE: polyneuridine aldehyde esterase

SAIL: Syngenta arabidopsis insertion library

TEMED: Tetramethylethylenediamine

TOF: time of flight

TriFFP: trifunctional fluorophosphonate probe

DECLARATION

No material presented here has previously been submitted for any other degree. Except where acknowledged, all material is the work of the author

STATEMENT OF COPYRIGHT

PUBLICATIONS ARISING FROM WORK DESCRIBED IN THIS THESIS

Gershater MC, Sharples K, Edwards, R (2006): Carboxylesterase activities toward pesticide esters in crops and weeds. Phytochemistry 67: 2561-2567

Gershater MC, Cummins I, Edwards R (2007): Role of a Carboxylesterase in Herbicide Bioactivation in *Arabidopsis thaliana.* Journal of Biological Chemistry 29: 21460-21466

ACKNOWLEDGEMENTS

First and foremost, I would like to express extreme gratitude to my supervisor, Rob Edwards, for his indispensable guidance, help and mentoring at every stage of this project.

Help from my colleagues in the lab has also been crucial: in particular, I'd like to thank Ian Cummins for his help in the early parts of the project, David Dixon for his advice throughout and technical expertise concerning protein identification in particular and Lesley Edwards for all her help with plants and tissue culture. I'd also like to thank the other members of the lab, past and present, who I've either pestered for advice regularly (thanks Melissa) or used as sounding boards for ideas (Ollie and Ed: thanks!).

On a financial note, I'd like to thank the BBSRC and Syngenta for their funding.

Lastly, I'd like to acknowledge endless help, guidance and support I've had from my Dad, and the support I have received from my family, my friends, and in particular my girlfriend Heather, who I'd especially like to thank for her support and incredible patience during the write-up stages in particular.

for Mum

CHAPTER 1: INTRODUCTION

Preface

This thesis describes the identification and characterisation of a carboxylesterase from *Arabidopsis thaliana* that has hydrolytic activity toward the proherbicide 2,4-D-methyl. This first chapter is primarily a review of the most important and relevant papers that discuss carboxylesterases, and plant carboxylesterases in particular.

What soon becomes apparent in an examination of the carboxylesterase literature is the lack of a coherent and consistent esterase classification system. Therefore a large portion of this chapter (section 1.3) is devoted to outlining the large diversity of esterases described to date and proposes an overall system for how such a diverse group of enzymes may be meaningfully classified.

Animal and microbial esterases are briefly considered (section 1.4), but most of the latter parts of the chapter chiefly deal specifically with plant carboxylesterases: firstly, publications concerning biochemical studies of carboxylesterase activities are examined (sections 1.5.1 and 1.5.2), then more recent papers detailing the identification and cloning of plant carboxylesterases are reviewed (section 1.5.3).

Firstly however, the role of carboxylesterases in xenobiotic metabolism is described (section 1.1), followed by a brief discussion of ester chemistry (section 1.2).

1.1 Xenobiotic metabolism in plants

Plants may be exposed to a great variety of potentially dangerous natural and synthetic compounds (xenobiotics). Natural chemicals may include fungal and bacterial toxins and alellochemicals produced by other plants. Man-made compounds may either be deliberately applied agrochemicals or pollutants. Many of these compounds would be toxic if allowed to accumulate inside the plant. However, plants are able to detoxify potentially harmful exogenous compounds through metabolism and sequestration, in a manner analogous to mammalian drug detoxification. For this reason, plants are regarded as "green livers" (Sandermann, 1994), as similar enzyme classes are involved in xenobiotic metabolism both in plants and in mammalian livers. This metabolism has a direct effect on the way a plant responds to a toxic agrochemical compound: in general, plants that quickly metabolise the active form of a given compound will be less affected by treatment than a plant whose metabolism allows the active form to persist in the plant. In the case of herbicides, differential metabolism may be the basis of selectivity (Owen 2000).

The routes by which plants metabolise xenobiotic compounds have collectively been termed to xenome (Edwards *et al.* 2005). The xenome is classically divided into three phases. Phase one metabolism functionalises the compound, either by adding functional groups through the action of enzymes such as cytochrome P450s, or by revealing functionalities in the compound through the removal of protecting groups, commonly through hydrolysis. Phase two metabolism involves the conjugation of the functionalised xenobiotic to hydrophilic endogenous compounds like glutathione or sugar molecules. Finally, phase three

is the sequestration of the metabolised compound through import into the vacuole, or by covalent binding to the cell wall. Phases one and two of detoxification are illustrated by the metabolism of bromoxynil octanoate in plants (Figure 1.1). The ester is rapidly hydrolysed, and the revealed hydroxyl group is then conjugated with glucose (Roberts (ed.), 1998).

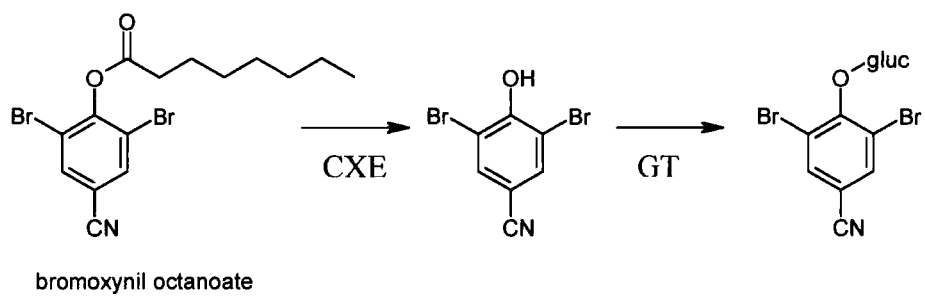

bromoxynil octanoate

Figure 1.1: One route of metabolism of bromoxynil octanoate (Roberts (ed), 1998). CXE: carboxylesterase, GT: glycosyltransferase

This thesis will focus on the carboxylesterases: phase one enzymes which hydrolyse xenobiotic carboxylic esters into a carboxylic acid and alcohol.

1.2 Ester Chemistry

Before proceeding with a review of the enzymes responsible for the hydrolysis of ester bonds, it is worth defining the ester chemistry that will be referred to throughout the rest of the thesis. An ester is defined as the product of a condensation reaction between an acid and an alcohol (McMurray, 1995). There are several types of ester (Figure 1.2) including phosphonate esters, sulphonate esters, thioesters and carboxylic esters, the last of which this thesis will be primarily concerned with.

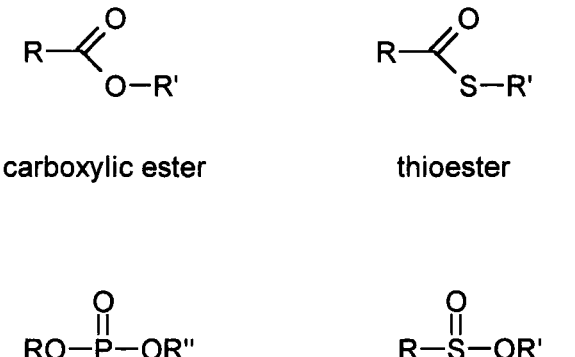

Figure 1.2: Different forms of ester

Ester hydrolysis

Ester hydrolysis can either be acid or base mediated. Base-induced hydrolysis is known as saponification and occurs via the nucleophilic addition of a hydroxide ion to the ester carbonyl carbon (Figure 1.3 **A**). Acid catalysed hydrolysis starts with the protonation of the carbonyl oxygen, which activates the carbonyl group for nucleophilic attack by a water molecule (Figure 1.3 **B**).

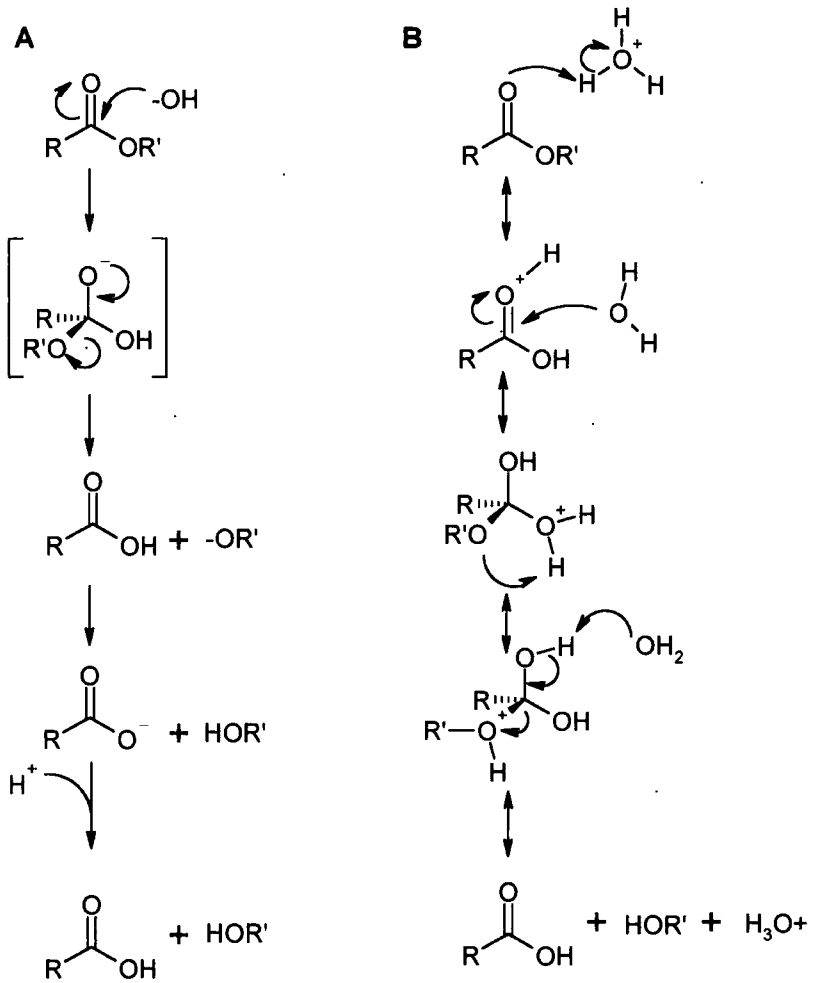

Figure 1.3: **A**: base-mediated and **B**: acid catalysed ester hydrolysis. (McMurray, 1995)

Carboxylesterases function via the base-mediated mechanism (Ollis *et al.* 1992). The reaction is not reversible in most cases: hydrolysis of the model ester substrate *p*-nitrophenyl acetate for example has a standard free energy of -9400 cal/mol (Leinweber, 1987). However, some enzymes that perform the hydrolysis of cyclic esters, such as limonin D-ring lactone hydrolase from citrus, have also been shown to perform the opposing condensation reaction (Merino *et al.* 1996).

1.3 Carboxylesterase classification

As is detailed in the following sections, plant esterases are both numerous and extremely varied in structure, substrate specificity, mechanism and function. Therefore, methods for esterase classification must be considered before carboxylesterases in plants can be meaningfully reviewed. Unlike other detoxifying enzyme families like the glutathione *S*-transferases (Dixon and Edwards, 2002) and the glycosyl transferases (Bowles *et al.* 2005), esterases are not all descended from a single progenitor enzyme. Instead, the capability to hydrolyse ester bonds has evolved independently in many diverse and structurally distinct enzyme families. This section will deal with how such diverse group of enzymes can be meaningfully classified. Firstly, methods of biochemical classification will be considered, followed by a review of how esterases may be further classified according to structural and sequence similarities.

1.3.1 Biochemical classification of carboxylesterases

Esterases (EC 3.1.-.-) catalyse the hydrolysis of ester bonds. As such they are a subset of the hydrolase superfamily (EC 3.-.-.-), which encompasses all enzymes with hydrolytic activity. Included under the general term of esterases are the carboxyl ester hydrolases (EC 3.1.1.-), as well as thiolester hydrolases (EC 3.1.2.-), phosphoric ester hydrolases (e.g. EC 3.1.3.-) and the sulphuric ester hydrolases (EC 3.1.6.-). Carboxylesterases (CXEs, 3.1.1.1) are specifically those esterases hydrolases that show activity toward xenobiotic carboxylic esters.

A more detailed biochemical classification of CXEs can be difficult and even misleading due to their wide and overlapping specificity toward the model ester substrates which are often used in their investigation (Figure 1.4).

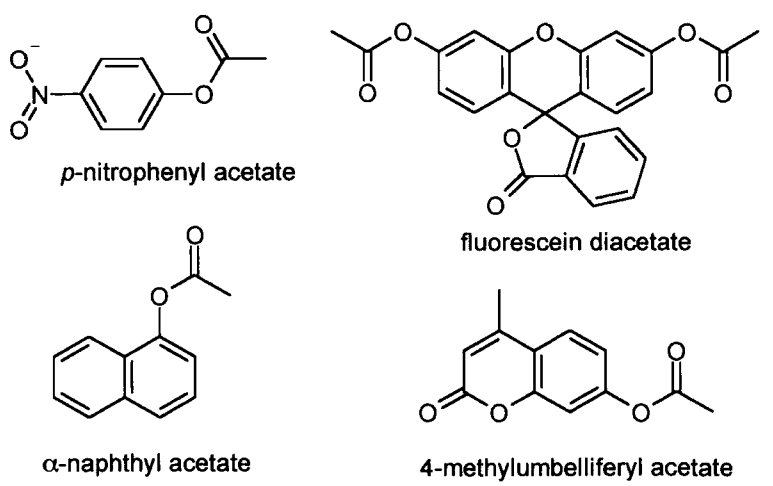

Figure 1.4: Examples of commonly used colorimetric or fluorometric carboxylic ester substrates

Despite this, there are some biochemical groupings into which carboxylesterases can usefully be delineated. Perhaps the most meaningful of these was originally proposed by Aldridge (1953): esterases were classified either as type A or type B, based on whether or not they were inhibited by organophosphate (OP)

compounds such as those in Figure 1.5. It has since been found that the OP-sensitive type B carboxylesterases possess a catalytically active serine residue which is irreversibly bound by the inhibitor. Hence type B esterases are now known as serine hydrolases (Leinweber, 1987). Sensitivity of different carboxylesterase isozymes to OPs therefore provides information about the nature of the catalytic residues of the enzymes under investigation.

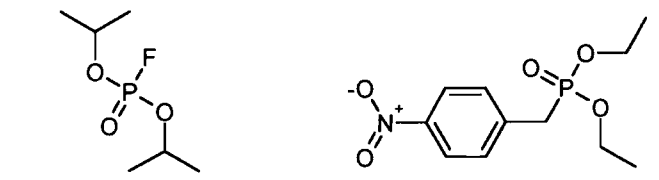

Figure 1.5: Organophosphate inhibitors

Another inhibitor that has been found in animals to specifically inhibit one type of esterase is eserine, an alkaloid which is also known as physostigmine after *Physostigma venenosum* (Calabar bean) from which it was originally isolated in the nineteenth century. Eserine was found to exclusively inhibit cholinesterases (Schrattenholz *et al.* 1993)- serine hydrolases that show selectivity for choline esters.

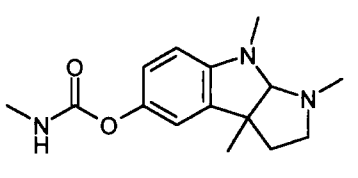

Figure 1.6: Eserine

A less well-defined distinction that is commonly made within the carboxyl ester hydrolases is between the carboxylesterases and the lipases. Classically, lipases work on insoluble substrates, usually with long acyl chains, whilst esterases

hydrolyse more hydrophilic molecules (Leinweber, 1987). However, the distinction is blurred by the capability of some lipases to effectively hydrolyse soluble substrates.

When used in conjunction, the above biochemical properties lead to a general carboxylesterase classification scheme as shown in Figure 1.7.

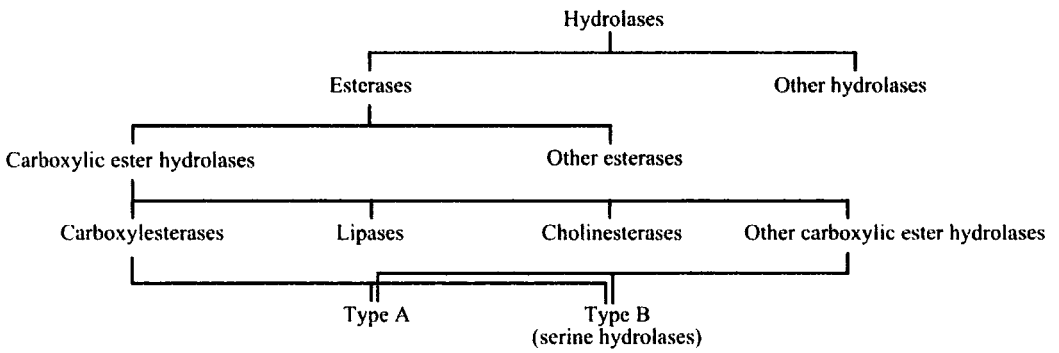

Figure 1.7: Biochemical esterase classification

Biochemical methods can therefore characterise carboxylesterases to a useful degree, but for full classification of any given esterase, consideration needs to be given to its sequence and structure and how these relate to other carboxylesterases.

1.3.2 Classification through sequence and structural homology

Homology between esterases is extremely variable: any two esterases may have anything from no sequence similarity at all, to being almost identical. The most dissimilar enzymes are from unrelated gene families that have evolved similar functionalities but exhibit completely distinct active site architectures and mechanisms of action. Conversely, two esterases may be the result of recent gene duplication events and so have almost complete sequence identity. In reality the vast majority of carboxylesterases are related to a degree which is somewhere between the two extremes. For clarity, the levels of esterase homology of relevance to this section are outlined below:

- **No homology**

  Enzymes have evolved to hydrolyse carboxylic esters independently, and show no sequence or structural homology.

- **Common catalytic core**

  Many hydrolases, including all carboxylesterases cloned to date, operate via a catalytic triad (see section 1.3.2.1). This triad has evolved in unrelated protein families through convergent evolution (Ollis *et al.* 1992), so very little to no sequence homology is observed.

- **Same enzyme superfamily (structural homology)**

  Enzymes belong to a common protein superfamily, which has evolved from a single progenitor through gene duplication followed by sequence divergence. The majority of carboxylesterases belong to the α/β hydrolase fold superfamily (see section 1.3.2.2). Members of the

superfamily may show very little sequence similarity, although they possess well-conserved structural features.

- **Same enzyme family (sequence homology)**

  A family of enzymes that show significant sequence homology to one another.

The specifics of how these levels of homology apply to carboxylesterase classification are detailed in the following sections.

1.3.2.1 Carboxylesterase mechanisms

All of the plant carboxylesterases that have been cloned to date (see section 1.5.3) have a common basis for their activity- a catalytic triad containing an active site serine. The catalytic mechanism of these enzymes is described below. However, it is clear from biochemical investigations (see section 1.5.1) that some carboxylesterases are not serine hydrolases, as they are not inhibited by OPs (Veerabhadrappa and Montgomery, 1971; Norgaard and Montgomery, 1968). Therefore pectin methylesterases are also considered in this section as they display a different, non serine-based mechanism by which carboxylic ester bonds may be hydrolysed (Johansson *et al.* 2002), which may be found in carboxylesterases in the future. In addition, acetylxylan esterases, which use a single metal ion in their active site (Taylor *et al.* 2006), are briefly discussed.

The catalytic triad

A very large number of hydrolases utilise a catalytic triad consisting of a nucleophile (serine/cysteine/aspartate), a histidine, and an acidic residue (aspartate/glutamate). The carboxylesterases described to date are all serine hydrolases (nucleophile = serine) and most have an aspartate as the acid residue. The mechanism by which catalytic triads perform hydrolyses has been studied in detail (reviewed in Dodson and Wlodawer 1998). The general mechanism has been well established (Figure 1.8), although details such as the exact role of the acid are not fully defined. The most recent proposal is that the acid residue hydrogen bonds to the histidine, holding the latter's side chain in the correct orientation for catalysis (Oakeschott *et al.* 1999). This hyphothesis is supported by the active site of a serine carboxylesterase from *Streptomyces scabies* (SsEst, Wei *et al.* 1995), where the acid residue is missing, but the backbone of a tryptophan residue hydrogen bonds to the histidine in a similar way, holding it in position.

The hydrolysis reaction proceeds via two main stages: the acylation of the enzyme and the release of the alcohol moiety from the ester, followed by the cleavage of the acyl group from the enzyme through hydrolysis (see Figure 1.8).

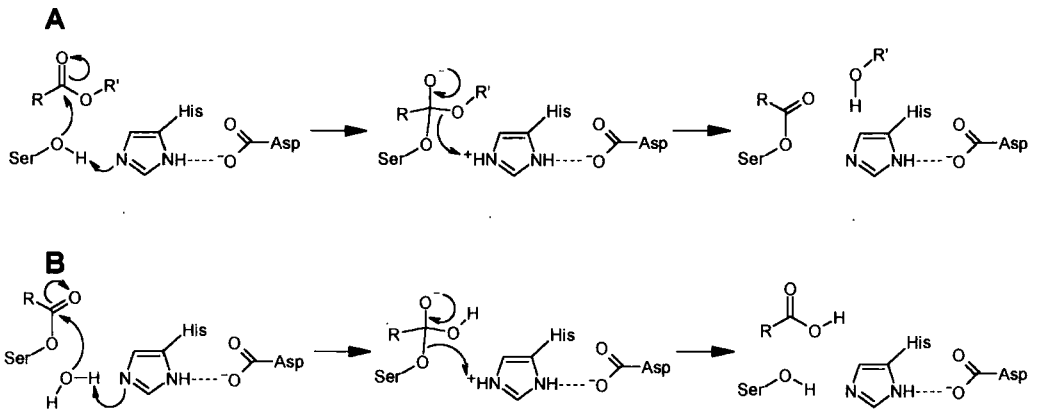

Figure 1.8: Reaction mechanism for the serine hydrolase mediated cleavage of a carboxylic ester bond. **A**: release of the alcohol moiety and acylation of the enzyme and **B**: hydrolysis of the acyl group from the enzyme.

Another feature of catalytic triad-based hydrolases is the oxyanion hole, which consists of residues that hydrogen bond to the carbonyl oxygen of the substrate. Two bonds are formed initially, then as the reaction proceeds and the oxygen becomes negatively charged, another hydrogen bond is thought to form, stabilising the tetrahedral intermediate (Ollis *et al.* 1992).

Pectin methylesterases: an aspartate based hydrolysis mechanism

Pectin methylesterases have a different catalytic mechanism (Johansson *et al.* 2002), which also involves a nucleophilic attack on the carbonyl carbon. In this case however, the attack is carried out by one of the active site aspartate residues, which is thought to be held in place though hydrogen bonds to a neighbouring arginine residue (see Figure 1.9). In this proposed mechanism, another aspartate residue acts as an acid/base during catalysis. Two glutamine residues provide a possible oxyanion hole.

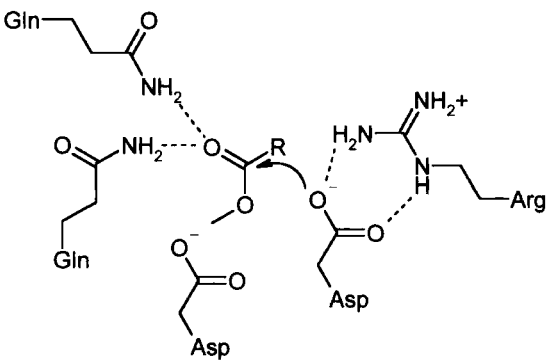

Figure 1.9: The proposed configuration of pectin methylesterase active site residues at the beginning of catalysis (Johansson et al. 2002).

Acetylxylan esterases: a metal ion-dependent mechanism

Acetylxylan esterases have a mechanism based on a single, divalent cation in the active site (Taylor et al. 2006). Hydrolysis is carried out by a nucleophilic attack on the carbonyl carbon by a metal-bound water molecule (Figure 1.10).

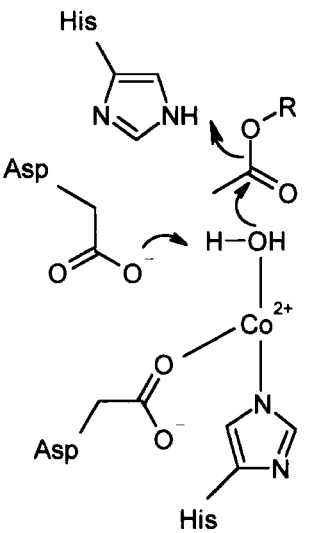

Figure 1.10 Initiation of hydrolysis by acetylxylan esterases (adapted from Taylor et al. 2006).

Although in future, an aspartate or metal ion-mediated hydrolysis mechanism may be found in carboxylesterases, all carboxylesterase sequences described to date show catalytic serine residues which are part of a catalytic triad. Carboxylesterase catalytic triads are found in two unrelated structural families of enzymes: the α/β hydrolase fold superfamily and the GDS hydrolase family. These structural classes are described in the next section.

1.3.2.2 Structural homology

The α/β hydrolase fold superfamily

The α/β hydrolase fold is typically composed of a mostly parallel β-sheet made up of eight strands linked by α-helices, arranged as shown in figure 1.11. Within this scheme, there is a central "minimal fold" that is common to all α/β hydrolases (Figure 1.11, Heikinheimo *et al.* 1999), although considerable variation is shown by enzymes within the superfamily outside of this area of high structural homology.

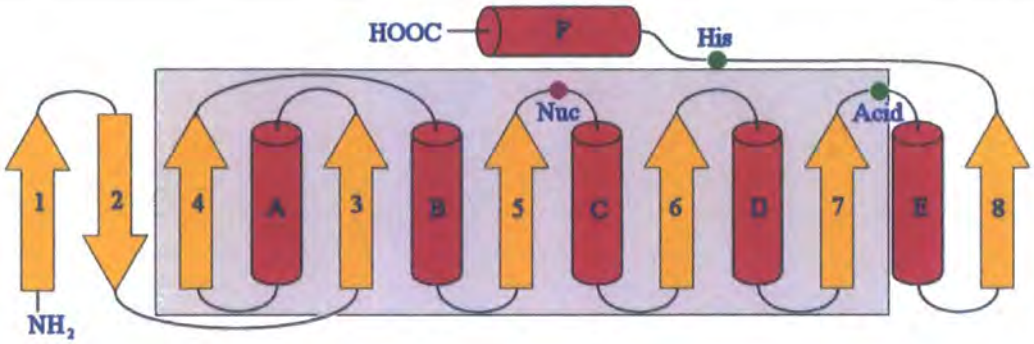

Figure 1.11: Schematic of a typical arrangement of the secondary structure in α/β hydrolase fold enzymes (not to scale, adapted from Ollis et al. 1992). β-strands are shown as yellow arrows and the α-helices are represented as red cylinders. The catalytic residues are marked: the nucleophile is purple while the other two residues are shown in green. The minimal fold is boxed.

The β sheet in α/β hydrolases exhibits a superhelical twist such that the first and the last strands can have a 90° difference in orientation. This can be seen in Figure 1.12, which shows the crystal structure of brefeldin A esterase (BFAE), a bacterial member of the superfamily (Wei *et al.* 1999). The catalytic triad residues all occur after a β-strand, positioning the active site on one edge of the sheet.

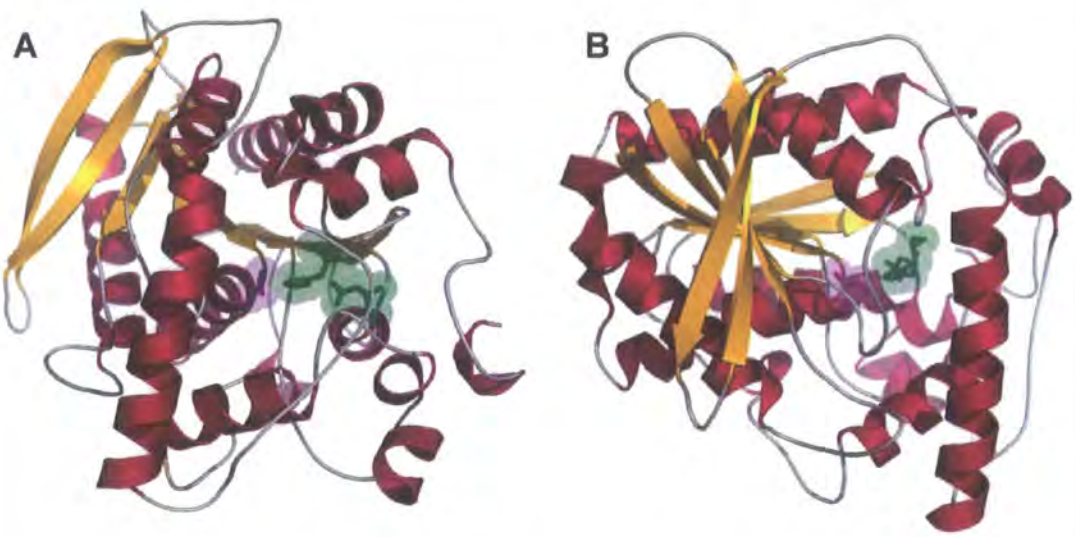

Figure 1.12: Crystal structure of BFAE, a bacterial α/β hydrolase (Wei *et al.* 1999, Protein Data Bank (PDB) accession: 1JKM). **A**: the active site residues in their position on the edge of the β-sheet. Part **B** is a rotated version of **A**, clearly showing the twist in the β-sheet. Using the nomenclature from Figure 1.11, β-strand 1 is on the left in **A** and the strand closest to the viewer in **B**. Colouration is as in Figure 1.11: the catalytic serine (Ser 202) is purple, while the other two catalytic residues (Asp 308 and His 338) are green. Images generated with PyMol using data stored in the protein data bank.

As well as the minimal fold and the nature of the β-sheet, there are other structural features that are characteristic of α/β fold hydrolases. The catalytic triad is held in a very well conserved three-dimensional conformation in which the residues are in close association with each other (Figure 1.12 **A**). The nucleophilic residue, serine in BFAE, is located on a "nucleophile elbow", an unusually sharp turn between β-sheet five and helix C (Figure 1.12 **B**). The elbow is thought to be necessary to ensure that the relatively short serine or cysteine side chain extends far enough into the active site for catalysis to take

place. An additional benefit is that the serine is directly at the end of helix C, where the helix dipole can contribute to stabilising the tetrahedral intermediate. A consequence of having such a sharp turn at the serine is that residues Ser+2 and Ser-2 are brought into unusually close proximity, which dictates that both residues have to be very small (see Figure 1.13 **B**). This creates a GXSXG motif, which is found in all α/β hydrolases.

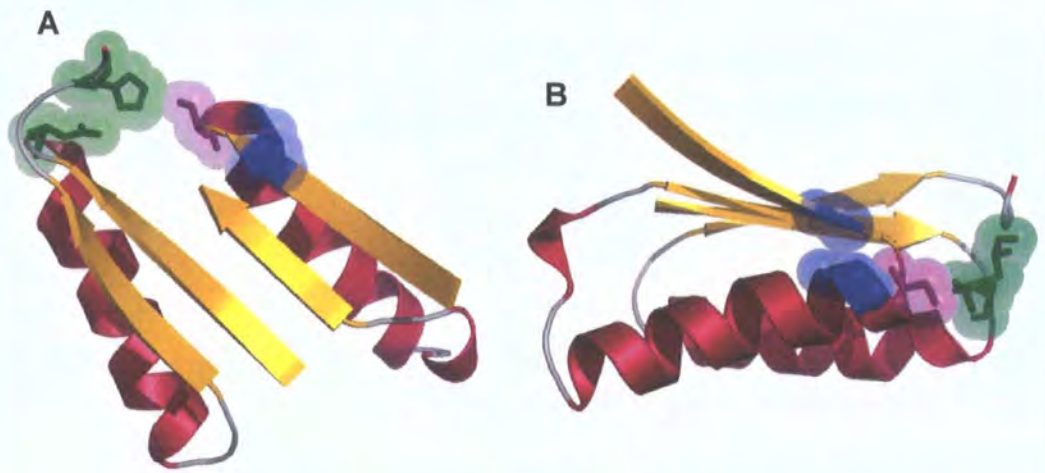

Figure 1.13: The catalytic triad of BFAE (Wei *et al.* 1999, PDB accession number 1JKM). Only the catalytic residues and their adjacent secondary structures are shown: strands five to eight are shown, as well as nearby helices. Coloured blue are Gly 200 and Gly 204 (Ser-2 and Ser+2), and all other colours are as in Figure 1.12. Van der Waals radii are shown around the atoms in the coloured residues as semi-transparent spheres. **B** is a rotated view of **A**, which views the nucleophile elbow from the side. The necessity for having two glycine residues at positions 200 and 204 (Ser - 2 and Ser + 2), due to their very close proximity, is clear. Images generated with PyMol using data from the protein data bank.

The α/β hydrolase superfamily encompasses a very large diversity of enzymes in addition to esterases, including lipases, epoxide hydrolases, halogen hydrolases, hydroxynitrile lyases and thioesterases. The structure of α/β hydrolases is similarly diverse: while they all have the structural features described above, variations in structure away from the minimal fold are common and can be very large. Members of the superfamily may show almost no sequence similarity whatsoever: excepting the GXSXG motif and the other catalytic residues, sequences can be completely diverged. Families of α/β hydrolase fold enzymes are found throughout nature and fulfil a wide range of roles. The classification of α/β hydrolase fold carboxylesterase families is described in section 1.3.2.3.

The GDS Hydrolases

Upton and Buckley (1995) described a family of lypolytic enzymes that showed sequence similarity to a lipase/acyltransferase (glycerophospholipid-cholesterol acyltransferase, GCAT) from *Aeromonas hydrophila* (Hilton and Buckley, 1991). Instead of a having GXSXG motif, GCAT has a sequence of FGDSLS around its active site serine. This alone showed that GCAT and related enzymes must have different structures to the α/β hydrolases. GCAT homologues were found in other prokaryotes and plants, and the resulting family became known as the GDSL lipases (Brick *et al.* 1995), after the consensus sequence around the active-site serine. More recent investigation has revealed that the leucine residue is not always conserved (Akoh *et al.* 2004), and the enzymes are not only active toward lipids, so this thesis will refer to the family as the GDS hydrolases in line with the suggested revised nomenclature of Cummins and Edwards (2004). Structurally, the GDS hydrolases are entirely distinct from the α/β hydrolase fold

superfamily, although they have a common catalytic mechanism based around a catalytic triad of serine, histidine and acid.

A subgroup of the GDS hydrolases is the SGNH family, named after four residues which are conserved in all family members. Two SNGH hydrolases, rhamnogalactonuran acetate esterase (RGAE) and SsEst (*Streptomyces scabies* esterase), have been crystallised and their structures determined (Wei *et al.* 1995, Molgaard *et al.* 2000). GDS hydrolase topology (Figure 1.14) is completely different to the α/β hydrolase fold. The active site serine occurs very near to the N-terminus, and the histidine and aspartate are only separated by two residues and are near the C-terminus.

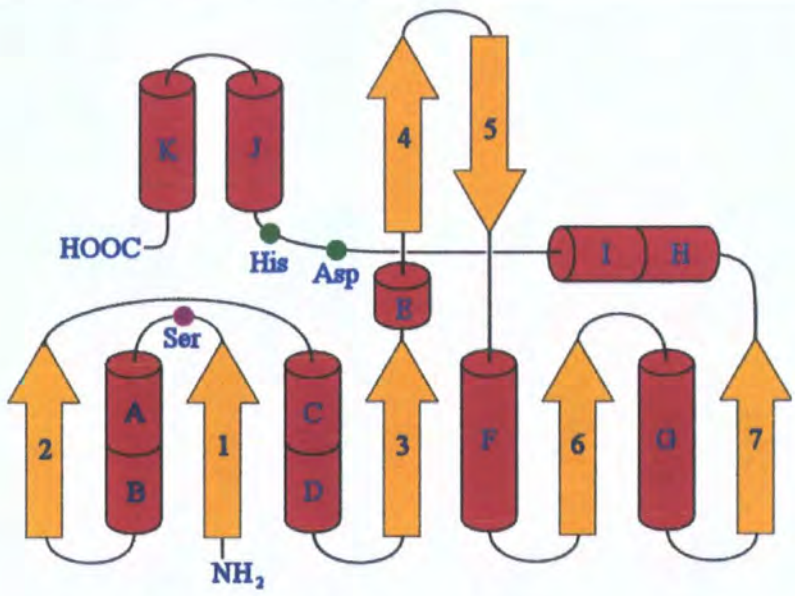

Figure 1.14: GDS hydrolase topology (Molgaard *et al.* 2000)

As well as the main β-sheet neighbouring the catalytic triad, there is an additional β-sheet (see Figures 1.14 and 1.15), the function of which is still unclear. GDS hydrolases have been shown to have a large degree of overall flexibility: while the central β-sheet and associated helices remained relatively rigid, the binding

pocket appeared to be highly flexible (Akoh *et al.* 2004). This flexibility possibly accounts for the wide range of ester substrates that may be hydrolysed by some GDS hydrolases (see section 1.5.3.2).

Figure 1.15: Structure of RGAE, a bacterial SGNH hydrolase. Colours of catalytic residues and secondary structure elements are as in Figure 1.12. Image generated with PyMol using data stored in the protein data bank.

Unlike the α/β hydrolases, GDS hydrolases do not have a nucleophile elbow. Instead the active site serine is part of a type one β-turn (Molgaard *et al.* 2000). The other active site residues are on a loop connecting two α-helices.

Although not nearly as diverse as the α/β hydrolase fold superfamily, the GDS hydrolase family does contain a large number of enzymes with diverse activities associated to them, including lipase, carboxylesterase and acyltransferase functionalities.

1.3.2.3 Classification of Carboxylesterase Gene Families

The GDS hydrolases have several areas of primary sequence homology, not just a motif around the active site serine, so they can be classified into one overall family (see section 1.5.3.2 for GDS hydrolase alignment). This is in contrast to the α/β hydrolases, whose extreme diversity dictates that they must be subdivided into several families, which may in turn be subdivided into subfamilies. The diversity of the superfamily is reflected in the fact that the ESTHER database (Hotelier et al 2004) has been established purely for the classification of members of the superfamily (http://bioweb.ensam.inra.fr/ESTHER/). Many of the families within the ESTHER database are outside the scope of this thesis in that they do not show carboxylesterase activities. The best classification of families of enzymes that include carboxylesterases/lipases has been made by Arpigny and Jaeger (1999), in their classification of bacterial lipases. The families included in this classification system encompass all the plant carboxylesterases characterised to date as well as the bacterial carboxylesterases, so is a suitable system to be used in this thesis. The classification system described by Arpigny and Jaeger, and how it relates to the cloned plant carboxylesterases described to date is summarised in Table 1.1 below. Characterised plant CXEs all fall into three of the microbial families I, II and IV.

Family	Structure	Cloned plant homologues	Example bacterial accession
I	α/β hydrolase fold	hydroxynitrile lyases, carboxylesterases (see section 1.5.3.1)	D50587
II	GDS hydrolase	plant GDS hydrolases (see section 1.5.3.2)	P10480
III	α/β hydrolase fold		M86351
IV	α/β hydrolase fold	carboxylesterases (see section 1.5.3.3)	X62835
V	α/β hydrolase fold		M58445
VI	α/β hydrolase fold		D90904
VII	α/β hydrolase fold		Q01470
VIII	α/β hydrolase fold		AAA99492

Table 1.1: Classification of bacterial carboxylesterases as proposed by Arpigny and Jaeger (1999)

This thesis will use a combination of the classification methods detailed above. The primary biochemical distinction applied is whether or not the carboxylesterases are sensitive to inhibition by OPs. Additionally, some information about whether enzymes have lipolytic activities as well as carboxylesterase activity can be inferred through use of substrates with long acyl chains. Finally, any enzymes for which sequence data are obtained will be classified according to the structural and sequence groupings described above.

1.4 Microbial and Mammalian Carboxylesterases

There is a considerable body of work in the public domain describing microbial and mammalian carboxylesterases, much of which has little obvious bearing on plant carboxylesterases, so this section is only intended as a very brief overview. The interested reader is referred to the numerous reviews of the areas (Redinbo and Potter, 2005; Satoh and Hosokawa, 1998; Leinweber, 1997; Bornscheuer, 2002, Wright 2005, Ro *et al.* 2004). Where specific microbial enzymes may offer insights into plant carboxylesterases, they are described in more detail along with their homologues in plants in section 1.5.3.

1.4.1 Bacterial Carboxylesterases

Bacterial carboxylesterases have attracted considerable interest for several reasons: carboxylesterases have been shown to have a role in antibiotic resistance, and along with bacterial lipases are used extensively in industrial processes where enzymatic hydrolysis is desirable (Panda and Gowrishankar, 2005). Additionally, esterases show high polymorphism when compared to other enzymes which allows them to be used as taxonomic differentiators: the different carboxylesterase isozymes may be effectively visualised through separation by gel electrophoresis followed by staining for esterase activity. Patterns of esterase expression generated in this way have been used to successfully distinguish between bacterial sub-species (Goullet and Picard, 1994).

1.4.1.1 Antibiotic resistance due to bacterial carboxylesterases

EreA is a gene cloned from erythromycin resistant *Escherichia coli* (Ounissi and Courvalin, 1985) coding for an esterase that can hydrolyse the macrocycle ester of erythromycin (Figure 1.16). While this detoxification is not a common resistance mechanism, it results in very high levels of resistance to the antibiotic (Wright, 2005).

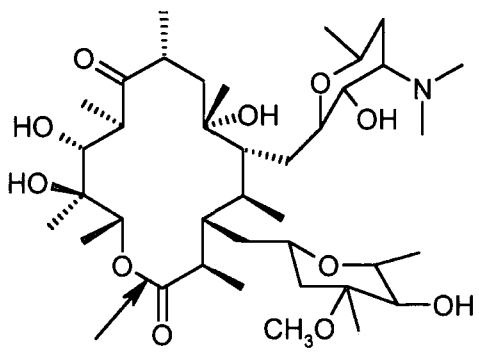

Figure 1.16: Erythromycin. The point of hydrolysis by EreA is arrowed.

1.4.1.2 Industrial Use of Bacterial Carboxylesterases

Carboxylesterases are used in a multitude of industrial applications from the extraction of hydroxycinnamic acids from residues of agro-industry such as wheat or rice bran to using carboxylesterases to selectively produce desired enantiomers of pharmaceutical drugs (Panda and Gowrishankar, 2005). An example of the latter case is the production of pure (R)- and (S)-ketoprofen using an esterase from *Trichosporon brassicae*. There is also potential for esterases which have been found to degrade plastics such as polyurethane to be used in the degradation of these otherwise very stable polymers (Jahangir et al 2003).

1.4.2 Mammalian Carboxylesterases

Mammalian carboxylesterases are enzymes of 55-60kDa, and have been investigated primarily with respect to their role in drug metabolism. They fall into family VII of the classification system presented in section 1.3.2.3, and have no plant homologues. Further classification of mammalian carboxylesterases has been problematic in that it was done primarily by substrate specificity, but such characterisations are often misleading due to the broad and overlapping substrate specificities exhibited by many carboxylesterases (Leinweber, 1987). In 1998, Satoh and Hosokawa proposed a subdivision of the family on the basis of sequence similarity, dividing the family into four subfamilies, of which two contain human enzymes. Human carboxylesterases are expressed in the epithelia of host organs, suggesting that they are there primarily to perform a protective function against xenobiotics. They have been shown to have hydrolytic activity toward a wide range of compounds, from pharmaceuticals like mevastatin to narcotic drugs like cocaine and heroin. Human carboxylesterase substrates also include compounds with amide and thioester bonds, showing that the enzymes are not completely specific to carboxylic esters.

Cocaine metabolism is of particular interest because it reveals an additional function of the carboxylesterases: when cocaine is taken in the presence of ethanol, cocaethylene is formed. This is as a result of a carboxylesterase replacing the methyl group of cocaine with an ethyl group (Satoh and Hosokawa, 1998). Such transesterification reactions are not conceptually difficult to understand in light of the carboxylesterase mechanism described in section 1.3.2.1: If an alcohol cleaves the acyl group off the carboxylesterase in the

second phase of the reaction instead of water, transesterification takes place instead of hydrolysis.

1.5 Plant Carboxylesterases

1.5.1 Activities toward xenobiotic substrates

Many older pieces of work have been published on plant carboxylesterases that have examined esterase activity toward various model ester substrates such as those in Figure 1.4. These are of limited use, as the substrates and assay conditions used vary between each study. However, they are of some value in that they give an overview of the numbers and types of esterase activities in different plant species. Studies have also been carried out which shed light on how esterase expression may change with development and in response to external stimuli. A selection of these studies is reviewed below.

Like with bacterial esterases, there have been several studies in plants in which the numbers of carboxylesterase isozymes have been assessed using gel electrophoresis separation followed by visualisation using naphthol ester substrates. These are summarised in Table 1.2. Of note is the large proportion of esterases that are serine hydrolases (inhibited by organophosphates), and also that large numbers of discreet enzymes found.

Species	Plant part	No. of esterase activities resolved	Number of activities inhibited by OPs	Reference
Pisum sativum (pea)	Seed	7	6	Veerabhadrappa and Montgomery (1971)
Phaseolus vulgaris (green bean)	Fruit	14	11	
Gossypium thurbereri	Leaf	4-6*	unknown	Cherry and Katterman (1971)
Aspidosperma polyneuron	Leaf	14	10	De Carvalho *et. al.* (2003)
Triticum aestivum (wheat)	Seed	17	17	Cubadda and Quattrucci (1974)

Table 1.2: Summary of numbers of isoenzymes found in different plant species and tissues, and their susceptibility to OP inhibition. (* different numbers of esterases were found in plants sampled from different localities)

Table 1.3 (next page): Summary of esterase activities described in selected investigations using non-specific substrates. (*: the number refers to the acyl chain length of the substrate assayed, + in parentheses indicate differences in comparable activities. †: + denotes full or close to full inhibition, (+) denotes partial inhibition, and 0 no inhibition; other numbers specify the number of enzymes of a group affected, PCMB: *p*-chloromercury benzoate. Empty cells: data not available.)

Species	Plant Part	No. of Observed Activities	M_r	pI	Substrate acyl group*	Inhibition†			Reference
						OP	eserine	PCMB	
Sorghum	Grain	2 (of 5)	60 kDa	6.6	2	+	0	0	Sae *et. al.* (1971)
Malus domestica (Apple)	Fruit peel	1 (of 5)			2				Bartley *et. al.* (1981)
		2 (of 5)			2, 3				
		1 (of 5)			3, 5				
		1 (of 5)			5, 6				
Daucus carota (Carrot)	Root	5 (of 6)			2>3>4>6>8	+			Carino and Montgomery (1968)
Cucurbita pepo cv. Little Gem	Fruit				2 (+++)				Schwarz *et. al.* (1964)
cv. Long White Bush	Fruit				2 (++)				
cv. Long Green Bush	Fruit				2 (+)				
cv. White Custard	Fruit				2 (+)				
cv. Golden Custard	Fruit				2 (+++)				
cv. Table Queen	Fruit				2 (+)				
cv. Grahamstown Marrow	Fruit				2 (+)				
Cucurbita andreana	Fruit				2 (++++)				
	Leaves				2 (++)				
	Stem				2 (+)				
Curcurbita maxima	Fruit	1	36kDa dimer	4.9	2	+	0	+	Nourse *et. al.* (1988)
Phaseolus vulgaris (Green beans)	Fruit	2 (of 13)			2>3>>4	(+)		0	Veerabhadrappa and Montgomery (1971)
		2 (of 13)			2>3>>4	(+)		(+)	
		3 (of 13)			2≈3>>4	+		(+)	
		3 (of 13)			2≈3>>4	(+)		0	
		1 (of 13)			2<3>>4				
		1 (of 13)			2≈3>4	+		+	
		1 (of 13)			2<3>4	+		0	
Pisum sativum (pea)	Seed	6			2<3≈4	5			Norgaard & Montgomery (1968)

Table 1.3 summarises selected activities which have been more extensively investigated using biochemical techniques including purification of esterase activities, assays for activity toward model ester substrates and inhibitor studies using organophosphates, *p*-chloromercuribenzoate (PCMB) and eserine. The esterases show great variability of expression between species, but also within different populations or cultivars of the same species (Cherry and Katterman, 1971; Schwarz *et. al.*, 1964), and different tissues of the same plant (Schwarz *et. al.*, 1964). Most of the esterases observed were inhibited by reaction with OP compounds, suggesting that the majority of esterases in plants are serine hydrolases. However, a minority were left unaffected, showing the presence of non-serine-mediated enzymes as well. Finally, where investigated, most esterases showed greater activity toward esters with shorter acyl chain lengths, although there were some exceptions (Carino and Montgomery, 1968; Veerabhadrappa and Montgomery, 1971; Norgaard and Montgomery, 1968).

Metabolism of Agrochemical Esters

Many herbicides are applied to plants formulated as carboxylic esters to increase their overall hydrophobicity, which aids absorption through the waxy cuticle (Hassal, 1990). Other herbicides have ester bonds as part of their active structure (Hassal, 1990; Roberts, 1998). It has been shown that the first step in the metabolism of these compounds is often the hydrolysis of the ester bond (Roberts, 1998). This leads either to activation of the herbicide, if the acid or alcohol is the active structure, or deactivation if the whole ester is necessary for phytotoxicity.

Not all plants show the same esterase activity toward herbicide substrates, and this can lead to herbicide selectivity. Jeffcoat and Harries (1975) reported that flamprop isopropyl showed toxicity toward wild oat (*Avena fatua*), but not toward barley (*Hordeum distychum*). Although flamprop isopropyl was hydrolysed in barley to the active flamprop acid, the rate was sufficiently slow to allow the flamprop to be metabolised further before it reached phytotoxic concentrations. In wild oat however, the rate of hydrolysis was considerably more rapid, and flamprop accumulated to a lethal dose, even though some was further metabolised to a more hydrophilic metabolite (Jeffcoat and Harries, 1975). In a study of *Triticum aestivum* (wheat) and the competing weeds blackgrass (*Alopecurus myosuroides*) and wild oat, Cummins *et. al.* (2001) also found differences in the carboxylesterase activities toward various xenobiotic substrates: it was found that while wheat hydrolysed model colorimetric substrates such as *p*-nitrophenyl acetate quicker then the weeds, the weeds showed higher hydrolytic activity toward the herbicides (diclofop methyl, bromoxynil octanoate and binapacryl) when compared with the wheat activities. Haslam *et. al.* (2001) observed the presence of at least 11 apoplastic esterases, at least some of which had activity toward aryloxyphenoxypropionate esters. It was speculated that these herbicides may be hydrolysed by these esterases before entering the cell. As well as being important for establishing the site of metabolism of xenobiotic substrates, establishing the localisation of esterases within the plant provides clues as to the endogenous roles of these enzymes.

The only esterase active toward a herbicide (clodinafop propargyl) that has been purified and cloned to date was isolated from blackgrass (Cummins and Edwards, 2004). The 40kDa enzyme purified was the dominant activity toward

clodinafop propargyl, although other more minor activities were also observed. MS-MS sequencing of peptides from the 40kDa polypeptide revealed a protein with homology to a rice (*Oryza sativa*) GDS hydrolase. Using primers designed from homologous GDS sequences, the blackgrass enzyme (AmGDSH1) was cloned and expressed in *Pichia pastoris* as an extracellular protein. The recombinant enzyme was confirmed to show activity toward clodinafop propargyl. *Am*GDSH1 was predicted to be glycosylated and exported from the cell into the apoplast, suggesting that it was related to the apoplastic esterases identified in wheat (Haslam *et al.*, 2001)

1.5.2 Plant Carboxylesterase Expression Patterns

Expression of carboxylesterases can be highly variable. In this section, carboxylesterase expression in different species is briefly examined, and levels of esterases in different plant tissues is also reviewed. Additionally, biochemical evidence that carboxylesterase levels change during plant development and in response to stress and pathogen infection is reviewed.

1.5.2.1 Taxonomic variation in esterase expression

As may be gathered from work reviewed in section 1.5.1, markedly different esterases are expressed in even closely related species, with patterns of esterase activities resolved by gel electrophoresis used to differentiate between closely related species, and even cultivars or different populations of the same species (Pereira *et. al.*, 2001; Cherry and Katterman, 1970, Schwarz *et. al.* 1964). While in closely related plants, the differences in esterase patterns often seem to be due to differential expression of very similar enzymes, plants which are further removed from each other appear to contain completely different enzymes, based

on activities, abundance and gel electrophoresis mobility. It should be noted that some of the differences in esterase expression observed between plant species could be due to variations in the stage of development or levels of stress the plants had been subjected to, as these factors also influence esterase expression

1.5.2.2 Expression of Esterases in Different Plant Tissues

Esterase activity has been reported in a wide range of plant tissues (see section 1.5.1). The expression of some esterases varies dramatically between tissues suggesting that these enzymes may have tissue-specific roles. In a study of many species and varieties of the Curcurbitaceae, Schwarz *et. al.* (1964) showed that many species show much higher esterase activities toward indophenyl acetate in their fruit tissue when in their leaves or stems, with the stems showing the lowest activity overall. However, one species (*Ecballium elaterium*) was an exception to this, and displayed higher activity in its leaves then its fruit. PAGE separation with α-naphthyl acetate activity staining revealed different patterns of esterase expression in the different tissue sources for all of the species investigated.

Interestingly, plant esterases also appear to be excreted on to the plant surface: Clifford *et. al.* (1977) found activity toward *p*-nitrophenyl esters in distilled water which had been used to wash marrow (*Cucurbita pepo*) leaves. Esterases were also found to be released by *Vicia faba* roots, with the release being proportional to time (Frossard and Voss, 1979). The release was stimulated to greater levels by the addition of increasing quantities of α-naphthyl acetate to the growth medium.

In a study of esterase activity toward α-naphthyl acetate in *Vicia faba*, Frossard and Voss (1978) reported that there was substantially more activity in the root

tips then in the middle part of the roots, with the root tip activity changing over time (see below, section 1.5.2.3). It was thought that these esterases may be involved in cell wall elongation.

1.5.2.3 Developmental Changes in Esterase Expression

Esterases possibly associated with cell wall elongation in the root tips of *Vicia faba* (Frossard and Voss, 1978), were found to increase dramatically after germination, peaking after seven days. Activities in the shoot behaved in a similar manner, although they were lower overall. Activities in the main body of the root and in the leaves remained relatively constant.

Chandra and Toole (1977) showed that esterases were released from germinating lettuce (*Lactuca sativa* L.) seeds following radicle protrusion from the seed coat. Esterases were not released from intact seeds to nearly the same extent as they were from half seeds, suggesting that they are located in the extraembryonic fluid. Release of esterases active toward indophenyl acetate peaked at 48 hours after imbibition of the seeds in water. By 80 hours the levels being released dropped to under 25 % of the levels observed at 48 hours. Peak release coincides with the rupture of the seed coat by the emergence of the radicle. Esterases were released from half seeds within 2-3 hours of imbibition, which suggests that the esterases are present in the extraembryonic fluid for many hours before being released into the medium when the seed coat ruptures.

In young fruit of *Malus pumila* (apple) there is very little esterase activity toward α-naphthyl acetate, but as the fruit grows in size, esterase activity increases as well (Goodenough and Riley, 1985). When the fruit reached its maximum size,

there was a further, more rapid increase in esterase activity, which continued to increase during ripening.

1.5.2.4 Post-Infection Changes in Esterase Expression

Expression of esterases has been found to change in response to infection by fungal or bacterial pathogens. Chigrin *et. al.* (1976) found an increase of esterase activity toward *p*-nitrophenyl acetate in wheat plants 18 hours after infection with stem rust (*Puccinia graminis*). This increase was larger in sensitive varieties of wheat then the non-sensitive, implying that it was not part of a response which conferred resistance to the plant. More likely, it seems part of a general stress response which occurs upon infection. There seems to be a similar situation in fingermillet seedlings infected with the major fungal disease, blast (*Pyricularia grisea*). The susceptible variety of fingermillet showed a much larger increase in non-specific esterase activity then the non-susceptible biotype (Muarlidharan *et al.*, 1995).

The bacterial pathogen responsible for halo blight, *Pseudomonas phaseolicola* was shown to induce the increased expression of an esterase in bean leaves (*Phaseolus vulgaris*, Rudolph and Stahmann, 1965). The esterase had activity toward α-naphthyl butyrate but not toward α-naphthyl acetate.

1.5.3 Plant carboxylesterase families

A significant number of plant carboxylesterases have been cloned in recent years, so the nature of the enzymes whose activities have been observed for so many years is starting to be revealed. What is emerging is a complex picture of many enzymes from several families with varied roles *in planta.* Plant carboxylesterases all fall into families I, II and IV as described by Arpigny and

Jaeger (1999) (see section 1.3.2.3). These families are described in the following sections.

1.5.3.1 Family I esterases

Cyanogenic plants produce hydrogen cyanide upon being wounded. Hydroxynitrile lyases perform the last step in the breakdown of cyanogenic glycosides that leads to hydrogen cyanide production (Hasslacher *et al.* 1996). Pir7b is a carboxylesterase from rice (*Oryza sativa*) which shows homology to hydroxynitrile lyases from the cyanogenic cassava (*Manihot esculaenta*; Hughes *et al.* 1994) and rubber tree (*Hevea brasiliensis*; Hasslacher *et al.* 1996). Rice is not cyanogenic, so Pir7b must have non-cyanogenic role. This was confirmed when active recombinant Pir7b was found to have no hydroxynitrile lyase activity (Wäspi *et al.* 1998). It has a mass of 32kDa, and activity toward both naphthol AS-esters (Figure 1.17) and naphthyl esters.

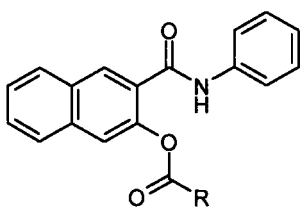

Figure 1.17: Naphthol AS-esters (R=CH_3; 2-naphthol AS-acetate, R=$CHClCH_3$; 2-naphthol AS-2-choroprionate)

Pir7b was first identified due to its upregulation during the response of rice to the non-host pathogen *Pseudomonas syringae* pv. *syringae*. Western blots confirmed the presence of Pir7b in rice leaves after inoculation, but more detailed localisation of the expression was not reported.

Ethylene-induced esterase (EIE) from *Citrus sinensis* is another family I esterase. This was discovered through a competitive hybridisation experiment designed to identify genes that are upregulated in response to treatment with ethylene (Zhong *et al.* 2001). Native EIE was shown to have activity toward α-naphthyl acetate, although bacterially expressed recombinant protein did not. This suggests that the recombinant protein was not in the correct conformation, or that there are post-translational modifications that occur *in planta* but are not carried out in bacteria. EIE is a protein of 31kDa, and like Pir7b shows no Hnl activity.

An experiment to find a methyl jasmonate-cleaving esterase (MJE) from tomato (*Lycopersicon esculentum*) revealed another Hnl-like esterase. After a multiple-stage purification of esterase activity toward methyl jasmonate, a protein of mass 28547Da (determined by electrospray ionisation time-of-flight mass spectrometry) and pI 4.7 was identified (Stuhlfelder *et al.* 2002). The protein was digested using endoproteinase LysC, and the fragments sequenced. Tomato MJE was subsequently cloned and expressed in *Escherischia coli* (Stuhlfelder *et al.* 2004) and transcript levels and activity were examined in different parts of the plant. High activity and transcript levels were found in roots and flowers, with much lower levels in stem and leaf tissue. MJE expression was transiently down-regulated one hour after treatment of plants with methyl jasmonic acid. There is no evidence of sub-cellular targeting of MJE, which suggests that it is cytosolic. It is speculated that MJE plays an important role in methyl jasmonate/jasmonate-related signalling (Stuhlfelder *et al.* 2004).

Polyneuridine aldehyde esterase (PNAE), a family one esterase, is involved in production of the complex alkaloid ajmaline in *Rauvolfia serpentina* L. (Figure

1.18), an Indian medicinal plant (Dogru *et al.* 2000). PNAE has a molecular weight of approximately 30 kDa, and a predicted pI of 5.9, and is notable for its extreme substrate specificity: it displayed high activity toward polyneuridine aldehyde, but no detectable activity at all toward any other substrates tested, which included the model substrates α-naphthyl acetate and *p*-nitro-benzoic acid methyl.

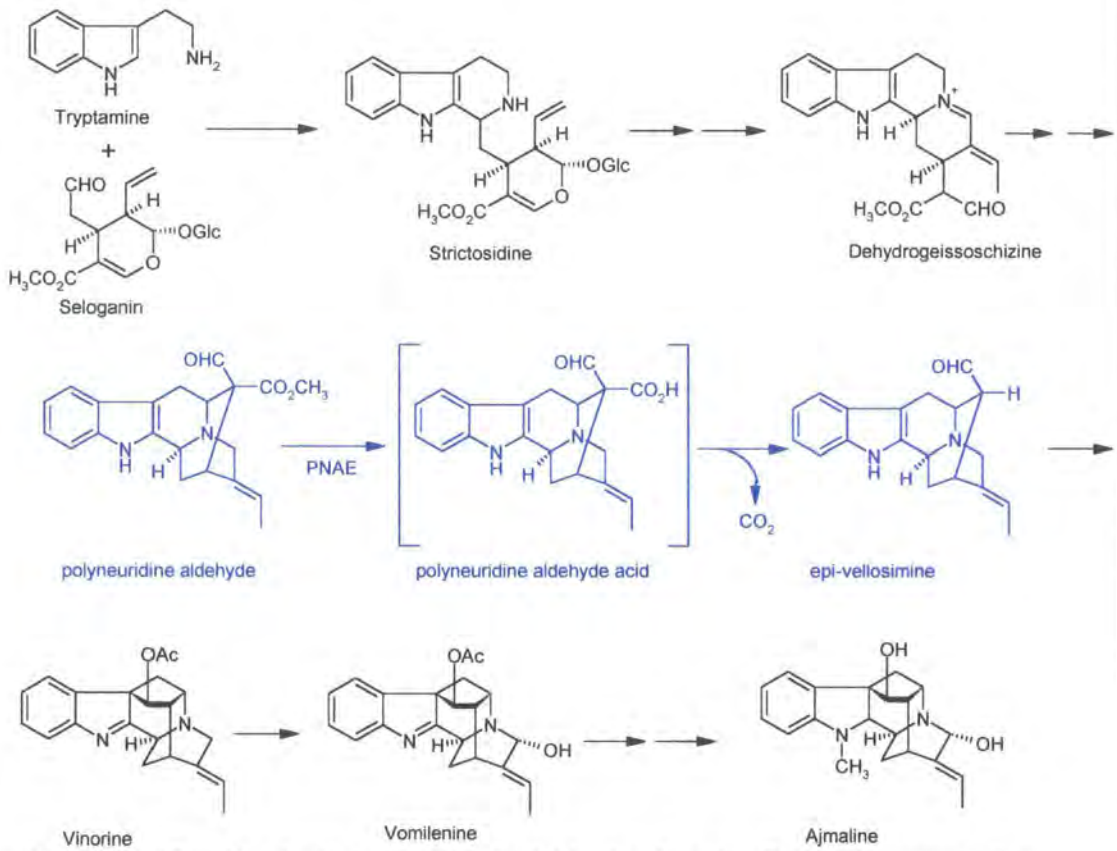

Figure 1.18: Production of the alkaloid ajmaline in *Rauvolfia serpentina* (adapted from Dogru *et al*, 2000). Reaction initialised by PNAE is in blue: the conversion of polyneuridine aldehyde acid to epi-vellosimine is spontaneous.

Salicylic acid-binding protein 2 (SABP2, Kumar and Klessig, 2003) is a 28kDa Hnl-like protein which has recently been identified in tobacco (*Nicotiana*

tabacum). Like Pir7b, it seems to be involved in defence against pathogens; when it is silenced, systemic acquired resistance is inhibited. It is also similar to EIE and MJE in that it is involved with a known plant signalling molecule. SABP2 showed activity toward *p*-nitrophenyl esters, including those with large carbon chain-lengths which is activity more normally associated with lipases. Intriguingly, this activity increases 3-6 fold in the presence of salicylic acid. Sice the original study, SABP2 has crystallised and its structure determined (Forouhar *et al.* 2005). In the same study it was also found that SABP2 has activity toward methyl salicylic acid, and it was proposed that this activity is involved in SABP2's possible endogenous role in the signal transduction pathway for systemic acquired immunity (Forouhar *et al.* 2006).

In summary, the Family I carboxylesterases reported to date are 28-31kDa whose divergence from the hydroxynitrile lyases seems to be complete in that they show no hydroxynitrile lyase activity. The proposed mechanism of the hydroxynitrile lyase from *Hevea brasiliensis* (Hanefeld *et al.* 1999) involves a cysteine residue (Cys81) adjacent to the active site serine (Ser80). This cysteine is missing from the homologous carboxylesterases, which could explain their lack of Hnl activity (see Figure1.19).

The predicted roles of the enzymes are varied, but seem to be related in that all but PNAE are involved in responses to signal molecules or, in the case of Pir7b, a pathogen which presumably causes the production of such molecules *in planta*.

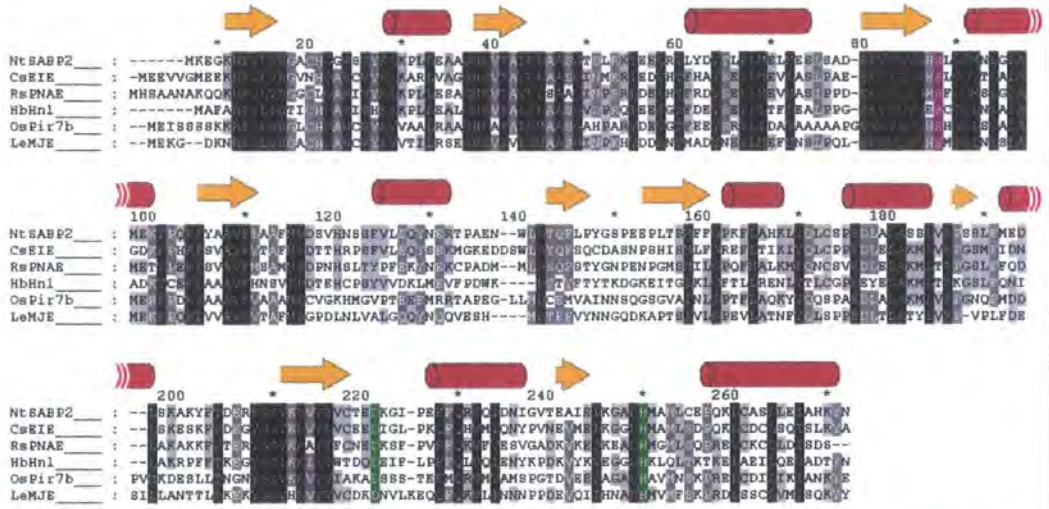

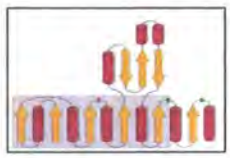

Figure 1.19: Alignment of plant family I esterases. Secondary structure elements are annotated as for SABP2 (Forouhar et al. 2006). The catalytic residues are coloured green except the serine, which is purple. Inset is a schematic of how the structural elements are arranged, showing the α/β hydrolase minimal fold boxed in grey. NtSABP2: *Nicotiana tabacum* salicylic acid binding protein 2, CsEIE: *Citrus sinensis* ethylene induced esterase, Rs PNAE: *Raufolvia serpentina* polyneuridine aldehyde esterase, HbHnl: *Hevea brasiliensis* hydroxynitrile lyase, OsPir7b: *Oryza sativa* Pir7b, LeMJE: *Lycopersicon esculentum* methyl jasmonate esterase.

1.5.3.2 Family II esterases (GDS hydrolases)

Family II esterases are of partcular interest, if only because they are not members of the α/β hydrolase fold superfamily. The structure of members of this family is discussed in section 1.3.2.2. One GDS hydrolase has already been described (section 1.5.2): *Am*GDSH1, which is involved in the metabolism of herbicide esters in blackgrass (Cummins and Edwards, 2004). Below, the other plant family II carboxylesterases that have been characterised to date are reviewed.

Lanatoside 15'-*O*-acetylesterase (LAE) is a GDS hydrolase from *Digitalis lanata* (Kandzia *et al*, 1998). Although it showed activity toward *p*-nitrophenyl acetate, it showed higher activity to the endogenous cardiac glycoside substrates lanatoside A, lanatoside C and α-acetyldigoxin (Figure 1.20).

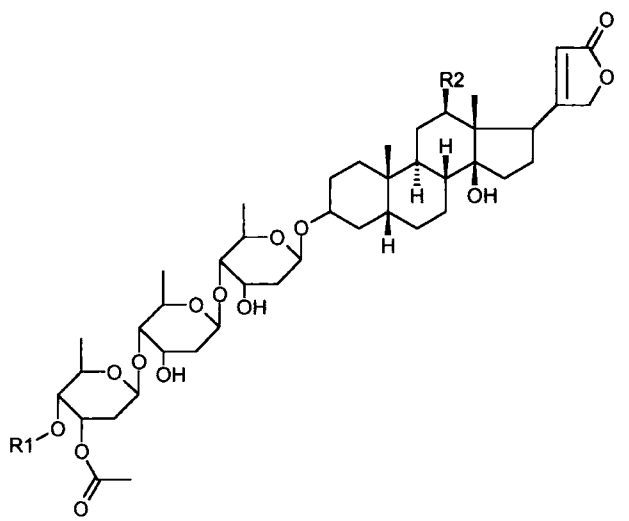

Figure 1.20: Cardenolides from *Digitalis* species (Lanatoside A: R1=glucosyl, R2=H; Lanatoside C: R1=glucosyl, R2=OH; α-acetyldigoxin: R1=H, R2=OH)

An SDS-PAGE gel of LAE revealed a subunit mass of 39kDa, but the protein appeared to function as a homodimer with an apparent mass of 80-90kDa.

Also involved in secondary metabolism is ajmaline acetylesterase AAE, which works downstream from PNAE (see above) in the biosynthesis of ajmaline in *Rauvolfia serpentina* (Ruppert *et al.* 2005). AAE could not be expressed in *E. coli*, despite many attempts using different expression conditions. However, successful expression was achieved in tobacco (*Nicotiana tabacum*): the AAE expression achieved was greater than that found in *Rauvolfia* plants.

Another GDS hydrolase was found associated with myrosinase, a defence-related enzyme from *Brassica napus* (Taipalensuu, 1996). Like *Am*GDSH1,

myrosinase-associated protein (MyAP) is a glucosylated 40kDa protein, but is not secreted into the apoplast, but is instead located with myrosinase inside myrosin grains. Expression of MyAP is induced by methyl jasmonate and wounding. It was also noted that MyAP shows homology to "proline rich, anther specific" genes from *Arabidopsis thaliana* and *Brassica napus* (Roberts *et al*, 1993), and ENOD8 from alfalfa (*Medicago sativa*). ENOD8 is an "early nodulation" protein, which was purified from alfalfa root nodules. Multiple forms of the enzyme were found, which all show activity toward acetyl and butyrl esters, but not toward substrates with longer acyl chain lengths (Pringle and Dickstein, 2004).

A plant acetylcholinesterase has been characterised from maize (*Zea mays*, Sagane *et al.* 2005). What is intriguing is that although it works on the same substrate, it shows no homology to mammalian acetylcholinesterase which is an α/β hydrolase related to mammalian carboxylesterases (see section 1.4.2). A previous piece of work (Momonoki, 1997) implicated acetylcholinesterase in the gravitropic response of maize seedlings.

In summary, family II esterases are larger enzymes than family I enzymes, with completely different structural features, except for the catalytic triad (see section 1.3.2.2). The enzymes don't seem to be linked to signalling compounds in the same way as family I esterases. Of note are the two members of this family that are involved in secondary metabolism- it is possible that the flexible nature of GDS hydrolases makes them good candidates for evolutionary recruitment to novel biochemical roles. A similar line of logic may explain why *Am*GDS1 can accommodate relatively bulky agrochemical esters.

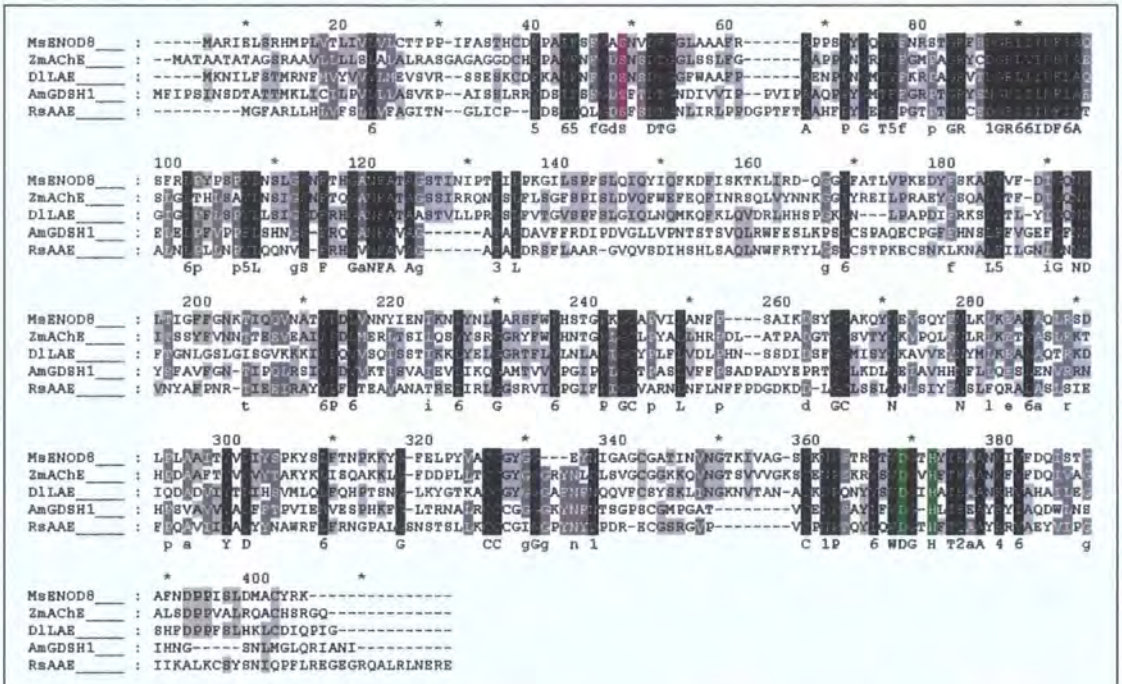

Figure 1.21: Alignment of Family II esterases. MsENOD8: *Medicago sativa* early nodulation protein, ZmAChE: *Zea mays* acetylcholinesterase, DlLAE, *Digitalis lanata* Lanatoside 15'-*O*-acetylesterase, AmGDSH1, *Alopecurus myosuroides* GDS hydrolase 1, RsAAE Rauvolfia serpentina ajmaline acetyl esterase.

Family IV plant carboxylesterases

HSR203J is the most characterised plant carboxylesterase to date. It is a serine carboxylesterase from tobacco that has a role in the hypersensitive response (HR) (Marco *et al*, 1990; Baudouin *et al*, 1997). Hybridisations with tobacco genomic DNA were carried out and revealed a gene family with at least six members (Marco *et al*, 1990). Studies of the *hsr*203j promoter with a GUS reporter gene (Pontier *et al*., 1994) showed that the expression of *hsr*203j is very rapid (3-6 hours) and localised to cells at the site of pathogen inoculation. Expression occurs upon infection of tobacco with an incompatible strain of the phytopathogen *Pseudomonas solanacearum*, but not when tobacco is infected

with a virulent form of the same species. Wounding also fails to induce significant levels of *hsr*203j expression. Maximum expression was observed nine hours after exposure to an HR-inducing pathogen (Pontier *et al.* 1994). Further studies to determine It was found that expression of *hsr*203j was correlated with hypersensitive cell death but was not elicited by auxin, cytokinin, ethylene, jasmonic acid or salicylic acid (Pontier et al 1998). Transgenic plants without functional HSR203J exhibited an accelerated HR and a corresponding greater resistance to phytopathogens. This suggests a role for HSR203J in the regulation of cell death during HSR. The enzyme itself has a mass of 38kDa and showed high activity toward *p*-nitrophenyl acetate and *p*-nitrophenyl butyrate, but little activity toward esters with larger acyl groups. It showed highest activity at pH 9, and little activity between pH 6 and 8. It also showed no amidase or protease activity, suggesting that it is a true carboxylesterase (Baudouin *et al*, 1997).

Another family IV carboxylesterase, PepEST from *Capsicum annuum*, is similar to HSR203J in that it is expressed in the plant's response to an incompatible pathogen (Kim *et al*, 2001). Like HSR203J, PepEST has activity toward *p*-nitrophenyl acetate, but much less activity toward *p*-nitrophenyl butyrate. It was found that recombinant PepEST inhibits fungal appressorium formation, although it is unclear whether this is related to its endogenous role. Application of PepEST on to the exterior of *Capsicum annuum* induced the production of hydrogen peroxide and the expression of defence-related genes within the plant.

E86 from pea (*Pisum sativum*) is expressed in response to polysaccharide elicitors of plant defence pathways (Ichinose *et al*, 2001), suggesting that it may

have a similar role to PepEST and HSR203J. E86 is a 41kDa protein, with activity toward *p*-nitrophenyl butyrate, but unlike HSR203J, it is expressed even when there is no noticable HR. Additionally, wounding induces *E86* but not *Hsr203j*, which further suggests that the two proteins do not have identical roles. It is possible that E86 is induced by chemicals such as jasmonic acid, which are produced by the plant as part to the wounding response (Hildman *et al.* 1992).

Although they have not been cloned, other HSR203J orthologues have been identified in the male cones of *Pinus radiata* (MC3; Walden *et al.* 1999), and in *Vitis vinifera* (BIG8.1; Bézier *et al* 2002). MC3 is expressed during meiosis while BIG8.1 mRNA was increased in *Vitis vinefera* that was infected with *Botrytis* cinerea. These proteins have not been biochemically characterised.

A group of 20 genes from *Arabidopsis* have been identified that show homology to *Hsr203j* (*AtCXE1-AtCXE20*; Marshall *et al*, 2003). RT-PCR analysis revealed that all 20 are expressed *in planta*, at variable levels depending on the stage of development and tissue type being examined. For example, *AtCXE11* and *AtCXE5*, were expressed in all tissues tested, while *AtCXE3* was only expressed in siliques and to a lesser extent in flowers. All *AtCXE* genes appeared to be constitutively expressed in unstressed plants, albeit in small amounts in some cases. This is in contrast to most other HSR203J-like plant esterases described, which are upregulated in response to pathogens.

Also related to HSR203J is hydroxyisoflavone dehydratase (HID), which

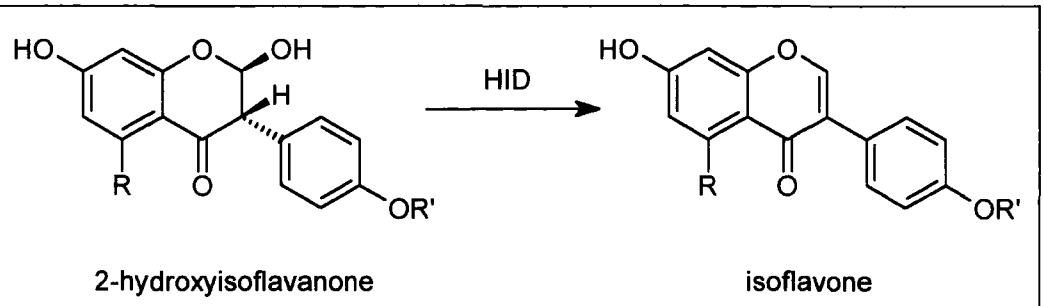

2-hydroxyisoflavanone isoflavone

Figure 1.22: 1,2 dehydration of 2-hydroxyflavanone.

performs the 1,2-elimination of water from 2-hydroxyisoflavones (Figure 1.22). Initially, a HID from *Glycyrrhiza echinata* was identified through screening of a cDNA library. A further HID was then identified from *Glycine max* through sequence homology. The *Glycyrrhiza echinata* HID was specific to 2,7-dihydroxy-4'-methoxyisoflavone while the *Glycine max* enzyme showed homology to 2,4'-dihydroxymethoxyisoflavone and 2-hydroxy-4'-methoxyisoflavone (Figure 1.23)

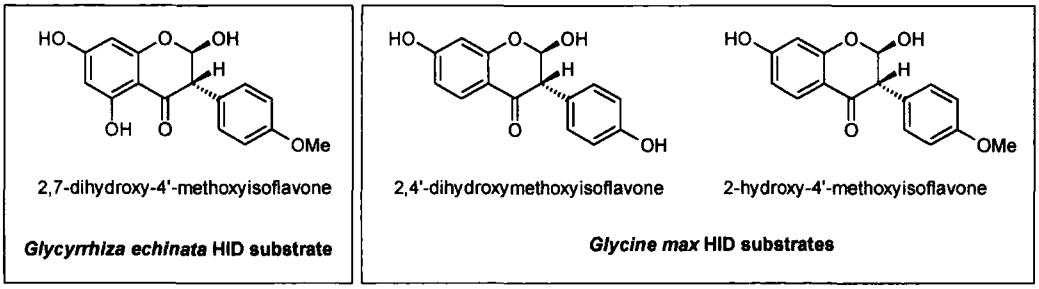

Figure 1.23: HID substrates from *Glycyrrhiza echina* and *Glycine max*.

This substrate specificity reflects the isoflavones found in the two species. A constitutive level of expression was found in cultures of *G. echinata* which was increased with yeast extract treatment, along with isoflavone synthase and hydroxyisoflavone-4'-O-methyltransferase. Interestingly, the HID enzymes have a threonine in place of a serine in the active site.

Interestingly, some CXE proteins have lost their ability to hydrolyse esters completely. A non-catalytic CXE-like protein has been identified in rice as a soluble gibberellin receptor (Ueguchi-Tanaka *et al.* 2005), . *GIBBERELLIN INSENSITIVE DWARF1* (*GID1*) encodes an esterase-like that has lost its hydrolytic capability. It is localised in the nucleus and its absence in knock-out plants resulted in stunted phenotypes typical for lines of plants with defective gibberellin signalling. It could be hypothesised that this gibberelin receptor has evolved from an esterase that was responsible for hydrolysing gibberellin ester conjugates.

There are a great number of bacterial homologues of HSR203J. Detailed below are two enzymes which have been crystallised and whose structural features have implications for the rest of the family.

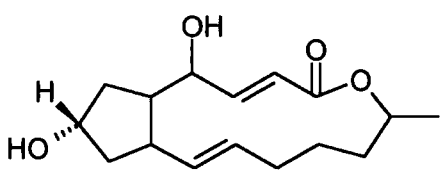

Figure 1.24: Brefeldin A

Brefeldin A (BFA, Figure 1.24) is a macrolide phytotoxin from *Alternaria carthami* which causes blight disease in safflower (*Carthamus tinctorius*). An esterase which is capable of metabolising BFA from *Bacillus subtilis* has been identified (Kneusel et al. 1994). BFAE also showed activity toward valeric acid methyl ester, but not with the macrolides erythromycin or zearalenone. The crystal structure of BFAE has been solved, confirming an α/β hydrolase-fold morphology and the presence of a closely interacting catalytic triad of ser-his-asp

(Wei et al. 1999). In addition to the general α/β hydrolase fold features, Wei et al. identified a residue in BFAE and related enzymes whose size affects the acyl length of the substrates which the enzyme of interest can hydrolyse. When the relevant position is occupied by a large amino acid residue, all activity toward esters with an acyl chain of length greater then C6 is impossible. To confirm this, Wei et al. mutated the appropriate residue in hormone sensitive lipase from alanine to phenylalanine. Although HSL's natural substrates are triacylglycerides, the A454F mutant could not cleave p-nitrophenyl esters with acyl chains of longer then six carbons. This shows that the structural difference between esterases and lipases can be as little as one amino acid residue.

EST2 is a thermostable carboxylesterase from *Alicylobacillus acidocaldarius*. It has been crystallised complexed with a Hepes sulphonyl derivative (De Simone *et al.* 2000), allowing the unambiguous identification of the oxyanion hole and the acyl-chain binding pocket.

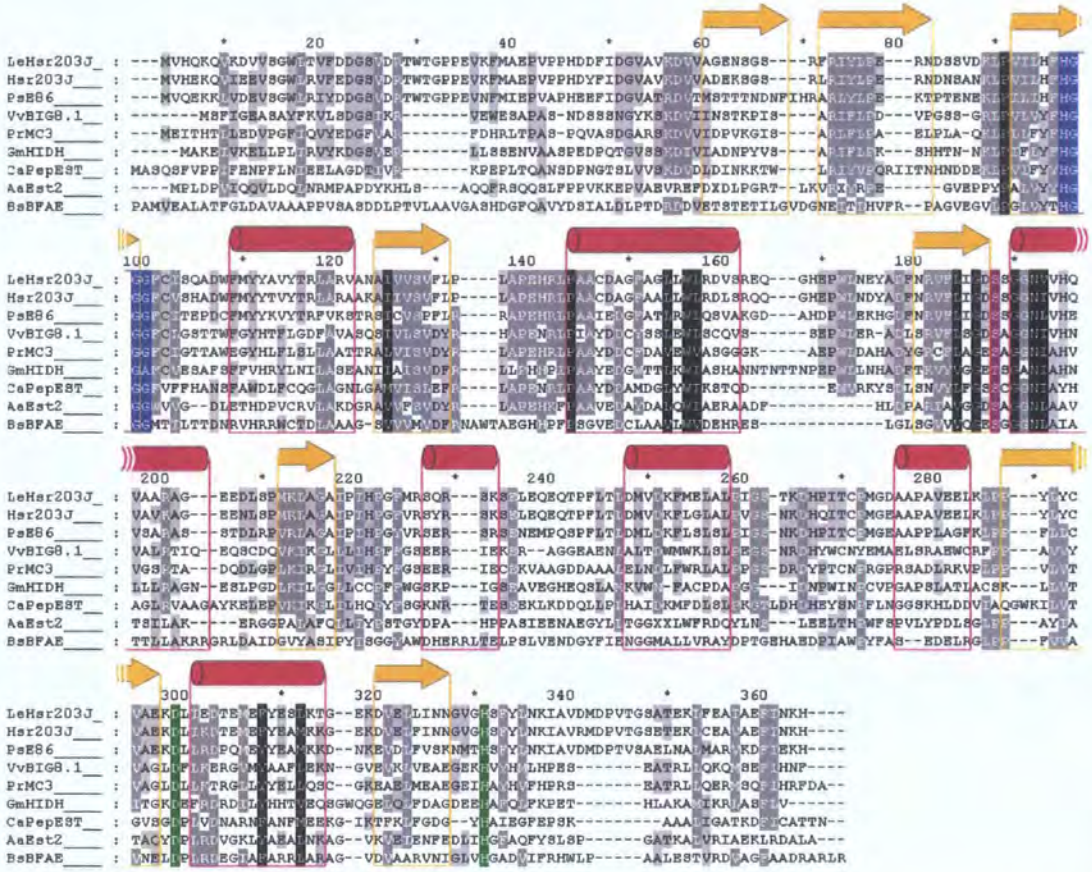

Figure 1.25: Alignment of selected family IV sequences. Secondary structure annotations are those for brefeldin A (Wei *et al.* 1999). The active site nucleophile is in purple. and the other catalytic residues are in green. The conserved region important for the formation of the oxyanion hole is in blue. LeHsr203J: Hsr203j homologue from *Lycopersicon esculentum* (tomato), PsE86: *Pisum sativum* E86, VvBIG8.1: Vitis vinifera BIG8.1, PrMC3: *Pinus radiata* MC3,

1.6 Conclusions

Plant carboxylesterases include a large number of enzymes with a surprising level of structural and functional diversity. There is an emerging picture in the literature of many enzymes involved in diverse roles *in planta*, with many linked to development, or responses to stress or pathogen attack. Other

carboxylesterases are involved in processes unique to one species, such as the biosynthetic roles of enzymes like PNAE and LAE.

It seems valid to conclude, based on the carboxylesterases characterised to date, that the catalytic triad provides a very flexible catalytic capability which evolution has exploited to fulfil many different cellular requirements. Combined with the broad substrate specificity of many of the enzymes characterised, this flexibility suggests that carboxylesterases are likely to play a significant role in xenobiotic metabolism in all plant species. However, information about plant carboxylesterases with importance in herbicide metabolism is very sparse. Studies to date have focused on small numbers of species, so the diversity of plant carboxylesterase activities is still largely unexplored. In addition, only one enzyme responsible for herbicide ester hydrolysis has been identified to date (Cummins and Edwards 2004). Thus, despite the importance of esterases in agrochemical metabolism, as enzymes that activate proherbicides and that can account for herbicide selectivity, a surprisingly small amount of information is available on their nature and activities. It is the aim of this project to characterise plant carboxylesterases to a much greater extent, so that esterase activities may be exploited in a much more systematic way in future crop protection strategies. The full aims of the project are detailed in the next section.

1.7 Aims and Objectives

The primary aims and objectives for the project were as follows:

- Due to the complex nature of the esterase part of the xenome, it would be advantageous to carry out work in a well characterised model system. *Arabidopsis thaliana* (arabidopsis) is the obvious choice due to the large amount of readily accessible genomic and transcriptional information, and the availability of large collections of T-DNA insertion lines. Therefore the first aim for the project was to establish the suitability of arabidopsis as a system to investigate plant carboxylesterases. Its hydrolytic activities were to be assessed and compared with activities found in plants of agronomic importance.
- Purification and identification of the enzyme primarily responsible for the hydrolytic activities observed in *Arabidopsis*.
- Cloning and heterologous expression of the identified carboxylesterase, to confirm it shows the activities observed during purification.
- Analysis of a T-DNA insertion line with knocked out expression of the carboxylesterase, to test its relative importance in xenobiotic metabolism *in planta*.
- Proteomic investigation of other carboxylesterases in *Arabidopsis* in order to identify other enzymes with potential importance in xenobiotic metabolism.

CHAPTER 2: MATERIALS AND METHODS

2.1 Materials

Fluorophosphonobiotin and the tri-functional probes described in Chapter 7 were custom-synthesised in house by Prof. Robert Edwards and Dr. Ian Cummins as described in Liu *et al.* 1999 and Adam *et al.* 2002 respectively. Analytical grade pesticide substrates were obtained from Greyhound Chromatography and Allied Chemicals Ltd., Birkenhead, UK and Fluka & Riedel-de Haën (part of Sigma-Aldrich, Poole, UK). Competent cells were obtained from Novagen (part of Merk, San Diego, USA). DNA primers were synthesised by MWG-Biotech, Ebersberg, Germany. Other reagents and enzymes for molecular biology were obtained from Boehringer-Mannheim (now part of Roche, Basel, Switzerland) and all other chemicals and materials were obtained from Sigma-Aldrich, except where stated otherwise. All chemicals were of analytical grade unless specified.

2.2 Methods

2.2.1 Plants

2.2.1.1 Whole Plants

One tray of moist potting compost for each species was sown with seed prepared as detailed in Table 2.1. These trays were kept in a growth room for a total growing time specified below.

Species	Seed preparation	Total growth time (days)
Abutilon theophrasti	Soak in water, 60 °C, 15 min	20
Arabidopsis thaliana	none	21
Echinochloa crus-galli	none	10
Glycine max	Soak in water, 25 °C, 60 min	13
Linum usitatissimum	none	34
Medicago sativa	none	14
Oryza sativa	germinate in dark on wet tissue, 2 days, 25 °C	21
Phalaris canariensis	none	23
Setaria faberii	none	23
Setaria viridis	none	20
Sorghum bicolor	none	20
Sorghum halepense	none	34
Zea mays	Soak in water, 25 °C, 60 min	10

Table 2.1: Preparation of seed and total time employed for growth of each of the species in this study.

Growth time depended on germination efficiency and growth rate, as plants were only harvested when they had produced sufficient material for extraction (~10 g or more). Growth room conditions were 16 hours light, 8 hours dark. In the light periods the temperature was maintained at 24 °C, which was dropped to 22 °C for the dark periods. The light intensity was 80 µmole of photons/m^2/s in the photosynthetically active range. The compost was kept moist with regular watering. At harvest, the plants were flash frozen in liquid nitrogen and then stored at -80 °C until extracted.

2.2.1.2 Arabidopsis Suspension Culture

Growth medium for arabidopsis suspension culture contained 30 g sucrose and 4.43 g Murashige and Skoog basal salts with minimum organics (MSMO), dissolved in distilled water. Then 0.5 ml 1 mg/ml NAA and 50 µl 1 mg/ml kinetin were added, and the pH adjusted to pH 5.7 using potassium hydroxide. The volume was made up to 1 l using distilled water. Conical flasks to be used for tissue culture were prepared by filling with water and autoclaving for 15 minutes at 121 °C to remove any residual detergent. Medium (80 ml) was decanted into each 250 ml flask. The flasks were stoppered with cotton wool, covered with foil, then autoclaved as above. Seven days after sub culture, a 10 ml inoculation of *A. thaliana* (Columbia) suspension culture was decanted into each flask under sterile conditions. The cultures were then incubated at 25 °C in the dark with shaking at 120 rpm. After seven days, the cultures were filtered to remove the medium and the cells flash-frozen in liquid nitrogen before being stored at -80 °C.

2.2.1.3 Arabidopsis Root Culture

Sucrose (10 g) and Gamborg B5 basal medium with minimal organics (3.2 g) was dissolved in distilled water, the pH adjusted to 5.8 with 1 M potassium hydroxide and the volume made up to 1 l. 12 flasks were prepared as described in section 2.1.2 and the medium divided between them in 80 ml lots. The flasks were then stoppered and covered with cotton wool and foil as above, and autoclaved.

A. thaliana seeds were washed using the regime detailed in Table 2. For each treatment, the samples were mixed constantly for the times indicated.

Wash solution	Time (min)
0.1 % (v/v) TX100	40
95 % (v/v) ethanol, 0.1 % (v/v) TX100	5
10 % (v/v) bleach, 0.1 % (v/v) TX100	10
5 sterile water washes	0.5

Table 2.2: Seed sterilisation regime for arabidopsis root cultures

Approximately 20 seeds were added to each flask and the resulting cultures were incubated at 25 °C in the dark for 18 days with constant shaking at 120 rpm. The medium was decanted off and the cultures were flash frozen in liquid nitrogen before being stored at -80 °C.

2.2.2 Protein Extraction

Frozen plant material was ground to a powder with a pestle and mortar under liquid nitrogen and was then extracted into 5 volumes of chilled 0.1 M Tris-HCl buffer pH 7.5, containing 1 mM DTT, 2 mM EDTA and 5 % w/v polyvinylpolypyrrolidone (PVPP). The extract was centrifuged at 10000 g for 15 minutes at 4 °C, and the supernatant was decanted and retained while the pellet was discarded. Ammonium sulphate was added to the supernatant to 40 % saturation, and the resulting suspension was recentrifuged (10000 g, 15 minutes). The pellet was discarded and ammonium sulphate was added to the supernatant to a saturation of 80 %, followed by a final centrifugation. The pellet from this final centrifugation was stored at -20 °C. Prior to use, protein was dissolved into 0.1 M potassium phosphate buffer pH 7.2, then desalted using a HiTrap™ desalting column (Amersham Biosciences). This was carried out on a Bio-Rad HRLC system, with a Bio-Rad model 1740 UV/Vis monitor used to observe when the protein eluted from the column. The concentrations of the desalted protein solutions were determined using Bio-Rad Protein Assay according to the manufacturer's instructions.

2.2.3 Esterase Assays

2.2.3.1 High-Performance Liquid Chromatography (HPLC)

Substrate (1 mM) was incubated with 50 µg protein in a total volume of 100 µl 0.1 M potassium phosphate buffer pH 7.2. The reaction was stopped using 100 µl methanol and the samples were centrifuged (16000 g, 5 minutes), to pellet precipitated protein. 150 µl of supernatant was decanted for analysis by HPLC:

System: Beckman System Gold 125P Solvent Module and 166 Detector with Gilson 234 Autoinjector

Mobile phase: A: 1 % H_3PO_4

B: HPLC grade acetonitrile

Stationary phase: 4.6 x 45 mm Beckman Ultrasphere ODS column

Flow rate: 1 ml/min

The column was equilibrated with 5 % B. Two minutes after injection of the sample (25 µl), a linear gradient increasing solvent B up to 100 % was carried out in eight minutes. The column was then washed with 100 % B for two minutes before returning to the start conditions in preparation for the next sample. Eluate from the column was analysed for UV absorbance at 264 nm. Standards were used to determine the retention time of the substrates and fully digested samples (using porcine esterase) were used to define the retention time of the hydrolysed product. Product formation was quantified by calibrating the HPLC with known amounts of product.

2.2.3.2 Fluorescence Spectroscopy

Protein extract (100 µg) was dissolved in 0.1 M potassium phosphate buffer pH 7.2 to a total volume of 198 µl at 37 °C. The protein samples were loaded into a multiwell plate, and 2 µl 100 mM 4-methylumbelliferyl acetate added (final concentration 1mM). The change in fluorescence emission at 450 nm was measured at five second intervals for a total of 30 seconds using a Labsystems Fluroskan Ascent, with excitation at 370 nm. A standard curve was established using 4-methylumbelliferone to quantify product formation.

2.2.3.3 UV spectrometry

Protein (100 μg) was dissolved in 990 μl of 0.1 M potassium phosphate buffer pH 7.2. Substrate (0.1 M in acetone) was added to a final concentration of 1 mM, and the rate of reaction at 37 °C determined through measurement of the change in absorbance at the wavelengths specified in Table 2.3.

Reaction product	Wavelength (nm)	Extinction coefficient ($M^{-1}cm^{-1}$)
p-nitrophenol	400	17000
naphthol	310	2300
fluorescein	491	57684

Table 2.3: Absorbance wavelengths and associated extinction coefficients of the colourimetric products as assayed by UV spectrometry.

2.2.4 Isoelectric Focussing

2.2.4.1 Protein Sample Preparation

Over 2 mg protein was desalted as described in section 3.2. 1 mg protein from each sample was inhibited with paraoxon: paraoxon was added to a final concentration of 1 mM, and the reactions were incubated at 25 °C for 30 minutes.

2.2.4.2 Isoelectric Focussing (IEF)

The IEF gel was made with 2.5 ml 40 % acrylamide:bis-acrylamide (mix ratio 37.5:1), 2 ml glycerol, 0.75 ml of each of three different ampholites (pH 4-6, pH 5-7 and pH 3-10, Fluka, now part of Sigma-Aldrich) and 13.25 ml deionised water. The resulting mixture was mixed then degassed under vacuum. TEMED

(20 µl) and 300 µl 10 % amonium persulphate solution was then added to initiate polymerisation.

The gel was cast between two 127x260 mm glass plates (Pharmacia), with GelBond electrophoresis film used to provide support for the gel. The gel was then run on a Pharmacia LK8 Multiphor II flat-bed rig with a Pharmacia Electrophoresis Power Supply (EPS 3500 XL) according to the manufacturer's instructions. The gel was pre-focussed for one hour at 200 V before the protein samples were loaded. In addition, 100 µg each of glucose oxidase, β-lactoglobulin, carbonic anhydrase, myoglobulin and cytochrome C were added as pI markers. After loading, the gel was run for a further hour at 200 V, before the voltage was increased to 500V for 90 minutes. Subsequently, the gel was washed with 0.1 M potassium phosphate buffer pH 7.2. The strip containing the markers was cut from the rest of the gel, fixed in TCA, then washed in water and stained with Coomassie blue stain.

2.2.4.3 Activity Staining

The main part of the gel was treated with the following solution: 100 ml 0.1 M potassium phosphate buffer pH 7.2 containing 20 mg α-naphthyl acetate and 50 mg Fast Blue RR. The gel was allowed to develop for 40 minutes at 25 °C, with gentle mixing. The reaction was stopped using excess deionised water, and the gel was then fixed with 3 % acetic acid.

2.2.5 Esterase purification

An initial attempt at esterase purification was made using ammonium sulphate precipitation followed by four chromatographic steps. This was then refined into a method that used the first three purification steps, prior to inhibition with FP-

biotin and subsequent affinity purification using streptavidin. The four chromatographic steps, FP-biotin inhibition and affinity purification methods are detailed below. Chromatography was carried out at 4 °C and protein fractions were kept on ice, or as precipitated ammonium sulphate pellets at -20 °C, between steps.

Protein was extracted from suspension cultured cells (250 g) as described in section 2.2.2. The 40-80 % ammonium sulphate saturation precipitated protein was dialysed overnight in 0.02 M potassium phosphate buffer pH 7.2, 1 mM DTT at 4 °C, using cellulose dialysis tubing with a molecular weight cut-off of approximately 10 kDa. The resulting protein solution was applied to a DEAE sepharose anion exchange column.

System:	Pharmacia GradiFrac unit in conjuction with Pharmacia LKB Pump P-1, Optical Unit UV-1, Control Unit UV-1 (set at 280 nm), and Rec 102 chart recorder.
Mobile phase:	Buffer A: 20 mM potassium phosphate buffer pH 7.2 + 1 mM DTT Buffer B: Buffer A + 500 mM NaCl
Stationary phase:	110 ml DEAE sepharose (Amersham Biosciences)
Flow rate:	5 ml/min

The column was washed prior to use with three column volumes of water, followed by three column volumes of buffer B. It was then equilibrated in buffer A before loading the protein extract (40 ml). From the start of loading, 10ml fractions were collected. After sample application, buffer A was run through the column until the UV absorbance returned to the baseline. A linear gradient to

100 % buffer B was then run over five column volumes. Finally, the column was washed with Buffer B until the UV absorbance had returned again to baseline levels.

Alternate fractions were assayed for esterase activity using *p*-nitrophenyl acetate, 2,4-D-methyl, clodinafop-propargyl and cloquintocet-mexyl as substrates. Fractions showing activity were pooled and applied onto a butyl sepharose column:

System:	As for DEAE sepharose column
Mobile phase:	Buffer A: 20 mM potassium phosphate buffer pH 7.2 + 1 mM DTT + 1 M ammonium sulphate.
	Buffer B: Buffer A minus ammonium sulphate
Stationary phase:	44 ml Butyl sepharose (Amersham Biosciences)
Flow rate:	5 ml/min

Prior to loading, ammonium sulphate was added to the protein to a concentration of 1 M. The column was equilibrated in buffer A, and after loading, washed with buffer A until the UV absorbance had returned to the baseline. 10 ml fractions were collected as with the DEAE sepharose column. A linear gradient to 100 % buffer B was then carried out over 5 column volumes. Finally, buffer B was run through the column until no more protein was eluted. Alternate fractions were assayed as before.

Subsequent purification was carried out on a Pharmacia Mono-Q HR 5/5 strong anion exchange column:

System:	Bio-Rad HRLC with Bio-Rad model 1740 UV/Vis

Mobile phase: Buffer A: 20 mM Bis-Tris-HCl pH 6.5 + 1 mM DTT

Buffer B: Buffer A + 0.5M NaCl

Stationary phase: Pharmacia Mono-Q HR 5/5

Flow rate: 0.5 ml/min

Buffer A was used for initial equilibration and to wash the column for 10 minutes after the sample had been injected. A gradient was started at 10 minutes that reached 100 % buffer B after 60 minutes. 100 % buffer B was maintained for 10 minutes before returning to 100 % buffer A. One millilitre fractions were collected and assayed for activity.

The final chromatographic step was carried out on a phenyl suparose column:

System: Bio-Rad HRLC with Bio-Rad model 1740 UV/Vis

Mobile phase: Buffer A: 0.02M potassium phosphate buffer pH 7.2 + 1mM DTT + 1M ammonium sulphate.

Buffer B: Buffer A minus ammonium sulphate

Stationary phase: Pharmacia Phenyl Suparose HR 5/5

Flow rate: 0.5 ml/min

The column was equilibrated in buffer A before loading. Buffer A was then used to wash the column until the UV absorbance returned to baseline levels. A gradient to 100 % buffer B was then run over 40 minutes. 100 % buffer B was then maintained for 20 minutes. 0.5ml fractions were collected and assayed for activity.

2.2.6 Affinity purification of FP-Biotin labelled serine hydrolases

Esterase samples in 0.1 M potassium phosphate buffer pH 7.2 were inhibited with successive additions of FP-Biotin until no activity toward *p*-nitrophenyl acetate remained. Sodium dodecyl sulphate (SDS) was then added to a concentration of 0.2 % w/v and the mixture heated to 95 °C for five minutes then cooled on ice. 20 µl of a 50 % slurry of streptavidin sepharose (Amersham Biosciences) in 20 % ethanol was added, and the mixture was then mixed end-over-end for one hour. The streptavidin sepharose was then washed with two washes of 0.2 % SDS w/v in distilled water, and then two further washes with just distilled water. After the last wash was removed, SDS-PAGE loading buffer was added to the beads and the resulting samples were mixed and then heated to 95 °C. The sepharose was centrifuged for 2 minutes at 500 g and the supernatant was run on a 12.5 % acrylamide gel, using a Bio-Rad Mini Protean II kit. After running, the gels were washed twice in distilled water for ten minutes, then stained overnight in colloidal coomassie-blue solution. Excess stain was washed out of the gel with a 3 hour wash in distilled water.

2.2.7 Identification of Purified Proteins with MALDI-TOF Mass Spectrometry

Bands of protein were submitted for MALDI-TOF-based proteomic identification (Applied Biosystems, Warrington, UK), which was carried out by a proteomics service as described in Chivasa et al. (2002). The resulting peptide mass ions were used to screen a non-redundant protein database using Mascot (http://www.matrixscience.com/).

2.2.8 Gene cloning and expression

The PCR primers referred to in the following section are:

AtCXE12F: TCAACTAACCATGGATTCCGAGATCGCCG

AtCXE12R: CGCCTCGAGGTTCCCTCCCTTAATAAACCC

These were designed to amplify AtCXE12 whilst mutating the stop codon and providing *Nco*I and *Xho*I restriction sites at the 5' and 3' ends of the coding sequence, allowing the amplified product to be inserted into pET24d.

2.2.8.1 mRNA extraction and reverse transcription

Arabidopsis thaliana suspension culture (100 mg) was ground in liquid nitrogen and extracted with 1 ml tri-reagent. The extract was spun at 12000 g for 15 minutes at 4 °C. The upper phase was retained and 0.5 ml isopropanol added. After five minutes incubation at room temperature, the mixture was spun again at 12000 g. The pellet was washed with 75 % (v/v) ethanol, then dried and dissolved in 25 µl sterile water, with 5 µl of the resulting RNA (1.74 mg/ml) incubated with 7 µl AtCXE12R (10 µM) for 10 minutes at 60 °C. The reaction was then transferred to ice for five minutes. 4 µl 5× incubation buffer (250 mM Tris-HCl, 200 mM KCl, 30 mM $MgCl_2$, 50mM dithiothreitol pH 8.3), 1 µl RNase block, 2 µl dNTPs (mixture of dATP, dTTP, dGTP and dCTP each at 10 mM) and 1 µl M-MuLV reverse transcriptase was then added, and the reaction incubated at 37°C for 90 minutes. The cDNA produced was kept at -20°C.

2.2.8.2 Polymerase chain reaction

The reaction mix listed below was made up in 0.5 ml PCR tubes.

4.5 µl 11× buffer (449 mM tris-HCl pH 8.8, 112 mM $(NH_4)_2SO_4$, 23 mM $MgCl_2$, 3 µM mercaptoethanol, 44 µM EDTA, each of dATP, dCTP, dGTP and dTTP at 2 mM, 1.1 mg/ml BSA)

5 µl 10 mM forward primer (AtCXE12F)

5 µl 10 mM reverse primer (AtCXE12R)

2 µl template (cDNA or genomic DNA)

1 µl Taq polymerase (concentration empirically determined)

The mixture was then subjected to the program detailed in Table 2.4 in an Eppendorf Mastercycler Gradient PCR machine

Step	Temperature (°C)	Duration (min:sec)
1	94	2:00
Repeat steps two to four inclusive 30 times		
2	94	0:30
3	55	0:45
4	72	1:20
After repeats, proceed to step five		
5	72	10:00
END		

Table 2.4: Temperature program used for PCRs

PCR products were analysed on a 0.8 % agarose gel, and if required, purified from the gel using a Promega Wizard® SV Gel and PCR Clean-Up kit (Promega UK, Southampton, UK).

2.2.8.3 Ligation

1 µl 10× ligation buffer (as supplied with enzyme) and 1µl T4 ligase (Promega) were incubated with equal volumes of the DNA fragments to be ligated (total reaction volume 10 µl) at 15 °C overnight.

2.2.8.4 Transformation

Competent *Escherichia coli* (Tuner (DE3) pLysS pRARE) were transformed following the manufacturer's instructions. In brief, 20 µl competent cells were incubated on ice with 1 µl plasmid for 5 minutes. The cells were then heat-shocked at 42 °C for exactly 30 seconds before being returned to ice for a further minute. 80 µl LB medium (10 g/l NaCl, 10 g/l bacteriological peptone, 5 g/l yeast extract) was added and the cells were then incubated at 37 °C for one hour. The cells were then plated on to LB agar (as for LB, with 15 g/l agar) with appropriate antibiotic selection.

2.2.8.5 Minipreps

10 ml cultures of transformed bacteria were grown and the cells were pelleted. Plasmids were purified from the cells using a Promega Wizard® Plus Minipreps DNA Purification System.

2.2.8.6 Restriction

Restrictions were carried out at 37 °C overnight in NE buffer 4 (New England Biolabs, Ipswich, UK). The restriction endonucleases that were used are detailed in Chapter 5.

2.2.8.7 Expression conditions and recombinant His_6-AtCXE12 purification

A single transformed *Escherichia coli* (*E. coli*) colony was used to inoculate a 10 ml LB starter culture, containing 100 μg/ml kanamycin and 35 μg/ml chloramphenicol. The culture was incubated overnight at 37 °C with shaking at 200 rpm. A 500 ml culture was then inoculated with 5 ml of the starter culture, and the cells grown under the same conditions until they achieved an optical density at 600 nm of approximately 0.6. The cells were then induced with 1 mM IPTG (isopropyl β-D-1-thiogalactopyranoside) and incubated for a further three hours. The bacteria were then centrifuged at 5000 g for five minutes. The pelleted bacteria were resuspended in 10 ml 0.1 M Tris-HCl pH 7.8 with 20 mM imidazole (buffer A) and sonicated three times for 20 seconds with 10 seconds between each burst. After the bacterial lysate had been centrifuged (4200 g, 15 minutes), it was loaded on to a HisTrap HP column (Amersham Biosciences). After washing with buffer A, retained protein was eluted by raising the imidizole

concentration to 300 mM. Further purification was carried out on a phenyl superose column as follows:

System:	Amersham Biosciences Acta FPLC with UV-900 ultraviolet detector and P-900 pump module
Mobile phase:	Buffer A: 0.1 M potassium phosphate pH 7.2, 1 M ammonium sulphate, 1 mM DTT
	Buffer B: 0.1 M potassium phosphate pH 7.2, 1 mM DTT
Stationary phase:	Pharmacia phenyl superose HR 5/5
Flow rate:	0.5 ml/min

The column was equilibrated in buffer A, and the protein (in buffer A) was loaded. After washing for 10 minutes, a gradient to 100 % buffer B was carried out over 20 minutes with the column then washed in buffer B for 40 minutes.

The method was subsequently adapted so that 0.02M MES buffer pH 5.7 was used to elute bound recombinant enzyme from the nickel chelate column in place of high imidazole concentrations. With the revised method, 2 ml fractions were collected directly into 0.5 ml 1 M potassium phosphate buffer with 5 mM DTT.

2.2.9 SAIL T-DNA insert characterisation

T-DNA Express (http://signal.salk.edu/cgi-bin/tdnaexpress)was used to identify T-DNA insertions which would be expected to disrupt AtCXE12 expression. The SAIL T-DNA insertion line (Sessions *et al.* 2002) SAIL_445_GO3 was identified and obtained from the Nottingham Arabidopsis Stock Centre (NASC: Nottingham, UK). Homozygous lines were selected using the protocol described on the SIGnAL website (http://signal.salk.edu/tdnaprimers.2.html), with the following primers:

Left product (LP): GACCAAGATCCACTAAAATTCATC

Right product (RP): GATGTTTGCTCCTGCACTGTC

SAIL left border (LB): TTCATAACCAATCTCGATACAC

Single leaves from each of the plants tested were ground in 100 µl nuclease free water. The resulting extraction was spun at 16000 g for 5 minutes and, 2 µl of the supernatant was used as a template for PCR as described below.

Reaction mix:

4.5 µl 11× buffer (449 mM tris-HCl pH 8.8, 112 mM $(NH_4)_2SO_4$, 23 mM $MgCl_2$, 3 µM mercaptoethanol, 44 µM EDTA, each of dATP, dCTP, dGTP and dTTP at 2 mM, 1.1mg/ml BSA)

5 µl of each of LP, RP and LB (all at 10mM)

2 µl template

1 µl Taq polymerase

The mixture was then subjected to the program detailed in Table 2.5 in an Eppendorf Mastercycler Gradient PCR machine.

Step	Temperature (°C)	Duration (min:sec)
1	94	2:00
Repeat steps two to four inclusive 35 times		
2	94	0:15
3	55	0:20
4	72	0:45
After repeats, proceed to step five		
5	72	5:00
END		

Table 2.5: Temperature program used for SAIL analysis PCRs.

2.2.10 Toxicity study

Four week old plants (*Arabidopsis thaliana* Columbia ecotype (WT) and SAIL_445_GO3 (*atcxe12*)) were sprayed with 360ml/m^2 of 0, 2, 5 and 10 mg/L 2,4-D methyl in 0.1 % (v/v) Tween 20. The plants were left in normal growing conditions (16 hours light, 8 hours dark, 25 °C and 22 °C respectively) for 96 hours to allow symptoms to develop.

2.2.11 Profiling serine hydrolases in *Arabidopsis* trifunctional fluorophosphonate probe (TriFFP)

2.2.11.1 Labelling and affinity purification of serine hydrolases

Frozen plant material, pulverised in a chilled mortar and pestle was extracted with 0.1M potassium phosphate buffer pH 7.2 with 1mM DTT and 5 % (w/v) cross-linked polyvinylpolypyrrolidone at 4 °C. The mixture was centrifuged at 15000 g for 15 minutes, then TriFFP added to the supernatant to a final concentration of 5 µM. The resulting solution was incubated at room temperature for one hour. The solution was then passed through a PD-10 desalting column (Amersham Biosciences) to remove excess probe. Subsequently, SDS was added to a final concentration of 0.2 % (w/v) and the resulting solution heated to 95 °C for 5 minutes. After cooling, 20 µl of a 50 % streptavidin sepharose bead slurry was added and the mixture was incubated for one hour at 4 °C with end-over-end mixing. The beads were then washed twice with 0.2 % (w/v) SDS, then twice with distilled water, and the bound proteins were eluted by heating the beads to 95 °C for five minutes in SDS loading buffer. Eluted bands were then run on an SDS-PAGE gel as described in section 2.2.6.

2.2.11.2 Visualisation, quantification and identification of purified serine hydrolases

The fluorescently labelled proteins in the gel were visualised using a Fujifilm FLA-3000, exciting at 532 nm and reading the emission at 580 nm. Quantification of fluorescence was carried out using Aida Image Analyser version 3.11.002. Bands were excised and submitted for MALDI-TOF analysis as described in section 2.2.7.

2.2.12 Bioinformatics

2.2.12.1 Determination of carboxylesterase gene families

Position specific iterative BLAST (PSI-BLAST, http://www.ncbi.nlm.nih.gov/BLAST/) was run through four iterations with an inclusion threshold of 10^{-10}, and the results were examined to identify all complete, non-redundant *Arabidopsis* sequences. Where needed, the TAIR accession was determined using the BLAST feature on the Salk Institute Genomic Analysis Laboratory (SIGnAL) website (http://signal.salk.edu/cgi-bin/tdnaexpress).

2.2.12.2 Tree production

Once the members of a given family had been identified, alignments were performed by first using DNA for Windows version 2.5a to create sequence files ([filename].seq) which were then aligned using ClustalW, version 1.83. Trees were produced from the alignments using the Phylip program package: protdist.exe was used with default settings, followed by neighbor.exe where UPGMA tree production was selected. Drawtree.exe was used to create the tree image. Where bootstrapping was applied, bootstrap replicates were created using

seqboot.exe prior to using protdist.exe. Consense.exe was used to create the consensus tree which was examined in Treeview (version 1.6.6).

2.2.12.3 Gene characterisation

Information about numbers of introns and ESTs/cDNAs was obtained from the SIGnAL website. Subcellular targeting predictions were performed using TargetP on the Centre for Biological Sequence Analysis (CBS) website (http://www.cbs.dtu.dk/services/). Secondary structure predictions were performed using SSpro and SSpro8 from the SCRATCH suite of analysis tools (http://www.igb.uci.edu/tools/scratch/). Where three dimensional structures are shown, the image was produced using PyMol. Other websites used are detailed with the relevant results.

CHAPTER 3: XENOBIOTIC HYDROLYSING CARBOXYLSTERASES IN CROPS AND WEEDS

3.1 Introduction

As discussed in section 1.5.1, little work has been published which describes the levels of esterase activity in a range of plants toward diverse crop protection agents, despite the potential for esterases to provide a basis for herbicide selectivity. Hoagland and Graf (1972) described a study in which 19 different plants representing 12 different families were assayed for hydrolytic activities toward herbicides containing amide bonds, notably the arylacylamide propanil. Of the plants tested, 14 showed activity toward propanil, but only one (wild cucumber (*Echinocystis lobata* L.)) showed activity toward the other herbicides tested (fenuron and propham). There is no such review of plant activities toward carboxylic ester-containing agrochemicals, despite the fact that many herbicides are applied as esters or have an ester bond as part of their active structure.

This chapter describes the analysis of hydrolytic activities toward xenobiotic carboxylic esters in 13 crop and weed species, representing five different plant families.

3.1.1 Plants Investigated in this Study

Background information on the plants used in this investigation is given below. Taxonomic and UK distribution information was obtained from The Flora of Northwest Europe (http://nlbif.eti.uva.nl/bis/flora.php). Information about the chemical control of weed species was obtained from the Pacific Northwest Weed Management Handbook (http://weeds.ippc.orst.edu/pnw/weeds). General

information was derived from the Encyclopaedia Brittanica except where stated otherwise.

3.1.1.1 Crops

***Glycine max* (L.) Merr.** (soybean)

Soybean is a leguminous crop of major economic importance, being a dominant source for both edible vegetable oil and high protein animal feed. Additionally, soy products such as soya milk and tofu are an important source of protein for millions of people. Industrially, oil from soybeans is used for a range of products including paints and insecticidal sprays. Soybean plants are grown in many countries, particularly in Asia and the United States of America.

***Linum usitatissimum* L.** (flax)

Flax was historically grown for its fibre, which can be made into linen. The expansion of the cotton industry has limited the amount of flax that is now grown to produce linen, but shorter cultivars are farmed for their seeds and the oil that is obtained from them.

***Medicago sativa* L.** (lucerne, alfalfa)

Lucerne is a leguminous crop known for it's tolerance to heat, cold and drought stress and its ability to produce large amounts of foliage which makes very good animal feed.

***Oryza sativa* L.** japonica cultivar-group (rice)

Approximately 50 % of the world's population is dependant on rice as a staple food. Rice is usually grown submerged under 5-10 cm of water, which has a result of suppressing weed growth. However, when constant irrigation is not possible weeds such as *Echinochloa* and *Setaria* species can establish

themselves, reducing rice yields. Such competing weeds can be successfully controlled with the herbicides propanil, butachlor, fluchloralin or nitrophen (Agribusiness Information Centre http://www.ficciagroindia.com/production-guidelines/field-crop/rice/weed-control.htm).

***Phalaris canariensis* L.** (canarygrass)

Canarygrass is grown primarily for the production of birdfeed particularily in Japan and other East Asian countries (Alternative Field Crops Manual, http://www.hort.purdue.edu/newcrop/afcm/cangrass.html). However, in cereal growing areas of Asia this species has the potential to be a problem weed.

***Sorghum bicolor* L.** (millet, sorghum)

Sorghum is grown predominantly in semi-arid tropical areas for food and animal fodder, although different cultivars are adapted to a wide range of growing conditions. The classification *Sorghum bicolor* includes all cultivated sorghums, as well as naturalised semi-wild strains which are regarded as weeds.

***Zea mays* L.** (maize, corn)

Maize is grown in abundance around the world: in terms of acreage it is the second most cultivated crop after wheat. The crop is grown mainly for its edible seeds although the non-edible parts are used in paper manufacture and other industry. Problem weeds include perennial grasses like quackgrass (*Elytrigia repens*) and johnsongrass, which can seriously affect crop yields.

3.1.1.2 Weeds

***Abutilon theophrasti* Medik.** (velvetleaf, china jute)

Native to southern Asia, *Abutilon theophrasti* is a dicotyledonous plant that reaches one to 2.5 metres tall and is cultivated in China for its fibre. It is a naturalised and widespread plant in North America where it is a significant weed (Washington State Noxious Weed Control Board: http://www.nwcb.wa.gov/) particularily in soybean (*Glycine max* (L.) Merr.), corn (*Zea mays* L.) and cotton (*Gossypium* spp.) crops. In the UK it is not naturalised, but is a regular contaminant of imported wool and oilseed. A wide range of herbicides has been reported to control *A. theophrasti*, including esters of 2,4-D and bromoxynil, which are included in this study.

***Arabidopsis thaliana* (L.) Heynh.** (arabidopsis)

Arabidopsis is a small Brassica weed that is found throughout the world. It has been included in this study because of its scientific importance as a model species.

***Echinchloa crus-galli* (L.) P. Beauv.** (barnyardgrass, barn Grass, barnyard millet)

Echinchloa crus-galli is an introduced, naturalised annual grass weed widespread across North America. Aryloxyphenoxypropionate (AOPP) herbicides such as clodinafop and fenoxaprop have been shown to be effective against it when it infests cereal crops such as barley and spring and winter wheat.

***Setaria faberi* Herrm.** (Giant Foxtail) and ***Setaria viridis* (L.) P. Beauv.** (Green foxtail)

Green foxtail is a naturalised weed in europe and can be a problem in wheat crops. AOPP herbicides are primarily used in its control. Both Giant and Green foxtails are naturalised weeds in the United States where they are major weeds in maize.

***Sorghum halepense* L. Pers.** (Johnsongrass)

Johnsongrass is a problem weed particularly in the United States. As with the other grass weeds, AOPP herbicides may be used in its control.

As illustrated in Figure 3.1, the plants selected in this study allow the comparison of species with many different degrees of relatedness: comparisons of esterase activity can be made between plants divergent at the subclass level at one extreme, to plants which share the same genus at the other. Information on whether similarities in esterase activity correlate with taxonomic classification is of interest because any such correlation would raise the possibility of predicting esterase activity to a given ester chemistry in a given species. In the case of agronomically important crops and weeds this could be very useful in developing new selective herbicides that are either activated or detoxified by esterases.

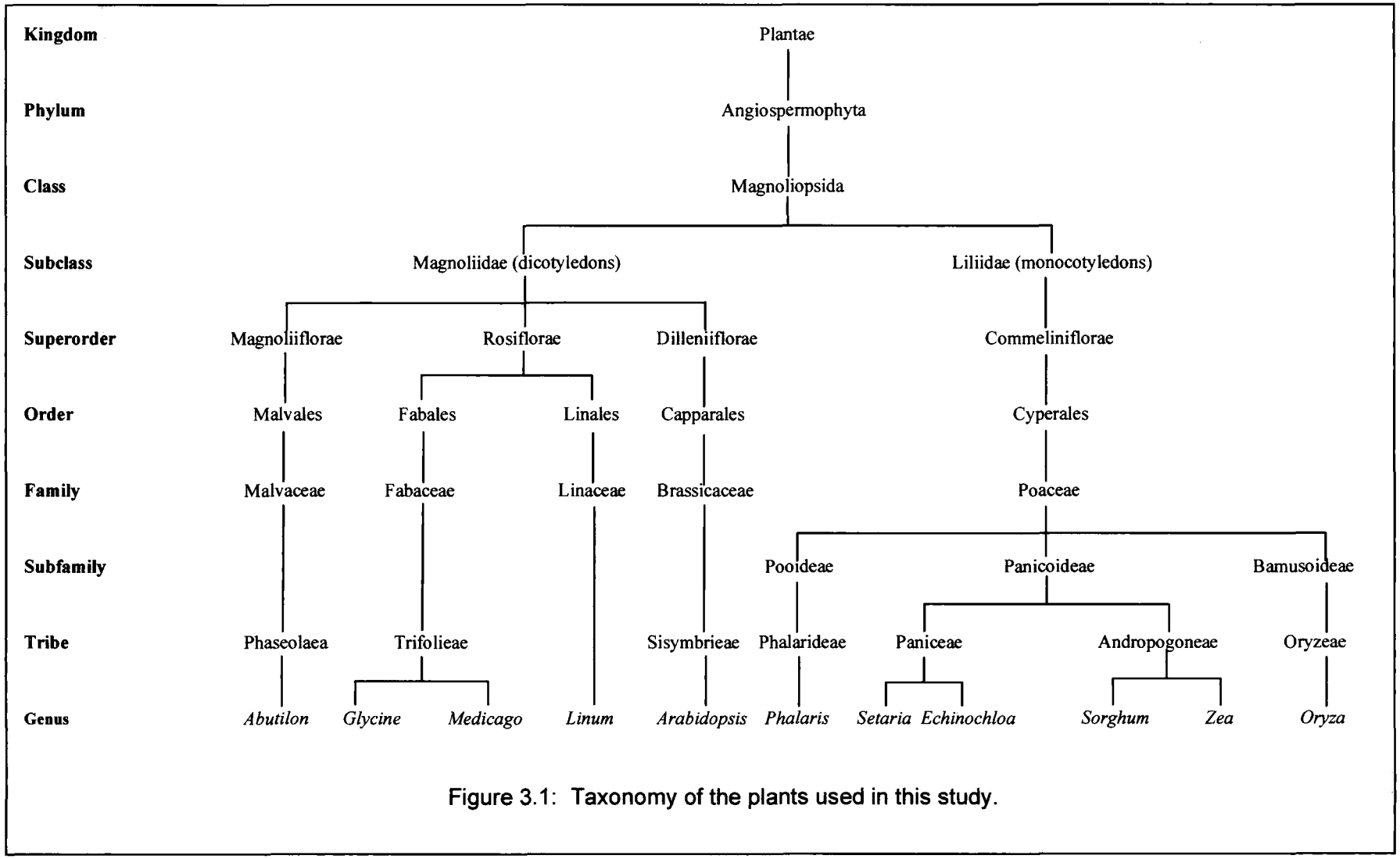

Figure 3.1: Taxonomy of the plants used in this study.

3.2 Results

3.2.1 Assay development

Protein extracts from arabidopsis cell suspension cultures were used to optimise conditions for the esterase assays. Protein dependency of esterase activity was confirmed, with a linear relationship between concentration of Arabidopsis cell culture protein and rate of *p*-nitrophenyl acetate hydrolysis observed, up to a protein concentration of 400 μg/ml (data not shown). Heat treatment (95 °C, 5 min) was found to abolish ester hydrolysis except for the low chemical rate. For all carboxylesterase assay results described, the chemical rate of hydrolysis has been subtracted. In all cases, under the conditions reported, the hydrolysis of each substrate was found to be linear with respect to time for the duration of the assays (30 seconds for colorimetric and fluorimetric substrates and 30 minutes for agrochemical esters).

3.2.2 Esterase activities toward agrochemical substrates

Hydrolytic activities of the selected crops and weeds toward the pesticide esters shown in Figure 3.2 were determined using HPLC with UV detection to monitor product formation.

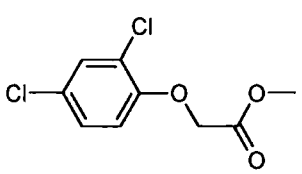

2,4-D methyl

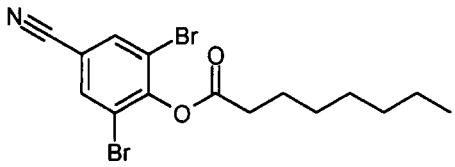

bromoxynil octanoate

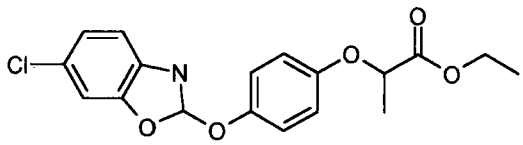

fenoxaprop ethyl

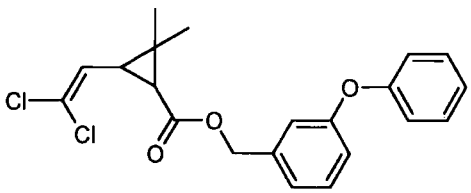

permethrin

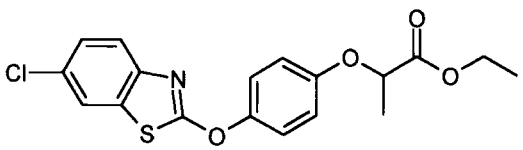

fenthioprop ethyl

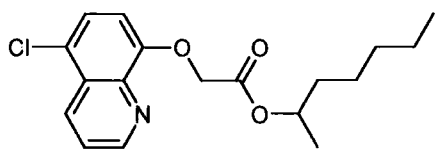

cloquintocet mexyl

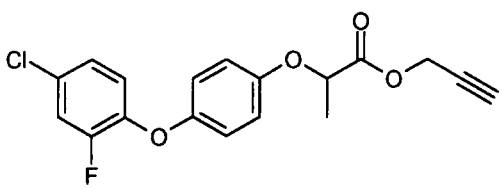

clodinafop propargyl

Figure 3.2: The structures of the seven agrochemical ester substrates investigated in this study. All compunds are herbicides except for permethrin (insecticide) and cloquintocet mexyl (safener).

		Species	Rate of carboxylic ester hydrolysis (pkat/mg)						
			2,4-D-methyl	clodinafop-propargyl	fenthioprop-ethyl	fenoxaprop-ethyl	bromoxynil-octanoate	permethrin	cloquintocet-mexyl
Dicots	Crops	*Glycine max* (Soybean)	**118.7** ± 4.3	**63.91** ± 7.20	-	**3.50** ± 0.42	**2.69** ± 0.76	**0.3** ± 0.0	**2.72** ± 0.14
		Linum usitatissimum (Flax)	**187.1** ± 26.4	**18.13** ± 0.28	**7.07** ± 1.25	**5.82** ± 1.15	**3.84** ± 0.02	**3.7** ± 0.5	**7.02** ± 0.80
		Medicago sativa (Lucerne)	**162.4** ± 32.7	**119.0** ± 13.1	**18.01** ± 5.62	**15.80** ± 8.14	**4.80** ± 0.81	**1.5** ± 0.2	**4.28** ± 0.62
	Weeds	*Abutilon theophrasti* (velvetleaf)	**127.8** ± 2.9	**20.35** ± 0.65	**7.03** ± 0.16	**6.09** ± 0.22	**5.29** ± 0.06	**6.3** ± 0.4	**0.97** ± 0.33
		Arabidopsis thaliana	**365.2** ± 54.8	**44.99** ± 0.00	**22.47** ± 0.23	**11.25** ± 0.24	**2.09** ± 0.31	-	**4.82** ± 1.29
Monocots	Crops	*Oryza sativa* (Rice)	**103.3** ± 1.4	**8.77** ± 1.06	**2.47** ± 0.32	-	**7.46** ± 0.10	**0.8** ± 0.2	**3.40** ± 0.22
		Zea mays (Maize)	**403.2** ± 15.9	**18.13** ± 0.28	**7.77** ± 1.43	**7.44** ± 0.11	**23.46** ± 1.25	**7.1** ± 0.2	**9.63** ± 1.72
	Weeds	*Echinochloa crus-galli* (Barnyardgrass)	**54.0** ± 3.7	**4.71** ± 0.51	-	**4.31** ± 0.00	**0.92** ± 0.10	-	-
		Phalaris canariensis (Canarygrass)	**65.8** ± 6.3	**10.06** ± 0.51	**5.86** ± 0.85	**5.27** ± 0.16	**1.78** ± 0.11	-	**2.60** ± 0.58
		Setaria faberi (Giant Foxtail)	**82.2** ± 0.5	**19.56** ± 1.15	**1.83** ± 0.90	**4.23** ± 0.08	**9.95** ± 0.58	**2.9** ± 0.4	**4.30** ± 0.10
		Setaria viridis (Green Foxtail)	**149.5** ± 11.1	**20.30** ± 0.05	**7.32** ± 0.56	**7.42** ± 0.08	**8.80** ± 0.24	**2.7** ± 0.2	**5.07** ± 0.22
		Sorghum bicolor (Sorghum)	**236.9** ± 9.1	**25.79** ± 0.55	**8.57** ± 0.69	**9.09** ± 0.16	**7.04** ± 1.91	**2.3** ± 0.2	**5.06** ± 0.03
		Sorghum halepense (Johnsongrass)	**189.5** ± 32.2	**18.27** ± 0.78	**4.55** ± 1.03	**5.90** ± 0.69	**4.11** ± 0.19	**2.5** ± 0.2	**6.49** ± 0.08

Table 3.1: CXE activities toward seven different agrochemical esters. Values are in pkat/mg protein, and are the means of biological duplicates ± the range.

2,4-D-methyl

All plants were most active toward 2,4-D-methyl. Extracts from arabidopsis and maize extracts were most active, whilst *Echinochloa crus-galli* and *Phalaris canariensis* protein showed significantly lower rates of 2,4-D-methyl hydrolysis.

Aryloxyphenoxypropionate (AOPP) Esters

Extracts from all species showed activity toward clodinafop-propargyl, although these were considerably lower then those shown toward 2,4-D methyl. As with 2,4-D methyl, clodinafop-propargyl was hydrolysed particularly quickly by the preparations from arabidopsis, lucerne and soybean. Interestingly, fenoxaprop-ethyl and fenthioprop-ethyl were hydrolysed at a much lower rate than clodinafop-propargyl by all the plant extracts tested. Most species showed similar activities toward both fenoxaprop-ethyl and fenthioprop-ethyl: presumably due to their structural similarity. The differences observed between the rates of hydrolysis of clodinafop-propargyl when compared to the other two AOPP esters shows that small changes in structure can significantly alter rates of xenobiotic ester hydrolysis. Therefore, predictions of activity towards a given ester based on activities toward similar substrates may be misleading, unless the compounds are very closely related, as in the case of fenthioprop-ethyl and fenoxaprop-ethyl.

Bromoxynil-octanoate

Bromoxynil-octanoate showed similar overall levels of activity to fenoxaprop-ethyl and fenthioprop-ethyl, although the pattern of activities from the different species was different. Most markedly, maize exhibited a significantly higher rate of bromoxynil octanoate hydrolysis than all the other plants.

Other pesticide esters

Most species showed minor activities toward the safener cloquintocet-mexyl. Still lower activities were displayed toward permethrin, with arabidopsis, *Echinochloa crus-galli* and *Phalaris canariensis* showing no detectable hydrolysis. These *in vitro* results are in line with *in vivo* studies which showed very slow rates of hydrolysis of permethrin when applied to whole plants (Lee *et al.* 1988).

3.2.3 Esterase activities toward model ester substrates

Assays were carried out to determine esterase activities toward the substrates in Figure 3.3 using assays based on UV or fluorescence spectroscopy to monitor product formation. Results are shown in Table 3.2.

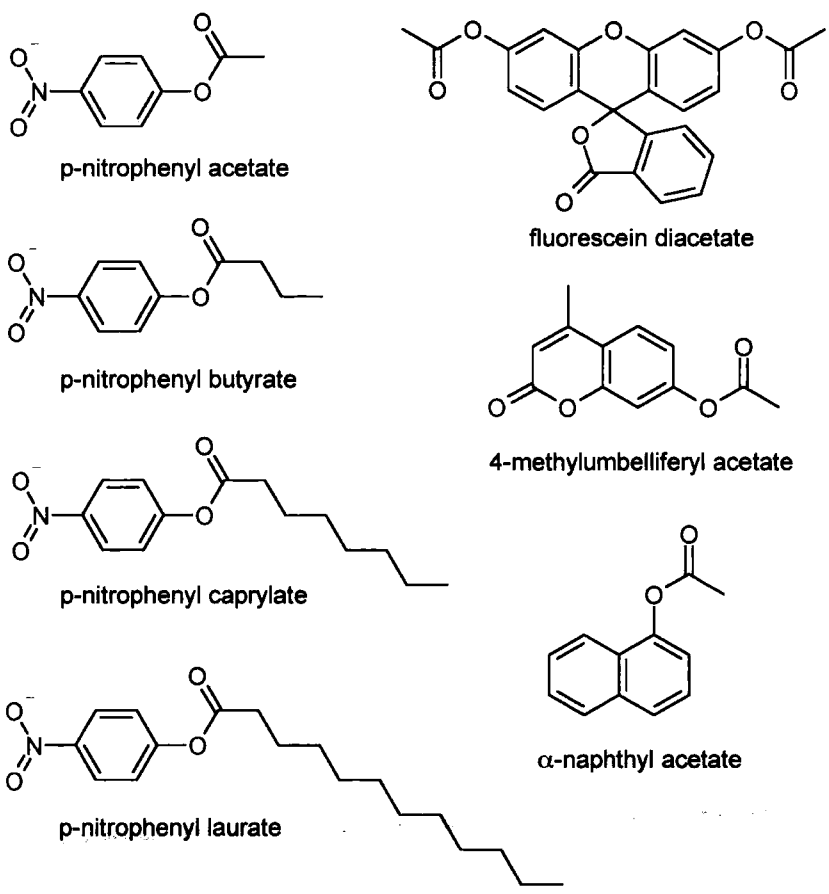

Figure 3.3: Colourimetric and fluorescent esterase substrates

		Species	Rate of carboxylic ester hydrolysis (pkat/mg)						
			α-naphthyl acetate	methylumbelliferyl acetate	fluorescein diacetate	*p*-nitrophenyl acetate	*p*-nitrophenyl butyrate	*p*-nitrophenyl caprylate	*p*-nitrophenyl laurate
Dicots	Crops	*Glycine max* (Soybean)	**6376** ± 36	**2574** ± 252	**48** ± 7	**510** ± 20	**426** ± 34	**382** ± 10	**29** ± 0
		Linum usitatissimum (Flax)	**2246** ± 145	**3636** ± 8	**33** ± 1	**559** ± 59	**260** ± 44	**172** ± 25	**34** ± 15
		Medicago sativa (Lucerne)	**6159** ± 580	**2843** ± 147	**35** ± 6	**578** ± 29	**387** ± 64	**470** ± 39	ND
	Weeds	*Abutilon theophrasti* (Velvetleaf)	**1159** ± 145	**2133** ± 760	**29** ± 6	**480** ± 69	**25** ± 25	**113** ± 5	**74** ± 44
		Arabidopsis thaliana	**2246** ± 507	**3728** ± 256	**29** ± 3	**990** ± 127	**490** ± 10	**294** ± 10	**10** ± 10
Monocots	Crops	*Oryza sativa* (Rice)	**942** ± 290	**1969** ± 63	**73** ± 13	**382** ± 20	**59** ± 10	**15** ± 15	ND
		Zea mays (Maize)	**2464** ± 217	**3998** ± 4	**30** ± 4	**789** ± 5	**691** ± 25	**779** ± 5	**49** ± 10
	Weeds	*Echinochloa crus-galli* (Barnyardgrass)	**616** ± 36	**937** ± 27	**23** ± 3	**289** ± 5	ND	ND	ND
		Phalaris canariensis (Canarygrass)	**6485** ± 109	**2401** ± 113	**39** ± 1	**343** ± 39	ND	ND	ND
		Setaria faberi (Giant Foxtail)	**760** ± 254	**2595** ± 38	**30** ± 7	**505** ± 54	**142** ± 5	**83** ± 44	ND
		Setaria viridis (Green Foxtail)	**2355** ± 181	**6848** ± 42	**32** ± 6	**873** ± 49	**113** ± 5	**98** ± 59	ND
		Sorghum bicolor (Sorghum)	**1739** ± 217	**2172** ± 192	**30** ± 7	**721** ± 44	**142** ± 5	**83** ± 44	**20** ± 30
		Sorghum halepense (Johnsongrass)	**3913** ± 72	**3531** ± 222	**46** ± 3	**1127** ± 10	**824** ± 49	**461** ± 0	ND

Table 3.2: CXE activities towards colourimetric and fluorescent substrates. Values are in pkat/mg protein, and are the means of biological duplicates ± the range.

In general, hydrolytic activities toward model substrates were significantly higher then those determined with the pesiticide esters. All species showed very large activities towards 4-methylumbelliferyl acetate and α-naphthyl acetate. In general, activities toward the *p*-nitrophenyl ester series decreased with increasing chain length. For example, none of the species in this investigation showed significant activity towards *p*-nitrophenyl laurate (C12). *Zea mays*, however, showed no decrease in activity up to and including *p*-nitrophenyl caprylate (C8), which shows that this species has esterases capable of cleaving esters with quite long aliphatic ester moieties. This conclusion is supported by the activity *Zea mays* showed towards bromoxynil octanoate, which was significantly higher than that of any of the other species (see Table 3.1). Most of the dicotyledonous species maintained some activity towards the substrates up to and including *p*-nitrophenyl caprylate. In contrast, the monocotyledonous species, with the exception of *Zea mays* and *Sorghum halepense*, showed very little activity even toward *p*-nitrophenyl butyrate. All species showed only minor activities towards fluorescein diacetate.

3.2.4 Isoelectric Focussing and Inhibitor Study

An isoelectric focussing gel was run with protein extracts from the crops and weeds, which had been treated ± paraoxon prior to electrophoresis. Esterase activity was then visualised using α-naphthyl acetate as substrate (Figure 3.4). This was carried out to obtain a qualitative indication on the relative numbers and diversity of esterases in the chosen crop and weed species. Paraoxon was used as a selective inhibitor of serine hydrolases, with the IEF gel analyses identifying which carboxylesterases used this type of catalytic mechanism.

The pIs of the enzymes were approximated using a curve of best-fit applied to the marker proteins of known pI. This generated a third degree polynomial curve with the equation

$pI = 2\times10^{-5}x^2 - 0.0013x^2 + 0.0442x + 5.1$

where x is the distance in millimetres above the pI 5.1 marker (β-lactoglobulin) on a 260×113mm image of the gel. Distances below the marker were denominated as negative values of x and yielded pI values below pH 5.1 accordingly.

The IEF gel shows a large range of different enzymes with activity towards α-naphthyl acetate. Related species such as the two *Sorghum* species and the *Setaria* species show similarities in their enzyme profiles, as do some of the dicotyledonous plants. *Abutilon theophrasti, Echinochloa crus-galli, Oryza sativa, Phalaris canariensis* and *Zea mays* each had unique esterase profiles.

The majority of the esterase activities have pIs between pH 5 and pH 6, but there are also a number of activities outside of this range, including a number of basic enzymes.

Overall, between four and eleven esterases with activity toward α-naphthyl acetate were resolved from each species. These figures represent the minimum number of esterases present in each case, as it seems likely that more remained unresolved. Most of the enzymes visualised on the gel were at least partially inhibited by paraoxon, indicating that most of the hydrolysis of α-naphthyl acetate in plants is mediated by serine hydrolases.

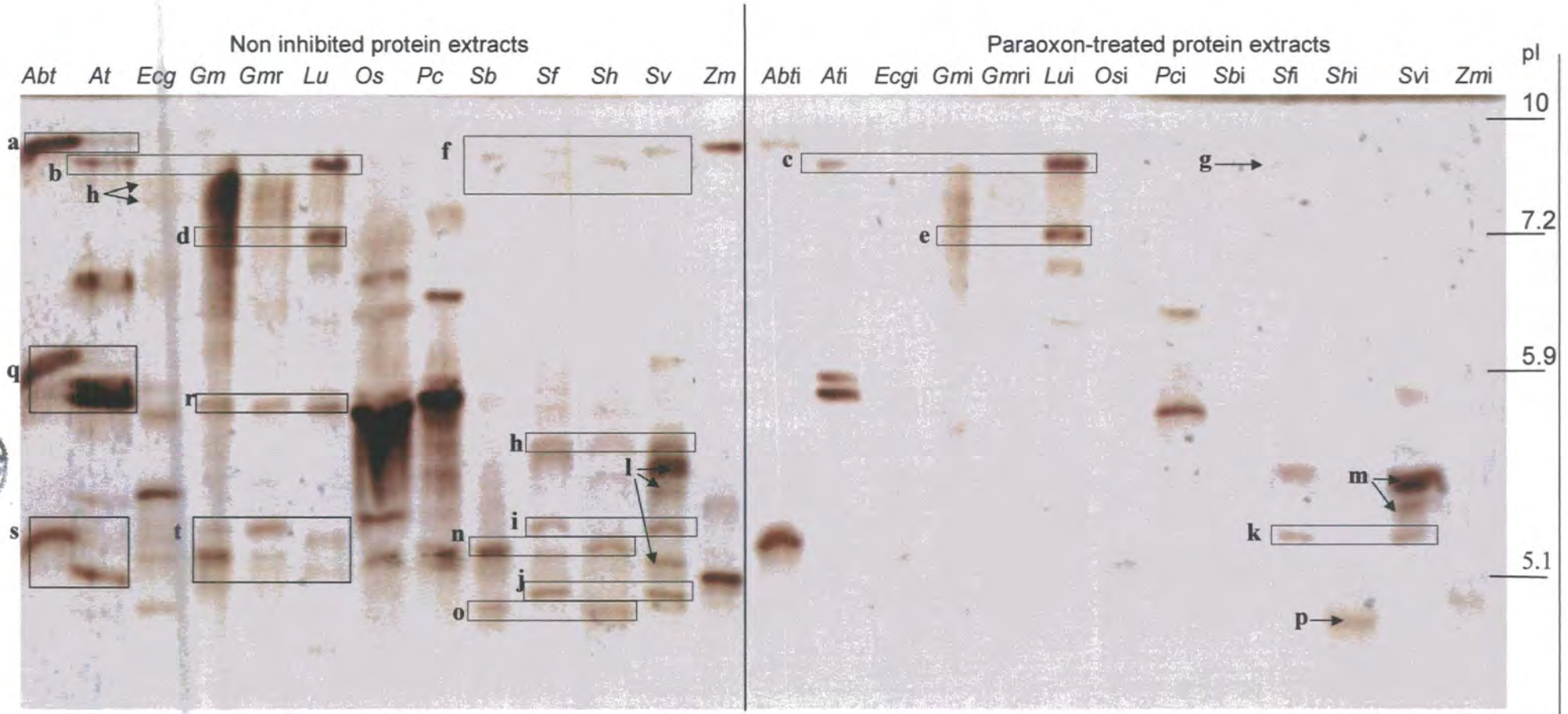

Figure 3.4: Isoelectric focussing gel with paraoxon-inhibited (designated by i) and non-inhibited protein samples from the foliage of the following crops and weeds: *Abutilon theophrasti* (*Abt*), *Arabidopsis thaliana* (*At*), *Echinochloa crus-galli* (*Ecg*), *Glycine max* (*Gm*), *Linum usitatissimum* (*Lu*), *Oryza sativa* (*Os*), *Phalaris canariensis* (*Pc*), *Sorghum bicolor* (*Sb*), *Setaria faberi* (*Sf*), *Sorghum halepense* (*Sh*), *Setaria viridis* (*Sv*) and *Zea mays* (*Zm*). Enzyme activity was visualised with α-naphthyl acetate as substrate. The suffix "r" indicates protein from root material. pIs are indicated on the right. Labelled and boxed activities are referred to in the main text.

3.2.4.1 Basic Esterase Activities

Many of the major basic carboxylesterases observed occur in the dicotyledonous plants (*Abutilon theophrasti, Arabidopsis thaliana, Glycine max and Linum usitatissimum*). In each case, esterases with pI between pH 7 and pH 10 were resolved. *Abutilon theophrasti* and *Arabidopsis thaliana* both have an esterase with pI 10 (figure 1, box **a**). The *A. theophrasti* enzyme is not fully inhibited by paraoxon. This might also be the case with the corresponding Arabidopsis enzyme, but the non-inhibited activity was low, so any residual activity following inhibition would fall below the threshold of detection. *Arabidopsis thaliana*, *Glycine max* and *Linum usitatissimum* all have an enzyme with an isoelectric point of pH 9.2 (box **b**), although the respective activity in G*lycine max* was not fully focused. These observed bands are likely to be caused by homologous enzymes: in addition to having the same isoelectric point, none of the three activities were affected by paraoxon (box **c**). *Glycine max* also seems to have an activity towards α-naphthyl acetate at pH 7.4, as does *Linum usitatissimum* (box **d**). The enzyme in *L. usitatissimum* was not inhibited by paraoxon and it was possible the *Glycine max* enzyme was also unaffected, but this could not be confirmed due to poor resolution (box **e**).

The monocotyledonous species investigated also showed evidence of basic carboxylesterases active toward α-naphthyl acetate, although their abundances are much lower then those from the dicotyledonous plants. The *Sorghum* and *Setaria* species showed esterases whose isoelectric points are between pH 8.5 and pH 9.8 (box **f**). *Sorghum bicolor* and *Sorghum halepense* both had an esterase with a pI of pH 9.3, whilst the *Setaria spp.* had a slightly more basic enzyme at a pI of 9.5. In addition, *Setaria faberi* has another basic activity that

focussed at an isoelectric point of 8.9, which was not affected by paraoxon treatment (**g**). *Echinochloa crus-galli*'s activities at pH 8.3 and pH 8.9, were unique within this study. *Phalaris canariensis* had an esterase at pH 7.8 which also does not appear in any of the other species. The only major monocotyledonous basic activity was in *Zea mays* (pH 9.8). The only basic monocotyledonous activity that was not inhibited by paraoxon was the enzyme from *Setaria faberi* (**g**).

3.2.4.2 Acidic Esterase Activities

The three main acidic esterases present in *Setaria faberi* are also present in *Setaria viridis*, focussing at pH 5.9, pH 5.5 and pH 4.9 (boxes **h**, **i** and **j** respectively). *Sorghum halepense* also has an enzyme of a pI at pH 5.9. The enzymes in the *Setaria* species at pH 5.5 were not inhibited by the paraoxon treatment (box **k**). *Setaria viridis* also showed at least three other acidic activities that were not evident in *Setaria faberi* (**l**: pIs 5.8, 5.7 and 5.3). The two most acidic of these enzymes were unaffected by paraoxon treatment (**m**). The two *Sorghum* species also had enzymes with common isoelectric properties, (pH 5.3 and pH 4.7, **n** and **o**). However, the *Sorghum halepense* enzyme at pH 4.7 was not inhibited by paraoxon treatment (**p**) unlike the equivalent *Sorghum bicolor* enzyme, which strongly suggests that the two are unlikely to be homologous.

The dicotyledonous species showed esterase activities towards α-naphthyl acetate between pH 5.7 - 5.9 (boxes **q** and **r**) and between pH 5.1 - 5.4 (**s** and **t**). In particular, the esterases in *Arabidopsis thaliana*, *Glycine max* and *Linum usitatissumum* at pI 5.1 may be homologous. The Arabidopsis enzyme shows incomplete inhibition by paraoxon, which could also be the case with the *Glycine*

and *Linum* esterases, but it is unlikely any remaining activity would be at detectable levels as the uninhibited activities were low. There was also a partially inhibited esterase of the same pH in *Phalaris canariensis*. However, it seems unlikely that an enzyme from such a distantly related species would be closely homologous to the dicotyledonous enzymes.

3.2.4 Further biochemical investigation of arabidopsis carboxylesterases

From the species investigated, the model plant *Arabidopsis thaliana* was confirmed as a good system to use for the further investigation of plant carboxylesterases: arabidopsis protein extracts showed high levels of carboxylesterase activity, especially toward 2,4-D methyl, clodinafop propargyl and the model substrates tested. Additionally, the whole arabidopsis genome is in the public domain, which would make the successful identification of purified carboxylesterases much more likely. Another major factor considered was the large collection of T-DNA insertion lines that are readily available, potentially allowing the characterisation of knockout lines deficient in the expression of any carboxylesterases identified in the course of the investigations.

Biochemical analysis as well as further isoelectric gel focussing was carried out in order to select a type of arabidopsis tissue which would be most suitable as a source of protein for esterase purification. Ideally, the source of tissue would be easy to obtain large quantities of, and would be grown heterotrophically to avoid the accumulation of large amounts of proteins related to photosynthesis. Protein extracts were prepared from arabidopsis suspension cultures, the foliage of four week-old seedlings and from 14 day-old root cultures. When analysed by

isoelectric focussing (Figure 3.5), the carboxylesterases expressed in arabidopsis foliage and roots were found to be very similar, whereas quite different patterns of expression were observed in suspension culture. The overall levels of carboxylesterase were qualitatively similar, but activity associated with a basic enzyme present in both root culture and foliage was present at much lower levels in extracts from suspension culture, while an activity with a pH of 5.1 was much more highly expressed in the cell culture. All of the arabidopsis carboxylesterases visualised showed at least partial inhibition by paraoxon.

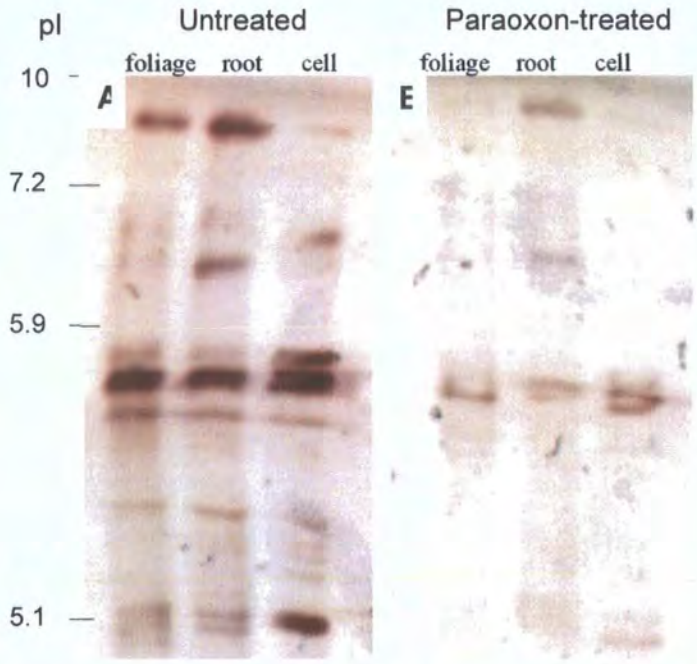

Figure 3.5: Isoelectric focussing gel, resolving activities toward α-naphthyl acetate from arabidopsis foliage, root culture, and cell suspension culture. Extracts were either untreated (**A**) or pre-treated with paraoxon (**B**).

A	2,4-D methyl	clodinafop propargyl	fenthioprop ethyl	fenoxaprop ethyl	bromoxynil octanoate	permethrin	cloquintocet mexyl
Arabidopsis thaliana (foliage)	**377** ± 57	**45.8** ± 1.3	**24.2** ± 1.6	**11.3** ± 0.2	**2.1** ± 0.2	ND	**4.9** ± 0.3
Arabidopsis thaliana (root culture)	**251** ± 19	**27.2** ± 0.7	**30.9** ± 0.3	**10.9** ± 0.3	**6.9** ± 0.6	ND	**3.0** ± 0.1
Arabidopsis thaliana (suspension culture)	**472** ± 0	**8.1** ± 0.2	**5.5** ± 0.1	**6.3** ± 0.2	**1.8** ± 0.3	**3.1** ± 0.2	**16.3** ± 2.4

B	α-naphthyl acetate	*p*-nitrophenyl acetate	*p*-nitrophenyl butyrate	*p*-nitrophenyl caprylate	*p*-nitrophenyl laurate	fluorescein diacetate
Arabidopsis thaliana (foliage)	**2750** ± 510	**990** ± 130	**490** ± 10	**294** ± 10	**10** ± 10	**29** ± 3
Arabidopsis thaliana (root culture)	**1590** ± 70	**930** ± 40	**456** ± 15	**230** ± 5	**78** ± 10	**46** ± 3
Arabidopsis thaliana (suspension culture)	**5330** ± 760	**1100 ± 30**	**5.5** ± 0.1	**6.3** ± 0.2	**1.8** ± 0.3	**3.1** ± 0.2

Table 3.3: Carboxylesterase activities of protein extracts from arabidopsis tissues toward **A** pesticide esters and **B** colorimetric and fluorimetric substrates. Activities are means of biological duplicates (pkat/mg) ± the range

Of the herbicides substrates, 2,4-D-methyl was the preferred substrate in all tissues followed by the AOPP esters and bromoxynil-octanoate. While activities toward 2,4-D-methyl were very high in the suspension cultures, this tissue was less active than the others in hydrolysing the other herbicides. Uniquely, the suspension culture preparation was able to hydrolyse the pyrethroid insecticide permethrin and also had the highest activity with the safener cloquintocet-mexyl. The three tissue sources each showed a specific preference for the AOPP herbicides. In the foliage, clodinafop-propargyl was the preferred substrate, whereas in the roots fenthioprop-ethyl was hydrolysed at similar rates. Given their structural similarity (Figure 3.1), it was surprising that fenthioprop-ethyl was a better esterase substrate than fenoxaprop-ethyl with the root and foliage extracts. Collectively, these results demonstrated that the relatively subtle qualitative changes in esterase expression in the cultures, roots and foliage observed in the IEF gels was reflected in significant differences in the ability of tissue extracts to bioactivate herbicides.

With the colourimetric and fluorimetric assays it was apparent that nitrophenyl acetate was not a good model substrate for identifying tissue specific differences in estrerase expression, with all extracts showing equivalent activities. Activities toward naphthyl acetate mirrored those determined with 2,4-D methyl (cultures > foliage > roots), even though the relative ratios were not identical. With respect to increasing the chain length of the acyl moiety, whereas root and foliar extracts showed a steadily declining activity from C-2 to C-8, the suspension culture preparations showed an intolerance toward any extension beyond the acetate. In all tissues, fluorescein diacetate proved to be the least preferred model xenobiotic substrate

3.3 Discussion

3.3.1 The effect of substrate structure on the rate of hydrolysis

What was most apparent in all species was that the smaller ester substrates were hydrolysed more rapidly than the larger substrates. This is not unexpected due to the supposition that smaller molecules would be able to access a larger number of esterase active sites than their larger counterparts, which are likely to be subject to a greater amount of steric hindrance. The size of the acid moiety possibly has more of a bearing on the rate of hydrolysis than the size of the alcohol part of a substrate: notably, where the chain length of *p*-nitrophenyl esters increased, this markedly reduced the activity in most cases, with few of the plants showing any activity toward *p*-nitrophenyl laurate. However, all of the species showed at least some activity toward fluorescein diacetate, which has a very bulky alcohol moiety. This observation about the relative role of the sizes of the different parts of the esters may account for why the pesticide esters showed lower activities than the model substrates: in all cases, the pesticides have larger acid moieties than the colorimetric and fluorimetric substates.

Another observation of note is that relatively small differences in substrate structure may translate into significantly different levels of carboxylesterase activity, as with clodinafop-propargyl when compared with the other AOPP esters investigated. Surprisingly, even the seemingly trivial difference between fenthioprop-ethyl and fenoxaprop-ethyl can also lead to significant differences in the rates of hydrolysis of the two pro-herbicides.

3.3.2 Relationship between plant taxonomy and carboxylesterase activities

The IEF profiles of carboxylesterase activities from species belonging to the same genus showed marked similarities: many isozymes were common to both *Seteria* species, and it was a similar situation with the *Sorghum* species as well. Similarily, the carboxylesterase activities shown by the two *Setaria* species showed strong similarities toward the substrates investigated, as did those of the *Sorghum* species, with the exception of the activities shown toward the *p*-nitrophenyl esters: *Sorghum halepense* showed much larger activities toward the butyrate and caprylate esters compared to *Sorghum bicolor*.

However, other than these similarities at the genus level, there were no consistent patterns of similarity between the species tested. Therefore, any ability to predict carboxylesterase activities of a given species based on data from related plants is restricted to closely related species. Any attempt to design herbicide esters that will be hydrolysed at a given rate in a target plant will have to be based on extensive characterisation of carboxylesterase activities exhibited by the species in question.

3.3.3 Limitations

It should be noted that the esterase profiles visualised in this study are not necessarily definitive for each of the species investigated; it has been shown in previous studies that esterase numbers and levels of expression may vary between cultivars (Schwarz *et. al.*, 1964) and even between different populations of the same species (Cherry and Katterman, 1971). Additionally, esterase expression has been shown to change during development (Frossard and Voss,

1978; Chandra and Toole, 1977), and in response to stress (Baudouin *et. al.*, 1997, Pontier *et. al.*, 1998), which could possibly have affected the profiles observed in this investigation. However, growth conditions were maintained as constant as possible, and the overall similarity of the esterase levels observed suggests that there have been no large perturbations in esterase levels due to stress. Additionally the plants were harvested at reasonably comparable developmental stages, minimising the effect of developmental changes.

3.3.4 Conclusions

This study is the first that describes the hydrolysis of a wide range of xenobiotic carboxylic esters by a large number of important crops and weeds. All the plants investigated exhibited several carboxylesterases in the IEF study, and activities towards a large structural diversity of substrates. Arabidopsis was confirmed as a good system in which to study carboxylesterases. Suspension culture was chosen as the source of material for further study of Arabidopsis enzymes, primarily as it provides a convenient source of large amounts of sterile tissue and the high level of activity it showed toward 2,4-D methyl and the model substrates.

Following the investigation of carboxylesterases in a wide range of species, further investigations of plant carboxylesterases were limited to arabidopsis. The next chapter describes the purification and identification of arabidopsis carboxylesterases involved in xenobiotic metabolism.

CHAPTER 4: PURIFICATION AND IDENTIFICATION OF ARABIDOPSIS CARBOXYLESTERASES

4.1 Introduction

To date, only one plant carboxylesterase has been unambiguously identified and cloned that has a role in pesticide metabolism, a family II carboxylesterase from black grass with activity toward AOPP esters (*Am*GDSH1, Cummins and Edwards 2004, see section 1.5.1.2). As discussed in Chapter 1, plant carboxylesterases are found in at least four gene families, and it is unknown whether any of the other families also contain enzymes active in pesticide metabolism. This is of particular importance, as in addition to gaining further insight into the role of these enzymes in herbicide bioactivation/detoxification, knowledge of which enzymes are responsible for pesticide ester hydrolysis would help determine their cellular location. This is important since hydrolysis can occur outside the cell (Haslam *et al.* 2001, Cummins and Edwards, 2004), which undoubtedly has an effect on the pesticides' final distribution and activity. In contrast, there has been no direct evidence of intracellular esterases that play a role in pesticide metabolism.

This chapter describes the purification and identification of the major 2,4-D methyl-hydrolysing enzyme from arabidopsis using a multi-step purification process. An initial attempt at purification was carried out using liquid chromatography as the primary method of separation, but it did not yield enough of the enzyme to allow for its identification. An alternative purification strategy was therefore devised where

the final step of the original purification was replaced with a procedure that exploited a chemical probe designed to covalently label serine hydrolases. The probe, fluorophosphono-biotin, and its mechanism of action are described below.

As is detailed in section 1.2.1, serine hydrolases are irreversibly inhibited by organophosphate compounds. This occurs as organophosphates covalently bind to the active site serine. FP-biotin (Figure 4.1 **A**) is a chemical probe which exploits this reactivity in order to enable serine hydrolases in any given proteome to be labelled with biotin (Liu *et al.* 1999) as shown in Figure 4.1 **B**.

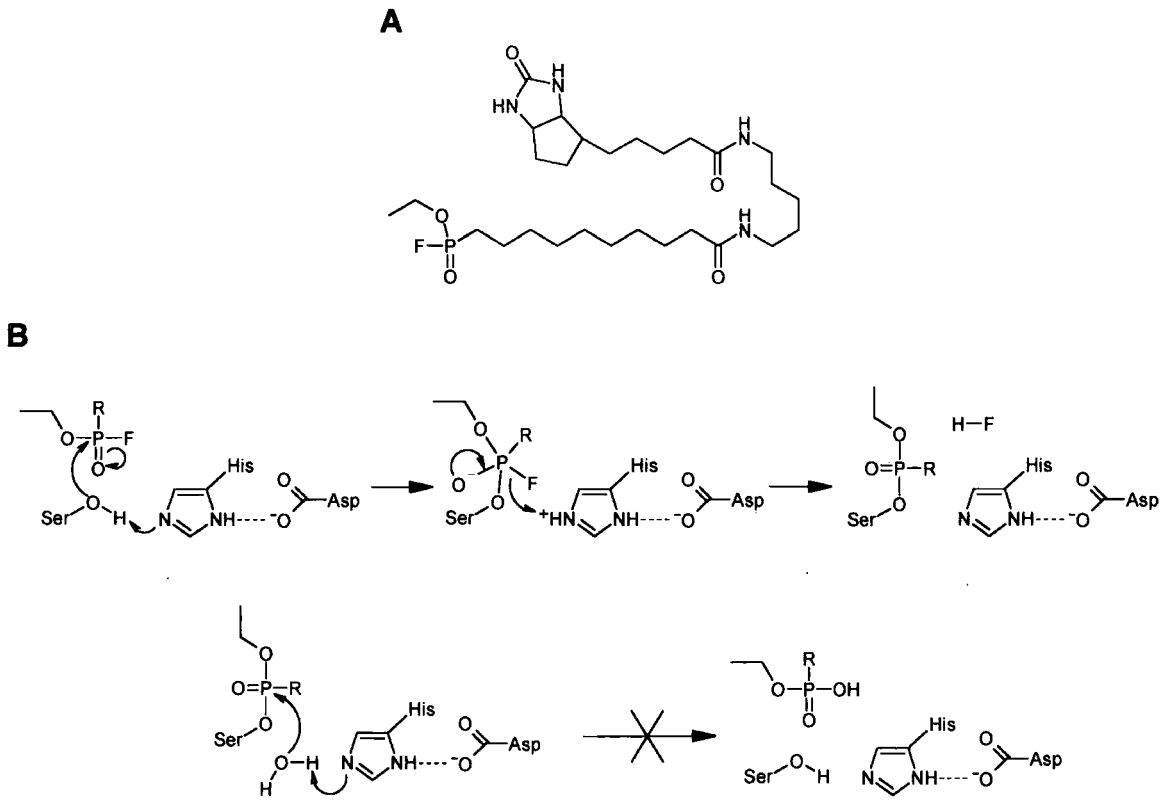

Figure 4.1: FP-biotin **A** and its mechanism of serine hydrolase inhibition **B**. R in part **B** represents the part of FP-biotin coloured blue in part **A**, the serine hydrolase is represented by the residues making up the catalytic triad. The second part of the reaction shown in part **B** cannot proceed, so the enzyme remains bound to FP-biotin.

Once labelled with FP-biotin, serine hydrolases may be easily distinguished from the rest of the proteome, using the very strong and specific affinity between biotin and streptavidin. To date FP-biotin has been used largely to profile serine hydrolases in mammalian systems (Liu *et al.* 1999). In view of the large size of the gene families of serine hydrolases and their complex regulation in plants, such a functional

proteomics probe would be a useful tool to help identify expressed carboxylesterases in crops and weeds. To this end, the FP-probe was used to purify and identify 2,4-D-methyl-hydrolysing esterases following their partial purification from arabidopsis.

4.2 Results and Discussion

4.2.1 Purification of carboxylesterase activity from Arabidopsis cell suspension culture

Two overall strategies were employed in order to purify and identify the enzyme responsible for 2,4-D methyl hydrolysis from *Arabidopsis* suspension culture. Both attempts are described in the following sections.

4.2.1.1 Initial purification strategy

A multi-step purification process was used to resolve esterase activities in *Arabidopsis* suspension culture (summarised in Figure 4.2). Hydrolytic activity toward 2,4-D methyl was followed through the purification process using the HPLC-based assays described in Chapter 3. The matrices used for the purification (DEAE sepharose, butyl sepharose and phenyl suparose), were chosen primarily because they were used successfully to purify *Am*GDSH1 from black-grass (Cummins and Edwards 2004).

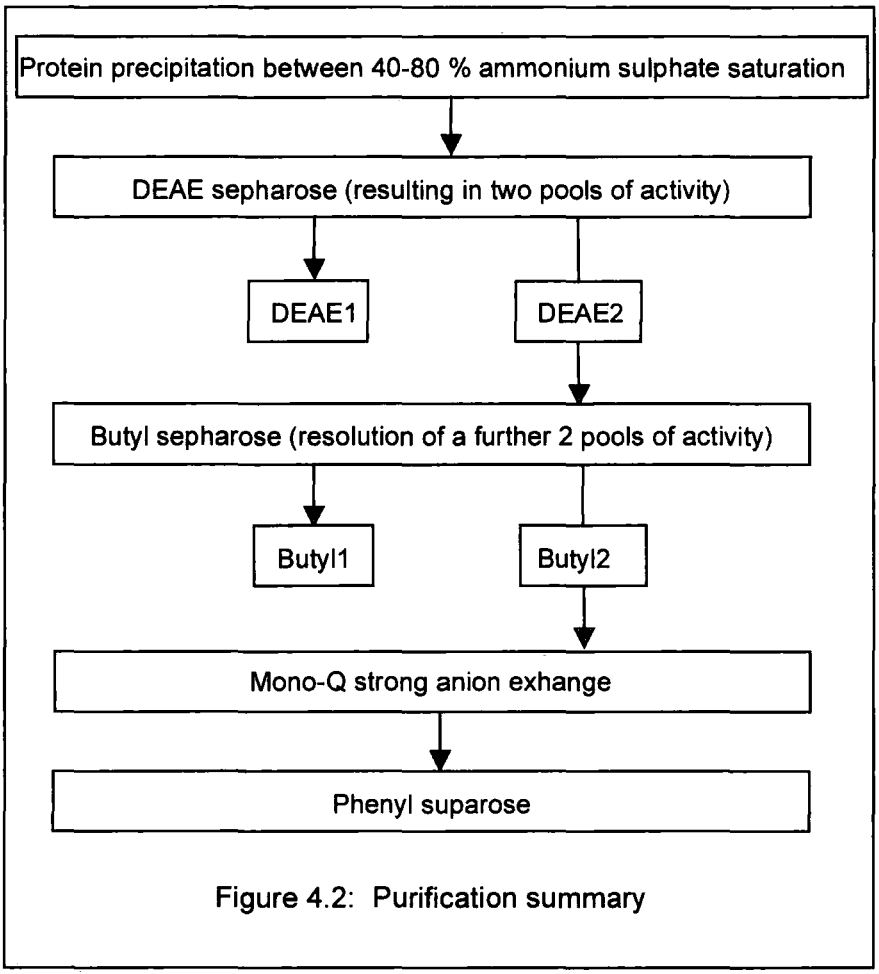

Figure 4.2: Purification summary

After ammonium sulphate precipitation, the protein was dissolved in buffer and dialysed overnight, before being loaded on to a 110 ml DEAE sepharose anion exchange column. After the unbound protein had been eluted, a salt gradient was carried out which resulted in two main pools of activity toward 2,4-D methyl being recovered (see Figure 4.3).

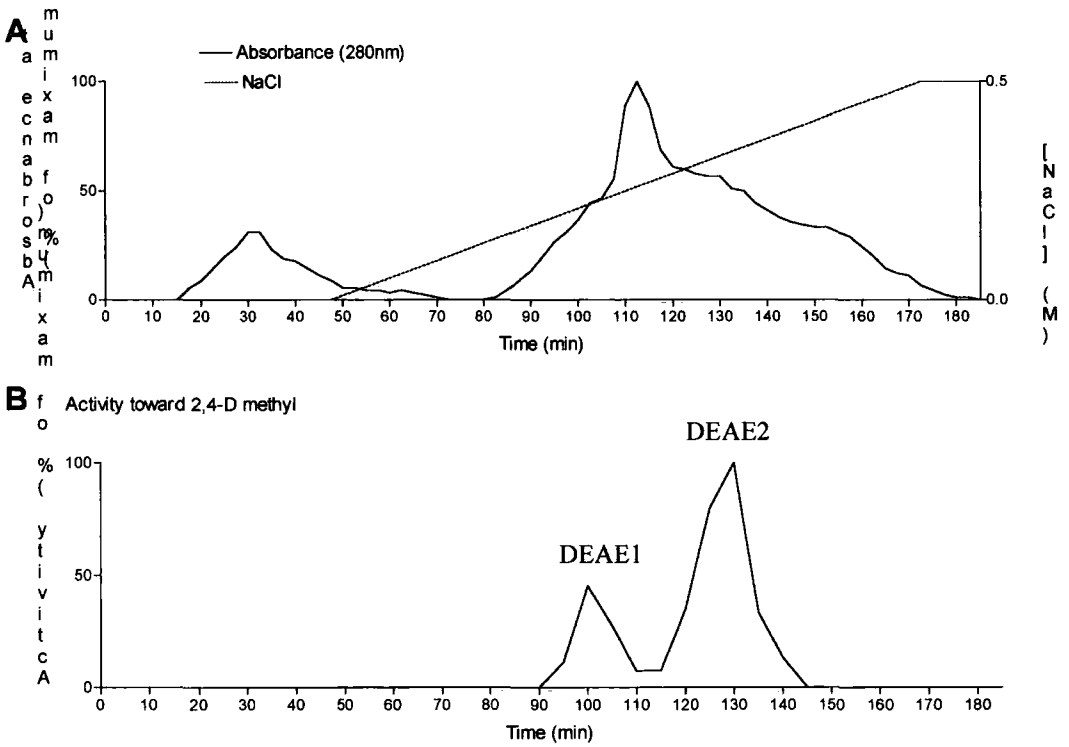

Figure 4.3: Chromatogram showing the first chromatographic step in the purification, with the UV absorbance of the eluant shown in **A** and carboxylesterase activity toward 2,4-D-methyl in **B**. The DEAE sepharose column resolved two pools of activity toward 2,4-D methyl, referred to as DEAE1 and DEAE2.

The second pool, DEAE2, accounting for most of the 2,4-D-methyl-hydrolysing activity, was applied to the second column, a 40 ml butyl sepharose (hydrophobic interaction) column. The protein was loaded in 1 M ammonium sulphate, which was maintained until the absorbance at 280 nm had dropped back down to baseline levels. A gradient that progressively reduced the salt content of the mobile phase was then run, eluting the bound protein. There was a small amount of activity in the

unbound protein, but the majority bound to the column and was eluted in two further pools, of which the second once again contained the most activity (see Figure 4.4).

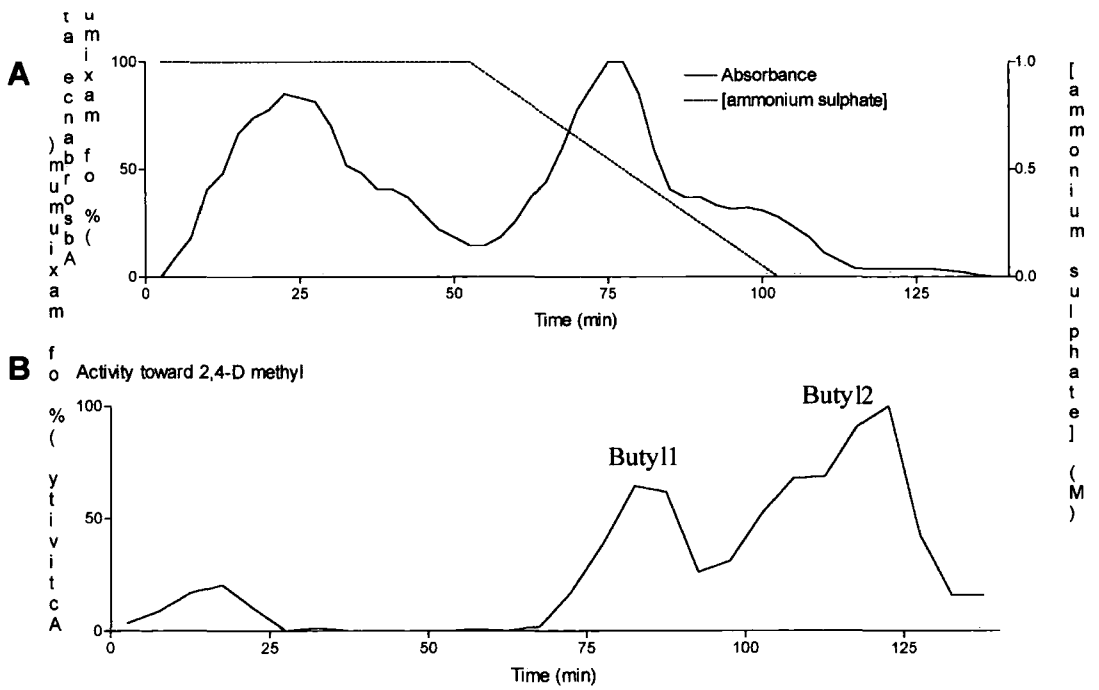

Figure 4.4: Chromatogram of the butyl sepharose separation, showing UV absorbance (**A**) and 2,4-D-methyl-hydrolysing activity (**B**) of the eluant. Two further activities were resolved, termed Butyl1 and Butyl2 respectively.

As pool Butyl2 contained most of the activity, it was then dialysed overnight to remove any remaining ammonium sulphate, in preparation for further separation on a Mono-Q strong anion exchange column. Protein was loaded in buffer at pH 6.5 and bound protein was eluted with a salt gradient (Figure 4.5).

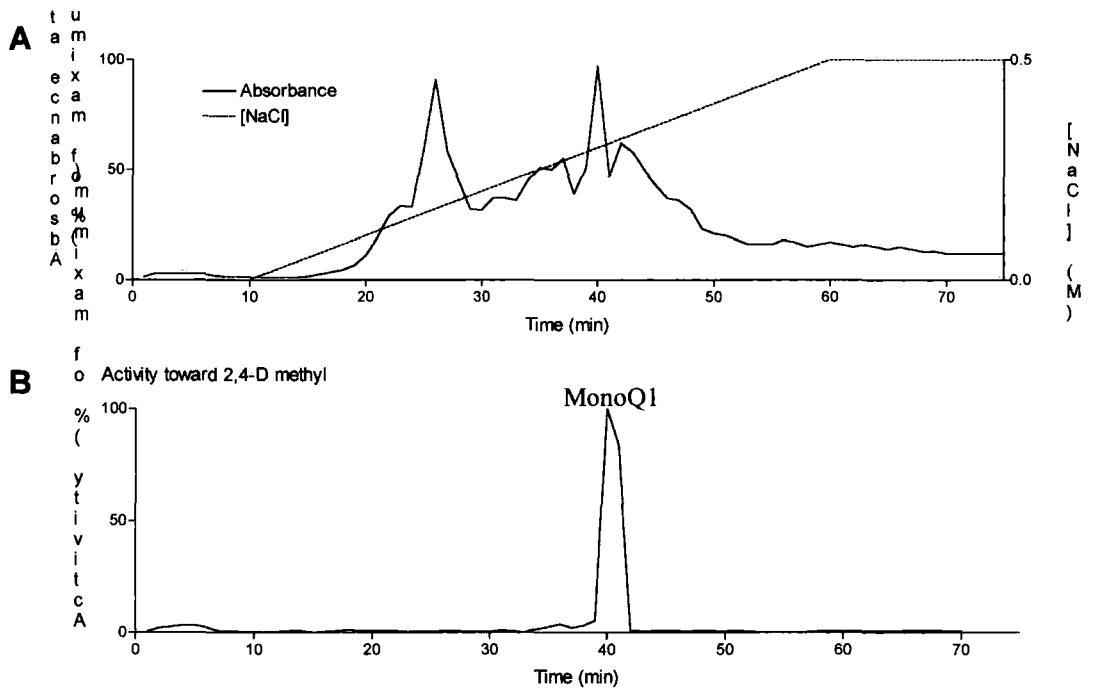

Figure 4.5: The results of the mono-Q separation showing the UV absorbance (**A**) and the 2,4-D methyl-hydrolysing activity (**B**) of the eluant.

The activity all came off the mono-Q column in a single peak (MonoQ1), which was then loaded on to the final column, a phenyl suparose hydrophobic interaction column (Figure 4.6).

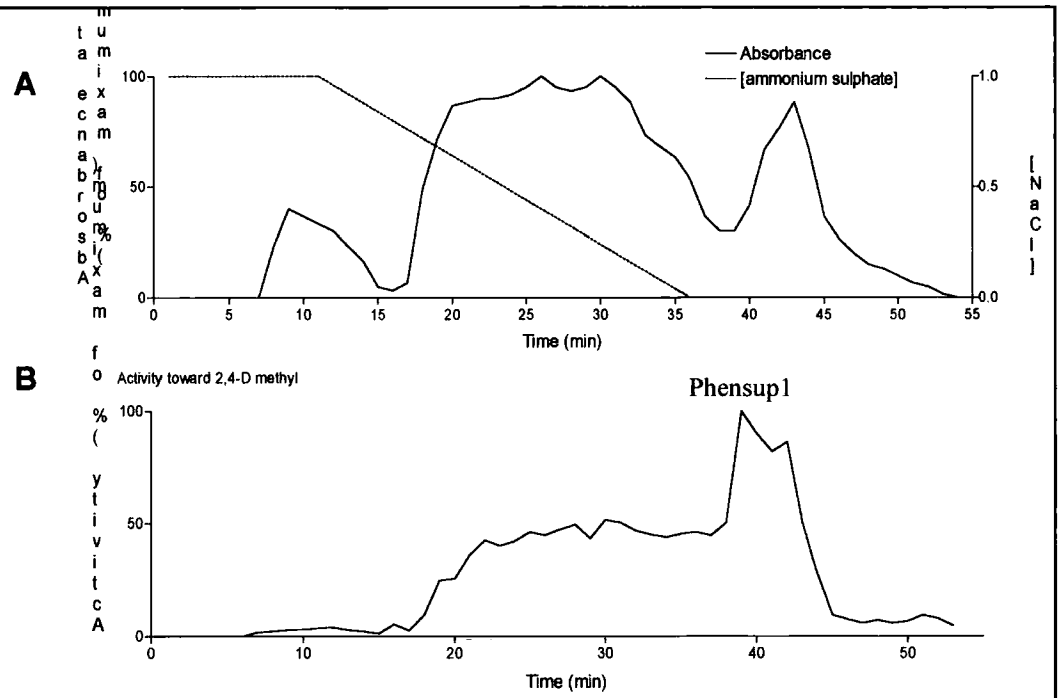

Figure 4.6: Phenyl suparose separation, showing the UV absorbance (**A**) and the 2,4-D methyl-hydrolysing activity (**B**) of the eluant.

Only limited 2,4-D-methyl hydrolysing activity was eluted from the phenyl suparose column (Phensup1), with the activity eluting over several fractions.

Samples from the purification run were inhibited with FP-biotin and the resulting labelled proteins run on duplicate 12.5 % SDS-PAGE gels, one of which was blotted and probed with streptavidin-linked phosphodiesterase to visualise biotinylated proteins (Figure 4.8). The other gel was stained with coomassie blue stain (Figure 4.7).

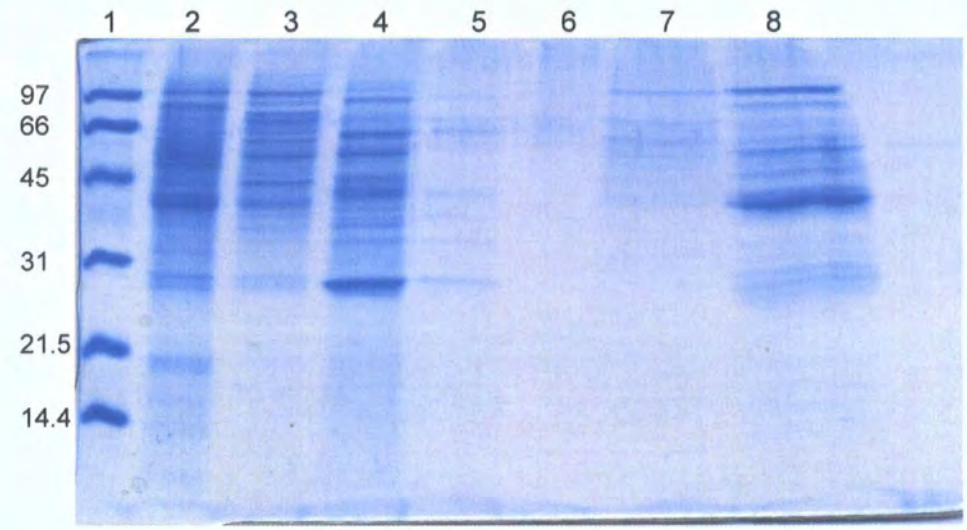

Figure 4.7: SDS-PAGE gel showing active fractions from each step in purification. 1: size markers (Mw as indicated, in kDa), 2: 40-80 % ammonium sulphate precipitated crude protein, 3: DEAE2, 4: Butyl2, 5: monoQ1, 6: phensup1. 7: Butyl1, 8: DEAE1.

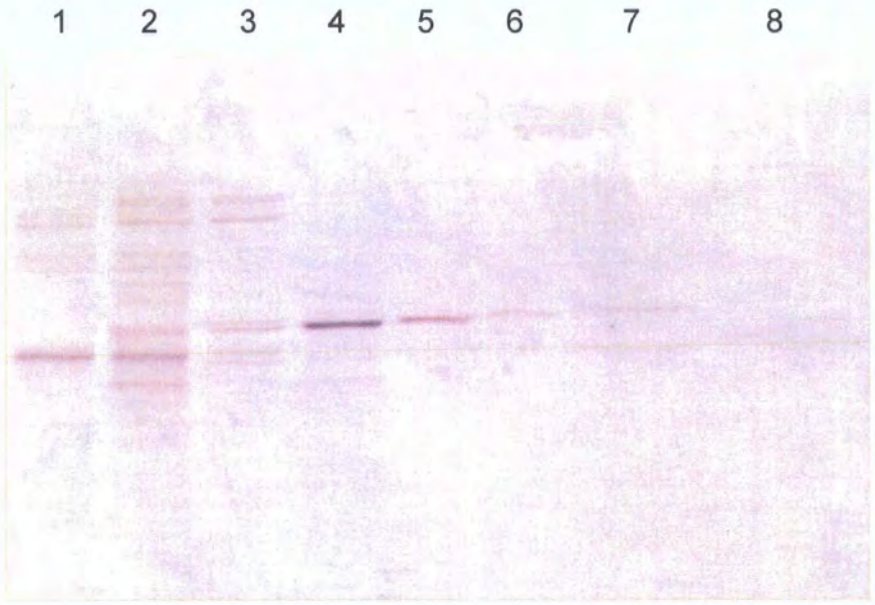

Figure 4.8: Western blot of samples shown in Figure 4.7 (lanes 2 to 8) which have been incubated with FP-biotin then probed with streptavidin. Lane 1 shows the identical protein preparation used in lane 2, but where pre-treatment with FP-biotin was ommitted.

Arabidopsis cultures contained a small number of endogenously biotinylated proteins (Figure 4.8). Following treatment with FP-biotin, the streptavidin-probed blot shows seven bands in the inhibited ammonium sulphate precipitate which were not visible in the non-inhibited sample, indicating the presence of a variety of different serine hydrolases in Arabidopsis suspension culture. This is consistent with the results of the IEF gel presented in Chapter 3, which showed the resolution of multiple activities toward α-naphthyl acetate that were susceptible to organophosphate inhibition (Figure 3.4). One of the serine hydrolases of Mr = 36kDa was greatly enriched in the early parts of the purification, especially by the butyl sepharose separation. Recovery of this hydrolase drops massively in the final purification stage. This pattern of enrichment and recovery of 2,4-D-methyl hydrolysing activities was quantitatively assessed at each stage of purification (see Table 4.1).

Fraction	Total Protein (mg)	Total Activity (nkat)	Specific activity (nkat/mg)	% recovery	fold purification
crude	504	573.2	1.14	100	1
DEAE2	266	349.5	1.31	61.0	1.1
Butyl2	36	237.2	6.59	42.4	5.8
MonoQ	3.9	107.8	27.65	18.8	24.3
Phensup1	0.10	23.8	238.24	4.2	209.0

Table 4.1: Purification table for the initial purification attempt

It was evident that much of the carboxylesterase was lost in the final purification step. Although staining for total protein showed several contaminating proteins present after the mono-Q separation, the strepatavidin-probed blot showed that there was only one serine hydrolase present. This suggested a strategy of repeating the purification up until after the mono-Q column, then inhibiting the carboxylesterase with FP-biotin. The inhibited protein could then be affinity purified using streptavidin sepharose, and identified.

4.2.1.2 Revised purification strategy

In addition to the modification of the purification strategy as described above, the second purification attempt was also used to gain more information about the carboxylesterases present in arabidopsis suspension culture. To this end, the fractions collected from the DEAE sepharose column were assayed with four carboxylesterase substrates. In addition to 2,4-D-methyl, clodinafop-propargyl, cloquintocet-mexyl and the model substrate *p*-nitrophenyl acetate were investigated. As before, the carboxylesterase activity resolved into two pools: DEAE1 and DEAE2. Unlike the previous purification, DEAE1 showed little activity toward 2,4-D methyl, but actively hydrolysed *p*-nitrophenyl acetate. Most of the activity shown toward 2,4-D-methyl, clodinafop-propargyl and cloquintocet-mexyl was present in the DEAE2 peak. In subsequent purifications hydrolase activity was monitored using *p*-nitrophenyl acetate as substrate.

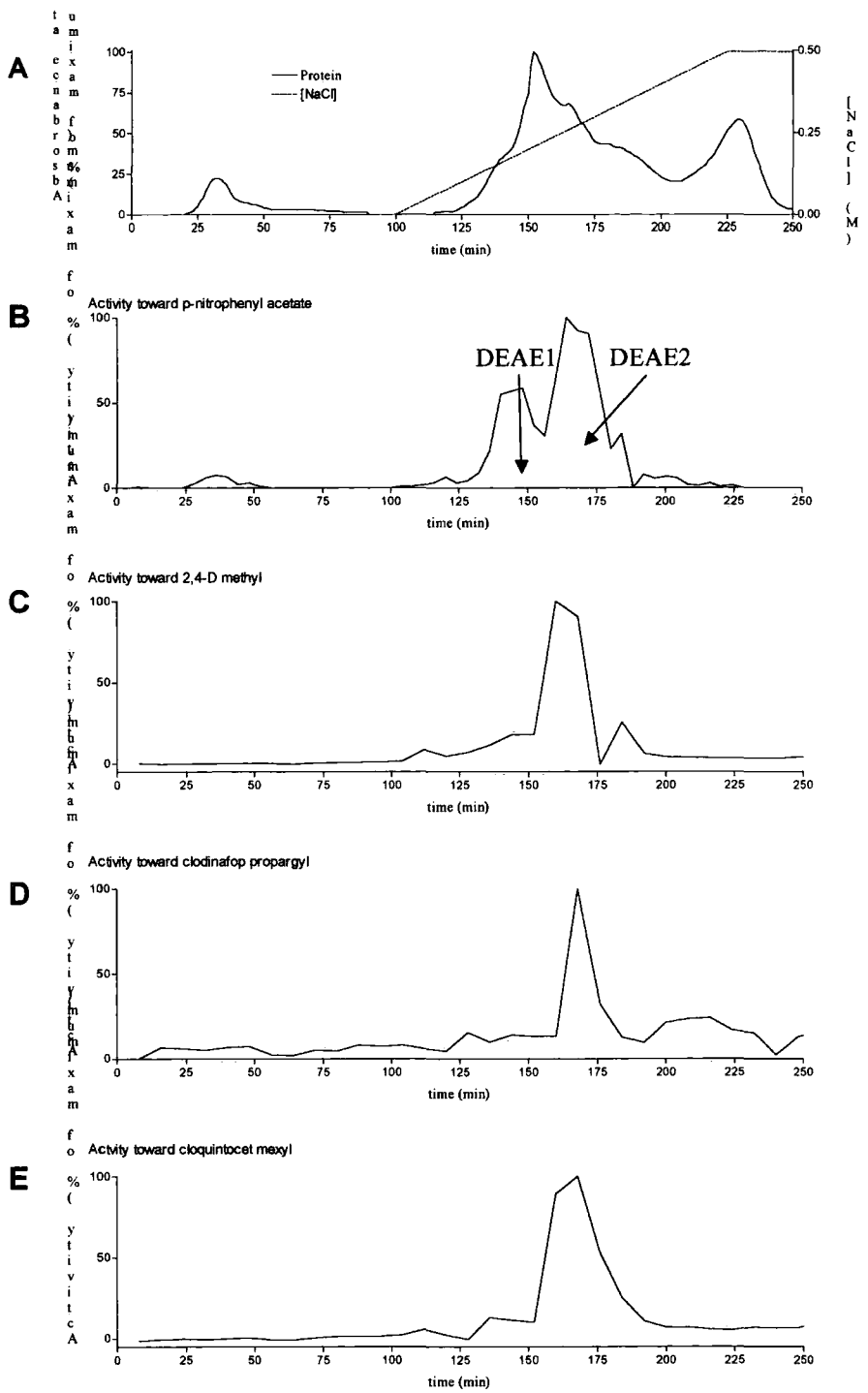

Figure 4.9: DEAE sepharose column separation: UV abosrbance (**A**) and elution of activity toward *p*-ntirophenyl acetate (**B**), 2,4-D-methyl (**C**), clodinafop-propargyl (**D**) and cloquintocet-mexyl (**E**)

The butyl sepharose column was then used to resolve the enzymes present in DEAE2. The carboxylesterase activity was resolved into Butyl1 and Butyl2 as before (Figure 4.10).

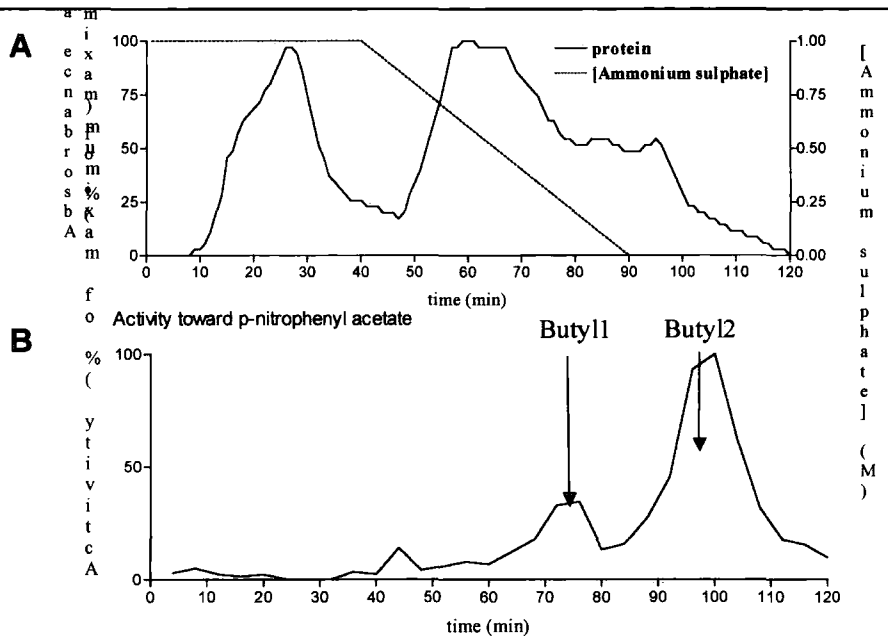

Figure 4.10: Separation of protein in DEAE2 by butyl sepharose, showing UV absorbance (**A**) and *p*-nitrophenyl acetate hydrolysing activity (**B**) of the eluant.

The proteins present in Butyl2 were then applied to the mono-Q strong anion exchange column (Figure 4.11).

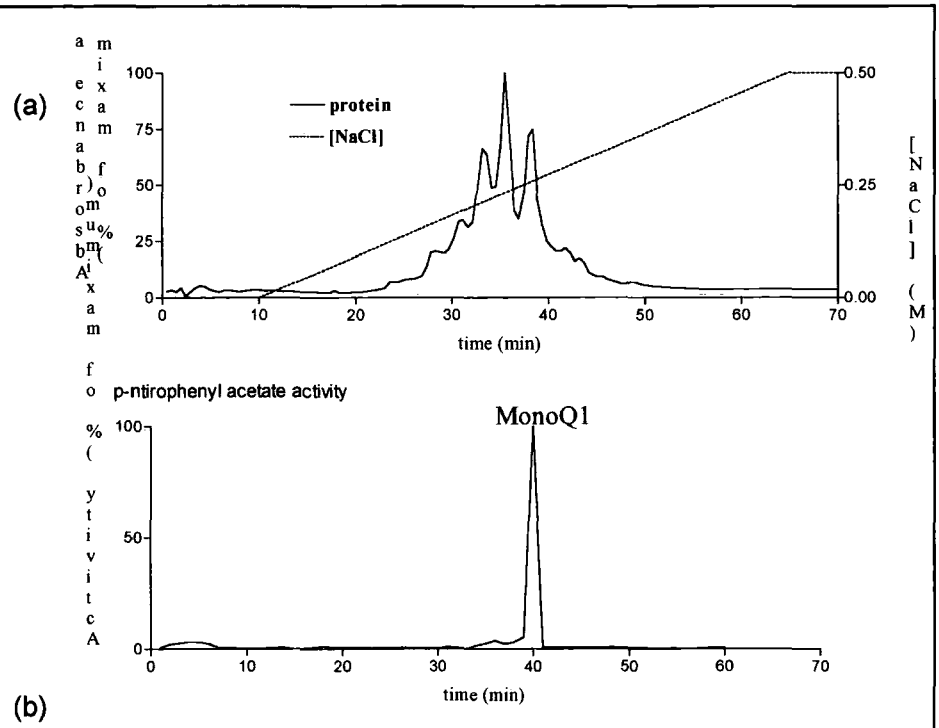

Figure 4.11: separation of Butyl2 using the mono-Q column, showing UV absorbance (a) and *p*-nitrophenyl acetate hydrolysing activity (b) of the eluant.

This resulted in the recovery of a discrete peak of *p*-nitrophenyl acetate hydrolysing activity (MonoQ1), which eluted at the same point as the 2,4-D methyl hydrolysing activity in the initial purification. The carboxylesterase activity present in this fraction was completely inhibited with fluorophosphonobiotin. The inhibited sample was then affinity purified using streptavidin sepharose. The bound protein was eluted by boiling the stationary phase in SDS-PAGE loading buffer, and then run on a 12.5 % SDS-PAGE gel (Figure 4.12 **A**). A duplicate gel was western blotted, using streptavidin-linked phosphodiesterase to identify biotinylated peptides (Figure 4.12 **B**).

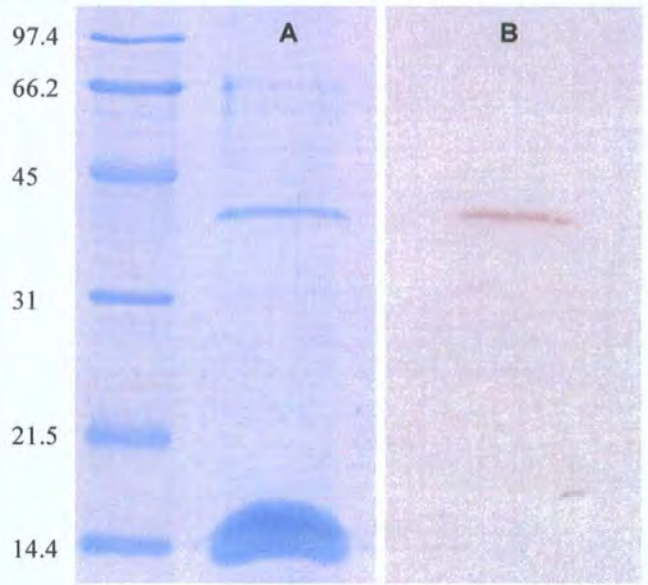

Figure 4.12: SDS-PAGE gel stained for total protein **A** and corresponding western blot using streptavidin phosphodiesterase **B** of the protein recovered from the mono-Q column, then inhibited with FP-biotin and affinity purified. Sizes of the size markers are given in kDa on the left.

Except for a very major band of streptavidin at 15 kDa, the gel revealed a single major polypeptide with a mass of approximately 36.6 kDa. The blot confirmed that the band visible on the gel had been selectively biotinylated by FP-biotin and therefore that it was a serine hydrolase. Two other polypeptides of approximately 60 and 66 kDa visible on the gel were not apparent on the blot, showing them to be non-specific contaminants, possibly keratin. A very minor signal was observed at 32 kDa on the blot, which was possibly a breakdown product of the purified carboxylesterase.

The 36.6 kDa band was excised from the gel and submitted for MALDI-TOF analysis. This identified the enzyme as a family IV enzyme, AtCXE12 (*Arabidopsis*

thaliana carboxylesterase 12) when searching the arabidopsis database ($p<0.05$). AtCXE12 is one of 20 *Arabidopsis* proteins that belong to family, which was first described by Marshall *et al.* (2003).

In order to investigate the other carboxylesterases resolved during the purification, the other pool of activity from the butyl sepharose separation, Butyl1, was then applied to the mono-Q column (Figure 4.13)

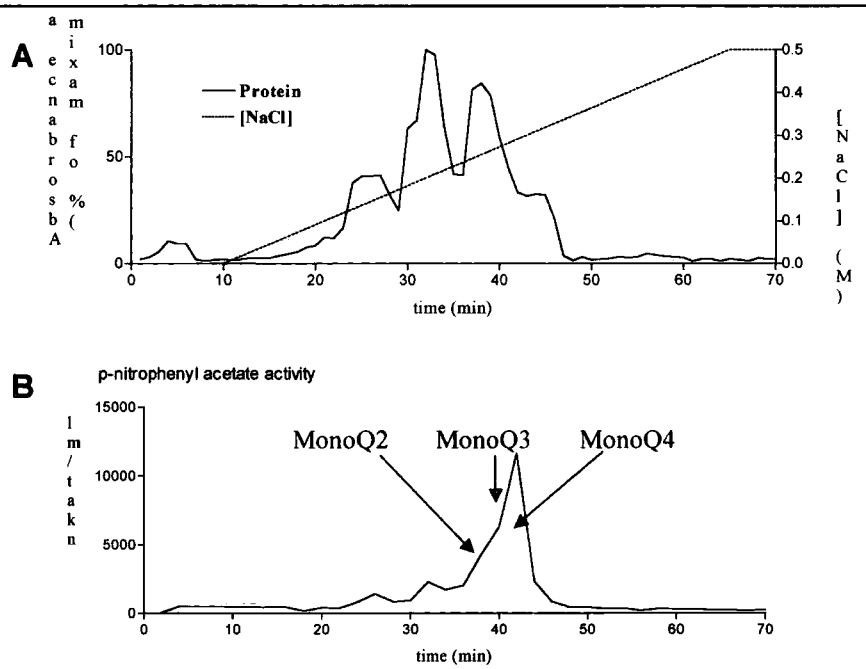

Figure 4.13: Separation of Butyl1 using the mono-Q column, showing UV absorbance (A) and *p*-nitrophenyl acetate hydrolysing activity (B) of the eluant.

The broad peak of activity recovered suggested that several carboxylesterases were present, so each of the three fractions making up the peak was inhibited with FP-biotin separately and the labelled enzymes affinity purified using steptavidin sepharose. The gel in Figure 4.14 shows the results of the affinity purifications,

along with a sample of MonoQ1 (AtCXE12), which was inhibited and purified to serve as a control. Except for the 60 and 66 kDa contaminants that were seen before, and the streptavidin bands at the bottom of the gel, the only polypeptides visualised were of an approximate mass of 36kDa (numbered 1-3, Figure 4.14).

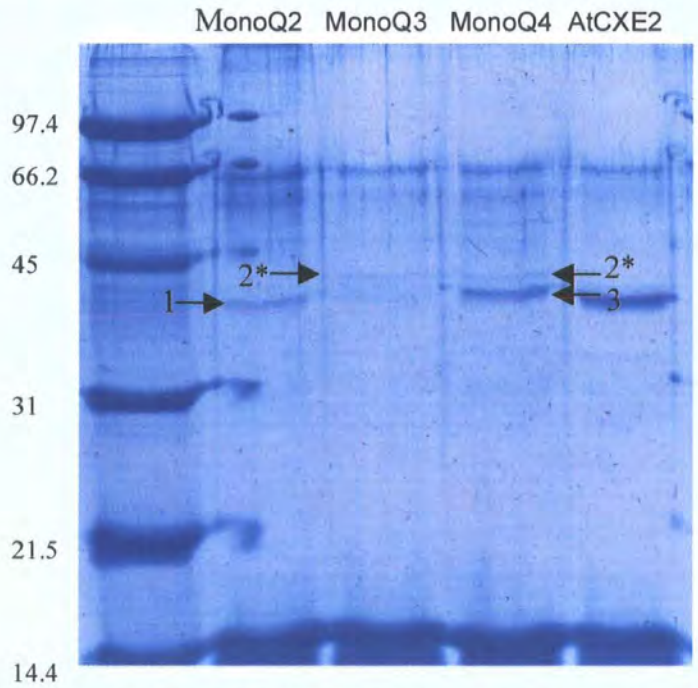

Figure 4.14: Showing polypeptides resulting from affinity purification of mono-Q fractions after inhibition with FP-biotin. Active fractions from the mono-Q separation of proteins in Butyl1 (MonoQ2-4) were inhibited with FP-biotin and biotinylated polypeptides were purified with streptavidin sepharose. Polypeptides that do not correspond to contaminants observed in the previous affinity purification (Figure 4.12) are arrowed and numbers are referred to in the main text. * These bands are exactly the same mass, so are likely to be the same polypeptide, which eluted over the collection of MonoQ3 and MonoQ4. Contrast of original image has been altered to allow minor bands to be seen.

The purified bands were excised from the gel and MALDI-TOF analysis was carried out. Band 3 was identified as AtCXE5 when the peptide fragment sizes were searched against the *Arabidopsis* protein database ($p<<0.05$). The minor band split across fractions MonoQ3 and 4 (band 2) was identified as AtCXE20 with a p value of less than 0.05 same protein database. Analysis of band 1 did not give a significant hit, however the arabidopsis protein with the best score was AtCXE12. All of the proteins identified in the purification are summarised in Table 4.2.

Fraction	**Carboxylesterase**	**AGI gene code**	**Predicted Mass (kDa)**	**Observed Mass (kDa)**	**Predicted pI**
MonoQ1	AtCXE12	At3g48690	35.8	36.6	5.22
MonoQ2	AtCXE12	At3g48690	35.8	36.6	5.22
MonoQ3	AtCXE20	At5g62180	36.4	40.1	5.11
MonoQ4	AtCXE5	At1g49660	35.4	38.1	5.33

Table 4.2: Summary of the carboxylesterases isolated from arabidopsis

Fraction	Total Protein	Specific Activity (pkat/mg)				Purification Fold				Total Activity (pkat)				Total Recovery (%)			
		p-NA	2,4-D	c'fop	c'cet	p-NA	2,4-D	c'fop	c'cet	p-NA	2,4-D	c'fop	c'cet	PNA	2,4-D	c'fop	c'cet
Total	2050	344	290	13	0.005	1.0	1.0	1.0	1.0	706000	592	25.7	10.0	100	100	100	100
40-80%	664	1181	940	18	0.005	3.4	3.3	1.5	1.0	784000	626	12.2	3.3	111	106	47.2	33.56
DEAE1	56	2352	1290	4	0.001	6.8	4.5	0.3	0.3	132000	72.3	0.25	0.08	18.7	12.2	1.0	0.8
DEAE2	66	6239	6070	263	0.010	18.1	21	2.1	2.0	412000	401	1.7	0.63	58.3	67.7	6.7	6.30
Butyl1	1.1	26115	17540	334	0.107	75.9	60.8	26.6	22.1	29700	20.0	0.38	0.12	4.21	3.4	1.5	1.23
Butyl2	0.91	98892	48930	222	0.087	287.5	169.5	17.7	17.9	89600	44.3	0.20	0.08	12.7	7.5	0.8	0.79
MonoQ1	0.22	303030	87900	387	0.106	880.9	304.5	30.8	21.8	66700	19.33	0.085	0.02	9.4	3.3	0.3	0.234
MonoQ2	0.21	37815	23810	199	0.107	109.9	82.5	15.8	22.0	7940	5.00	0.042	0.02	1.1	0.8	0.2	0.22
MonoQ3	0.24	38807	12800	177	0.052	112.8	44.4	14.1	10.7	9310	3.07	0.043	0.01	1.3	0.5	0.2	0.12
MonoQ4	0.26	43363	6570	195	0.028	126.1	22.8	15.5	5.7	11300	1.71	0.050	0.01	1.6	0.3	0.2	0.07

Table 4.3: purification table monitoring the purification activities of protein fractions toward four xenobiotic substrates. Abbreviations of substrates: p-NA: *p*-nitrophenyl acetate, 2,4-D: 2,4-D-methyl, c'fop: clodinafop-propargyl, c'cet: cloquintocet-mexyl.

Table 4.3 shows the carboxylesterase activity toward *p*-nitrophenyl acetate, 2,4-D-methyl, clodinafop-propargyl and cloquintocet-mexyl at each stage of the protein purification. From this, AtCXE12 could be shown to be a major 2,4-D-methyl and *p*-nitrophenyl acetate hydrolysing enzyme in Arabidopsis. The other purified enzymes did not have such clearly defined hydrolysis of the xenobiotic ester substrates used in the investigation.

4.3 Analysis of identified carboxylesterases

4.3.1 The *Arabidopsis* carboxylesterases (AtCXEs)

All three of the enzymes identified in the above purification belong to the recently defined AtCXE family (Marshall *et al.* 2003). An RT-PCR study of the gene expression of each of the AtCXE family members showed that *AtCXE12*, and *5* are expressed in all tissues, although AtCXE12 was only weakly expressed in the roots. *AtCXE20* was expressed at much lower levels, predominantly in the stem and flower (Marshall *et al.* 2003). This low level of expression correlates with the very low levels of the enzyme observed in cell culture in this study. The AtCXEs were assumed to be carboxylesterases because of their sequence similarity to cloned family IV carboxylesterases from other plants (Marshall *et al.* 2003). The purification studies show that the respective AtCXEs are expressed *in planta* and are associated with carboxylesterase activity toward both model xenobiotic and pesticide esters. Figure 4.15 shows how the three AtCXEs purified fit into the proposed classification scheme (Marshall *et al.* 2003) and shows their relationship with selected family IV carboxylesterases from both plants and bacteria.

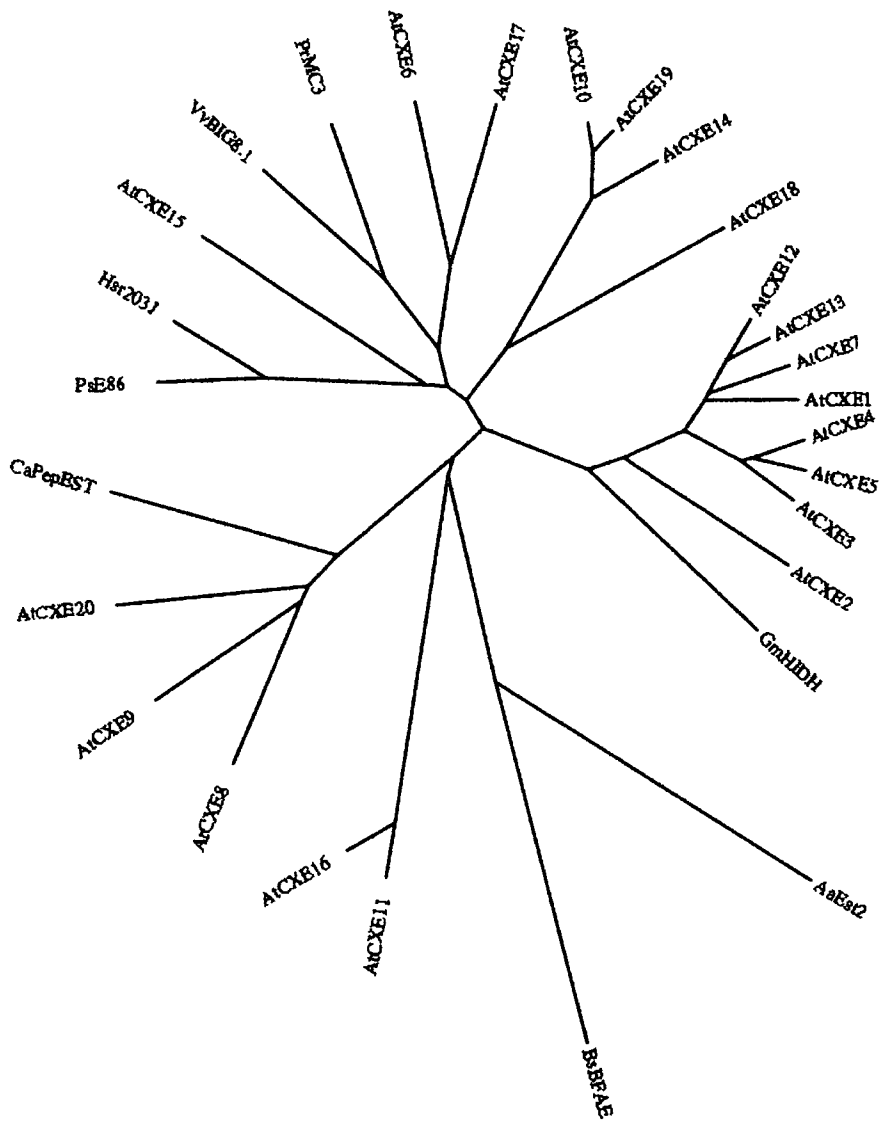

Figure 4.15: Tree showing family IV carboxylesterases. Related sequences were identified using four iterations of PSI-BLAST (http://www.ncbi.nlm.nih.gov/BLAST/) and the tree was produced from a CLUSTAL W alignment using the Phylip program package. AtCXE1-20: arabidopsis proteins as classified by Marshall *et al.* 2003, GmHIDH: *Glycine max* hydroxyisoflavone dehydratase, CaPepEST: carboxylesterase from *Capsicum anuum*, AaEst2: *Alicylobacillus acidocaldarius* esterase, BsBFAE: Bacillus subtilis brefeldin A esterase.

AtCXE5 and AtCXE12 are relatively closely related, and show similarities to GmHIDH (*Glycine max* hydroxyisoflavone dehydratase, see section 1.5.3.3), whilst AtCXE20 is further removed and is related to CaPepEST (*Capsicum anuum* Pepper Esterase, also described in section 1.5.3.3). Figure 4.16 shows an alignment of the three arabidopsis enzymes isolated, together with GmHIDH and CaPepEST. In each case the catalytic triad has been identified.

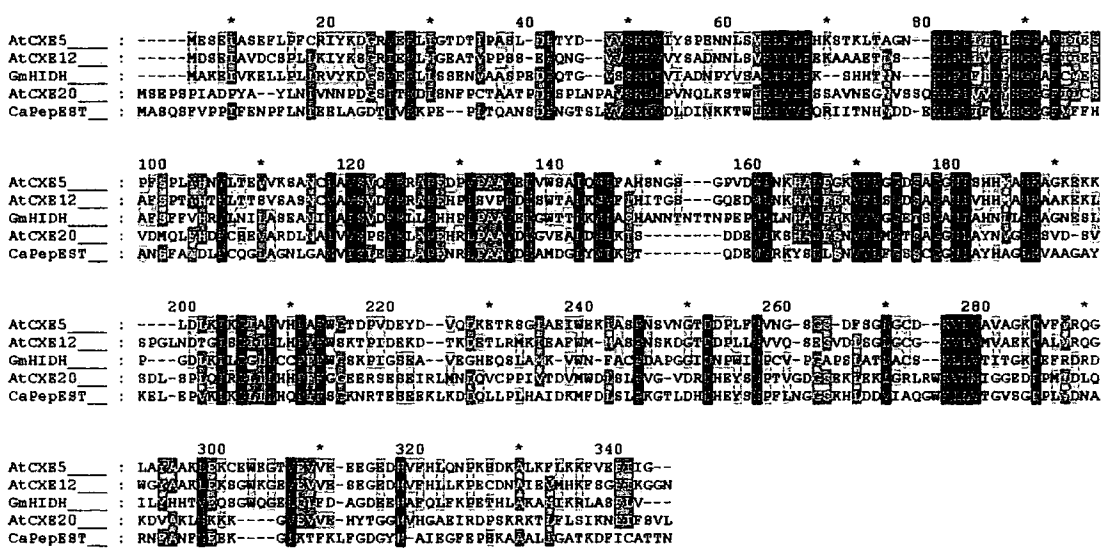

Figure 4.16: Alignment of the three purified *Arabidopsis* carboxylesterases with GmHIDH and CaPepEST. The active site serine (threonine in GmHIDH) is shaded purple, and the other catalytic residues are in green.

AtCXE12 showed by far the greatest hydrolytic activity toward 2,4-D-methyl of the three enzymes identified. For this reason, it was chosen as the primary subject for further analysis. The following section describes a more detailed analysis of its sequence and presents results from web-based protein analysis tools.

4.3.2 AtCXE12

One of the more intriguing aspects of the purification was that AtCXE12 was identified as part of two separate pools of activity from the butyl sepharose column. The presence of AtCXE12 in the smaller pool of activity could be interpreted as spill-over from the major pool, but the two peaks of activity are chromatographically completely distinct. Additionally, AtCXE12 protein eluted from the mono-Q column at slightly different times when isolated from the two butyl fractions. Perhaps most significant of all are the very different specific activities shown by the two mono-Q fractions containing AtCXE12: the activity shown by the enzyme in Butyl1 toward 2,4-D-methyl is considerably lower than that shown in Butyl2. These observations indicate that two forms of the enzyme are present in suspension culture, showing that AtCXE12 must undergo some form of post-translational modification. In order to gain an insight into this modification, the sequence of AtCXE12 was analysed using several web-based protein bioinformatics tools as detailed in the following section.

4.3.3 Prediction of post-translational modification

This section presents results from the analysis of the AtCXE12 amino acid sequence by web-based sequence analysis programs. No predictions made on the basis of protein sequence are perfect or infallible, so where available, more than one program was used for each type of prediction in an attempt to reduce the probability of obtaining spurious results.

TargetP is one of a suite of protein analysis tools provided by the Center for Biological Sequence Analysis (CBS, http://www.cbs.dtu.dk). It is designed to predict the subcellular localisation of a protein from its sequence, and is able to

do so with an overall accuracy of 85 % for plant proteins (Emanuelsson *et al.* 2000). The program predicted that AtCXE12 is a cytosolic protein with a high degree of confidence. MultiLoc, a similar but independent program (Hoeglund *et al.* 2006, http://www-bs.informatik.uni-tuebingen.de/Services/MultiLoc/), also predicted a cytosolic localisation for the protein. While experimental evidence would be required for confirmation, this biofinformatic prediction suggests that it is unlikely that AtCXE12 is glycosylated in the same fashion as an esterase like *Am*GDSH1.

With glycosylation less likely, the most probable form of post-translational modification that AtCXE12 may undergo is phosphorylation. Phosphorylation is a common, reversible modification which can dramatically alter the activity of an enzyme. In plants, phosphorylation events have been implicated in responses to many signals, including stress and pathogen attack. This makes carboxylesterases good candidates for possible regulation by phosphorylation, as so many of them are associated with such responses, as discussed in Chapter 1.

Two programs were used to identify possible phosphorylation sites in the AtCXE12 amino acid sequence. These were NetPhos, from the CBS suite of analysis tools (http://www.cbs.dtu.dk/services/NetPhos/, Blom *et al.* 1999), and PredPhospho (http://pred.ngri.re.kr/PredPhospho.htm, Kim *et al.* 2004). NetPhos predicted 15 separate phosphorylation sites, including the active site serine, which seems highly unlikely. The only conclusion can be that NetPhos produces many false positives, so results should be regarded with a high degree of scepticism and refined in order to identify those sites with the potential to be more accurate predictions. To this end, the phosphorylation predictions made by

NetPhos were compared with those made by PredPhospho, and the predictions of both were put into the context of AtCXE12's predicted secondary structure (see Figure 4.17). NetPhos does not make predictions of which kinases act on each residue, but PredPhopho specifies the family or group of kinases likely to act at a predicted phophorylation site. It predicted that Ser81 and Ser181 were likely to be phophorylated by kinases from the CMGC group, which includes MAP kinase, while Thr203 and Ser292 were assigned kinase families CDK and CK2 respectively.

In addition to the predictions of phosphorylation sites, the AtCXE12 amino acid sequence was submitted to a high stringency analysis by ScanSite (Obenauer *et al.* 2003), which searches for kinase binding domains. ScanSite identified a potenital MAP kinase binding domain, which is also shown in Figure 4.17.
The secondary structure predictions were made by SSpro (part of the SCRATCH suite of prediction tools: http://www.igb.uci.edu/tools/scratch/, Cheng *et al.* 2005) and PSIPRED (http://bioinf.cs.ucl.ac.uk/psipred/, Jones, 1999).

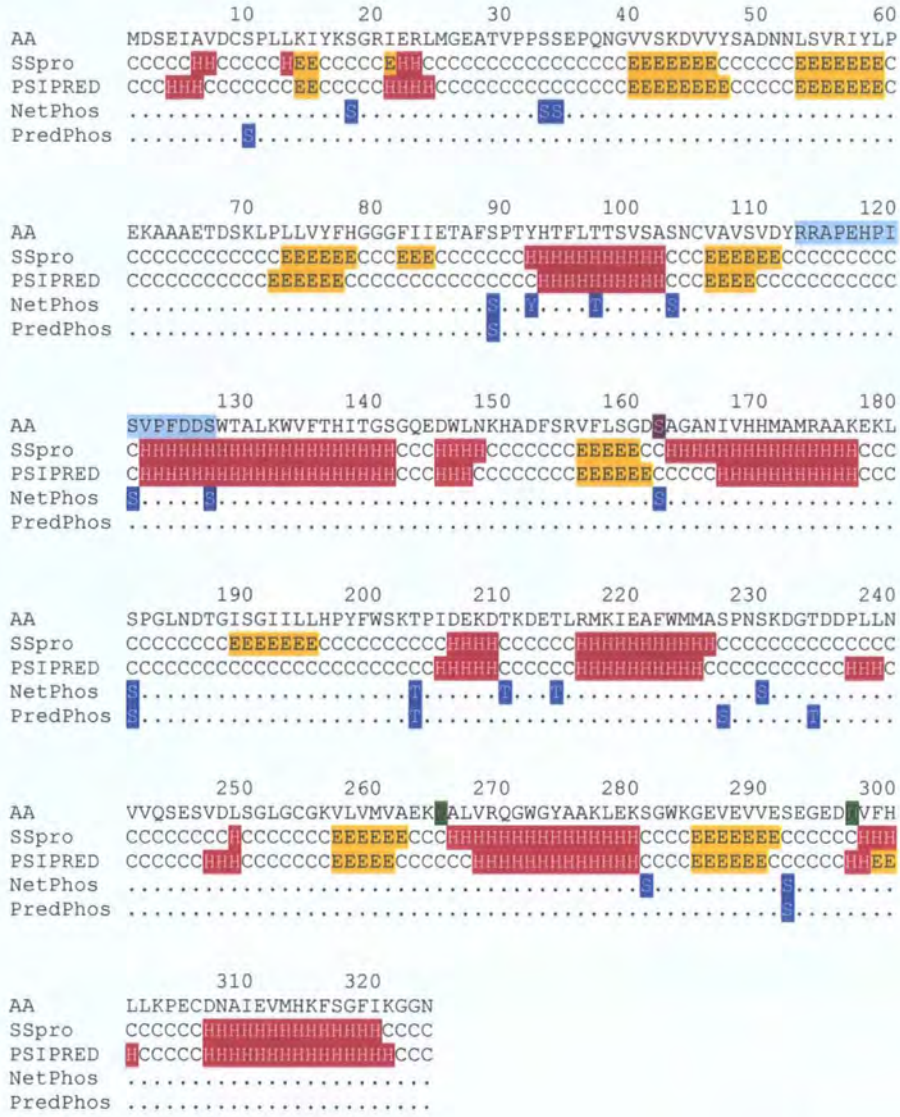

Figure 4.17: AtCXE12 potential phosphorylation sites in context of secondary structure predictions. Legend: AA: amino acid sequence, sequence highlighted in light blue is the predicited kinase binding site, H: predicted α-helix, E: predicted β-strand, S, T or Y: phorphorylation site predictions. Active site residues are highlighed in purple (serine) or green (histidine and aspartate).

Four of the predictions made by NetPhos and PredPhospho concur, and all four occur at the end of a predicted α-helix or β-strand, suggesting that they may be in accessible locations on the enzyme. In order to further assess the accessibility, and thus the feasibility, of the potential phosphorylation sites, AtCXE12 was

submitted to two structural prediction programs. The first, mGenTHREADER (Bujnicki *et al.* 2001), is a program that uses PSIPRED secondary structure predictions to align submitted sequences with homologous enzymes with known crystal structures. ESyPred3D, the second program employed, uses neural networks to produce a similar alignment, and then produces a model of the submitted enzyme using the alignment (Lambert *et al.* 2002). ESyPred3d aligned AtCXE12 with AaEst2 (*Alicylobacillus acidocaldarius* esterase: a bacterial carboxylesterase of known 3D structure) and produced a three-dimensional model in the form of a protein data bank file. Supporting this model was the fact that mGenTHREADER also aligned AaEst2 with AtCXE12 with a very high level of confidence. The two alignments are shown in Figure 4.18, with the AtCXE12 predicted secondary structure and the known AaEst2 secondary structure shown. The alignments seem remarkably good, considering the low level of sequence identity between AtCXE12 and AaEst2, perhaps reflecting the high level of structural homology shown by α/β hydrolases in general, even when sequence similarity is low (Ollis et al, 1992).

Figure 4.18: Alignments produced by mGenTHREADER and ESyPred3D between AtCXE12 and AaEst2. The AaEst2 sequence is shown twice, labelled with the programme that generated each of the alignments. Red highlight indicates α-helix, yellow indicates β-strand.

Figure 4.19 shows a 3D representation of AaEst2 with the residues corresponding to the predicted AtCXE12 phophorylation sites coloured blue. The predicted kinase binding site is shown in light blue. In the centre of the image is the threonine residue in AaEst2 that corresponds to Ser89 in AtCXE12. The other three potential phosphorylation sites were also on the proposed surface of the enzyme, on the reverse of the enzyme as it is viewed in Figure 4.19.

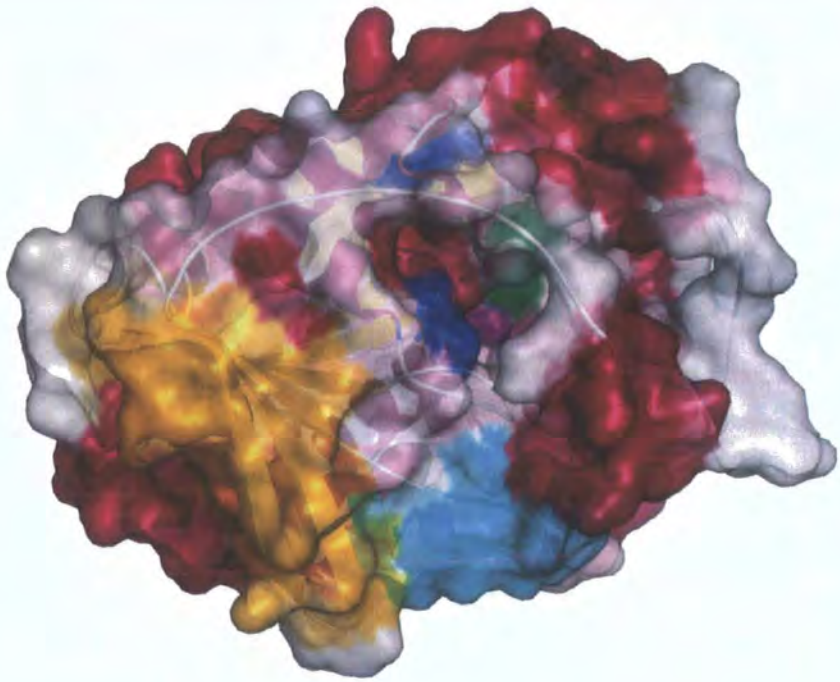

Figure 4.19: AtCXE12 threaded on to the crystal structure of AaEst2. α-helices are shown in red, β-strands in yellow, active site residues are purple (serine) and green (histidine and aspartate). Putative phosphorylation sites are shown in dark blue, whilst the predicted kinase binding site is in cyan. Image generated with PyMOL (http://pymol.sourceforge.net/). The enzyme is orientated such that the N-terminus of the β-sheet is closest, and the active site serine and histidine residues may be seen through the active site entrance.

The model produced by ESyPred3D showed the location of Ser89 in a similar position. The positioning of Ser89 has the potential to be very significant, as it is placed very close to the entrance to the active site, so its phosphorylation would have dramatic effects on the enzyme's activity. The supposition that it is a true phosphorylation site is supported by the close proximity of the kinase binding site predicted by ScanSite. The potential phosphorylation site and the kinase

binding site correlate in that both are sites potentially associated with MAP kinases. Plant MAP kinases are known to be involved with signal transduction events associated with biotic and abiotic stress responses (Morris, 2001).

4.4 Conclusions

A carboxylesterase associated with the hydrolysis of 2,4-D-methyl has been purified from Arabidopsis cell suspension cultures and identified. It is a family IV carboxylesterase, while the AOPP ester-hydrolysing enzyme from black-grass was a GDS hydrolase (family II carboxylesterase). Also, unlike the black-grass enzyme, which was predicted to localise to the apoplast, AtCXE12 was an intracellular enzyme. Although this prediction would have to be confirmed by experimental data, but it suggests that plants have carboxylesterases capable of xenobiotic metabolism on both sides of the plasma membrane. The very different substrate specificities of AtCXE12 and AmGDSH1 suggest that different herbicide esters may be hydrolysed in different locations. This would mean that herbicides could enter the cell at different rates depending on whether they are hydrolysed before or after they cross the plasma membrane.

As a family IV carboxylesterase, AtCXE12 is related to several cloned and characterised plant carboxylesterases (see section 1.5.3.3). These enzymes are implicated in pathogen responses (HSR203J from tobacco, CaPepEST), or secondary metabolism (GmHIDH), suggesting that AtCXE12 may also be involved in one of these processes *in planta*.

Sequence analysis of AtCXE12 revealed it may be phosphorylated *in vivo*, providing a possible explanation for the two forms of the enzyme resolved during purification. Once again however, this prediction needs to be confirmed

experimentally, especially as the prediction software used in this study is optimised for predicting mammalian phosphorylation events, and has been shown to be much less reliable for predicting the phosphorylation of plant proteins (Peck, 2006). That said, the utilisation of a combination of many predictive methods in this chapter allow a slightly greater degree of confidence in the predictions than if phosphorylation-prediction software had been used in isolation.

It is known that many plant carboxylesterases are involved in responses to stress, and several carboxylesterases have been shown to be upregulated under such conditions. This is the first indication of what may be another level of carboxylesterase response to stress and plant signalling compounds- regulation by phosphorylation would enable the very rapid modification of AtCXE12 activity, allowing a much faster response than that achieved by regulation at the transcriptional level. Therefore, even though AtCXE12 has been shown to be expressed in high levels in all aerial parts of arabidopsis (Marshall *et al.* 2003), the level of its activity toward carboxylic esters may depend on its phosphorylation state, and accordingly depend on the biotic and abiotic conditions the plant is growing in.

As mentioned above, it would be highly desirable to confirm whether or not AtCXE12 undergoes phosphorylation *in planta*. Investigations using mass spectrometry to identify phosphorylated forms of the enzyme could be carried out, and in conjunction with tryptic digests, identify the section(s) of the AtCXE12 sequence that undergo(es) phosphorylation. Further investigations could then be carried out to identify the conditions under which the enzyme is

phosphorylated, and assays used to determine the hydrolytic activities of the different phosphorylated forms.

Initially, however, it was important to unequivocally confirm that AtCXE12 was responsible for the esterase activities observed during the purification. To obtain this confirmation, the AtCXE12 coding sequence was cloned and expressed in *Escherichia coli*, and the resulting recombinant enzyme was assayed for carboxylesterase activity. The results from this study are described in the next chapter.

CHAPTER 5: CLONING AND EXPRESSION OF ATCXE12

5.1 Introduction

Following the purification of AtCXE12 in the major 2,4,-D-methyl hydrolysing fraction from arabidopsis suspension cultures as described in the last chapter, confirmation of its activity toward 2,4-D-methyl was needed. To this end, this chapter describes the cloning, expression and biochemical characterisation of AtCXE12.

5.2 Results and Discussion

Primers were designed to each end of the AtCXE12 coding sequence. The *atcxe12* sequence contains an *Nco*I restriction site (CCATGG), which includes the start codon, and the 3' primer was constructed such that the stop codon would be replaced with an *Xho*I restriction site (CTCGAG).

As the genomic sequence of *atcxe12* does not contain any introns, both genomic DNA and cDNA were used as templates for attempted PCR of the *atcxe12* coding sequence. When the PCR products were run on an agarose gel, it was evident that while both PCR reactions produced products of ~1 kb, the genomic product was a single band whilst other bands were also visible from the cDNA template (see Figure 5.1).

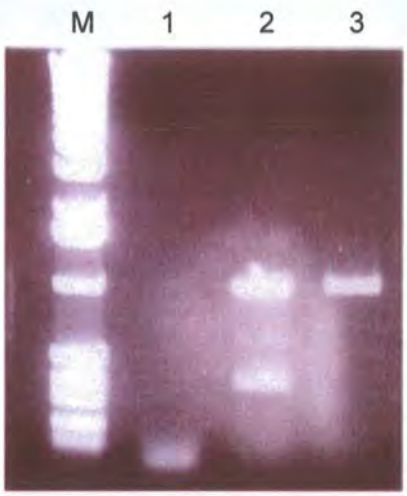

Figure 5.1: PCR products obtained using sequence specific primers designed to *atcxe12*. M: size markers (sizes indicated in kb), 1: no template, 2: cDNA template, 3: genomic DNA template.

The genomic PCR product was excised from the gel and purified, then ligated into pGEM®-T Easy plasmid. The resulting recombinant plasmid was used to transform XL10-Gold® ultracompetent cells. Seven colonies resulted, two of which were confirmed by PCR to contain *atcxe12*.

Mini-preps of both colonies were performed and the plasmid inserts sequenced. Single PCR errors were found in both inserts when the sequences were compared with the predicted *atcxe12* PCR product (see Figure 5.2). Translation of the DNA sequence established that neither mutation was silent, so a strategy to obtain the whole sequence without errors was devised, whereby the two PCR products would be restricted between the two errors, and the error-free sections ligated together. To this end, a unique restriction site for the enzyme *Aat*II was identified between the error-bearing sequences using the restriction site analysis tool in DNA for Windows (version 2.5a). Clone 1 was restricted with *Aat*II and *Nco*I, whilst Clone 2 was cut with *Aat*II and *Xho*I.

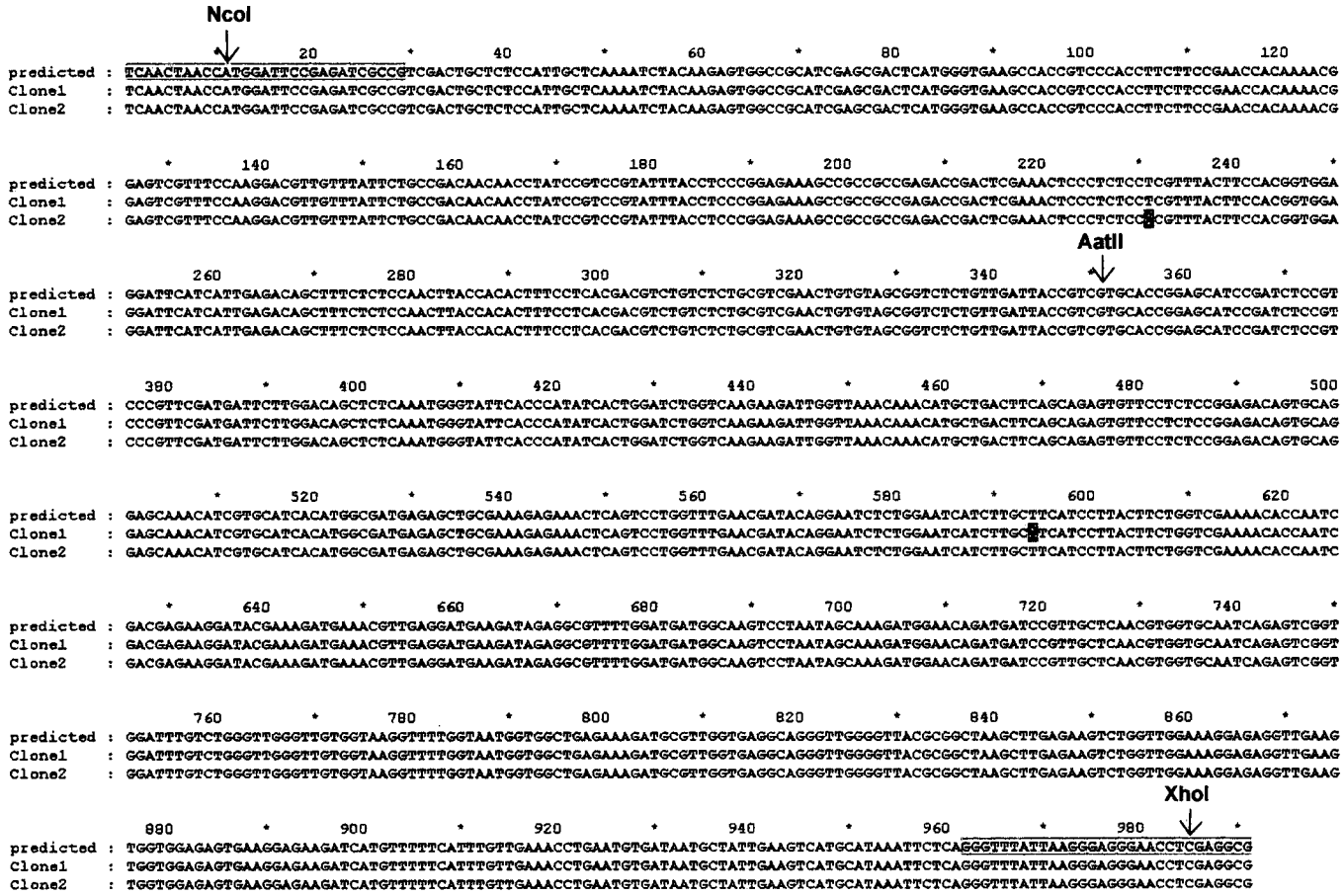

Figure 5.2: Sequences of the two mutant *AtCXE12* clones. The top line is the predicted PCR product, derived form the authentic *atcxe12* coding sequence. Errors in each of the clones are shown shaded black, whilst the parts of the predicted PCR product which correspond to the two primers are shaded grey. Relevant restriction sites are indicated.

The products of the restrictions were run out on an agarose gel and imaged (Figure 5.3).

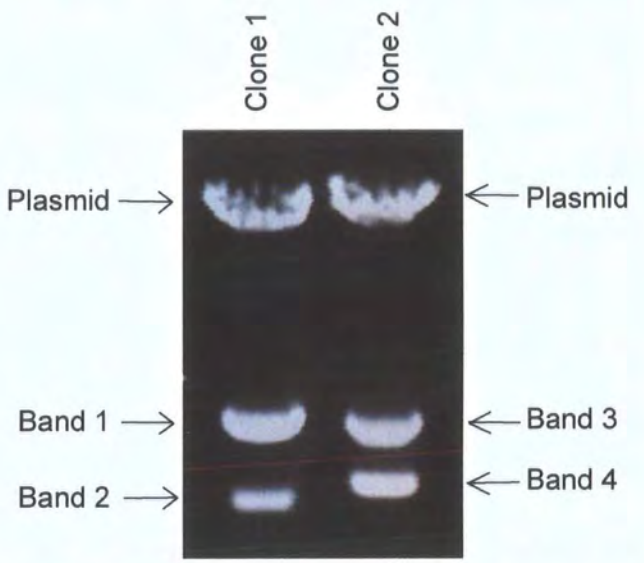

Figure 5.3: Digest results from restricting Clone 1 with *Aat*II and *Nco*I and Clone 2 with *Aat*II and *Xho*I. Approximate sizes of the bands were determined as Band 1: 680 bp, Band 2: 310 bp, Band 3: 590 bp, Band 4: 350 bp.

Each restriction produced three products, with linearised plasmid being the largest product in each lane, while the two other products accounted for as explained in Figure 5.4.

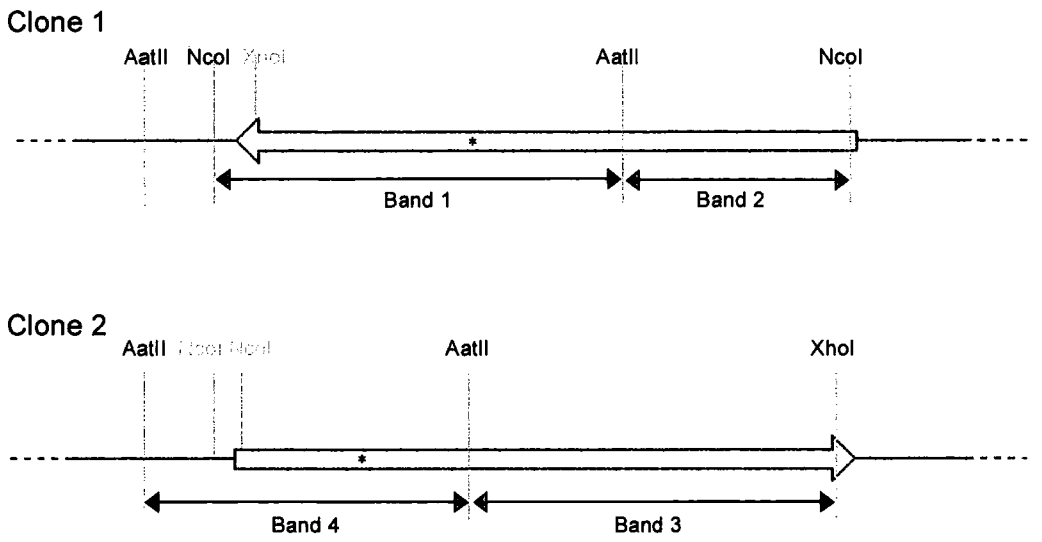

Figure 5.4: Schematic of the restriction of Clone 1 with *Aat*II and *Nco*I, and Clone 2 with *Aat*II and *Xho*I (not to scale). The inserted PCR products are shown as large arrows, the direction indicating the orientation of the AtCXE12 coding sequence in the plasmid. Also shown are the *Nco*I and *Aat*II restriction sites on the pGEMT-Easy plasmid, which neighbour the insertion site, leading to the additional restriction products. The approximate locations of the errors in the clones are marked with *.

Band 2 and Band 3 were excised and purified from the gel. The resulting DNA fragments were then ligated into pET24d in a tripartite ligation. The resulting ligation was used to transform Rosetta (DE3) pLysS competent cells, which were then plated on to LB agar containing kanamycin and chlorampenicol. A resulting colony was used to initialise a 10 ml LB starter culture with kanamycin and chloramphenicol selection, which was in turn used to inoculate a 100 ml culture after being allowed to grow overnight. When the larger culture had reached an optical density of approximately 0.6, it was induced with 1 mM IPTG, and left for an hour at 37 °C. The recombinant protein expressed under these conditions was then purified using a 2 ml nickel-chelate column. However,

the activity that was eluted was lower than expected, and it was established that the recombinant enzyme was not stable in the high concentrations of imidizole used to elute from the column. Therefore an alternative method was developed which used low pH (0.02 M MES pH 5.7) instead, with eluted fractions collected into 0.5 M buffer at pH 7.2. Further purification was then carried out on a phenyl suparose column to remove any remaining contaminating proteins. The two-step process yielded pure AtCXE12 (Figure 5.5).

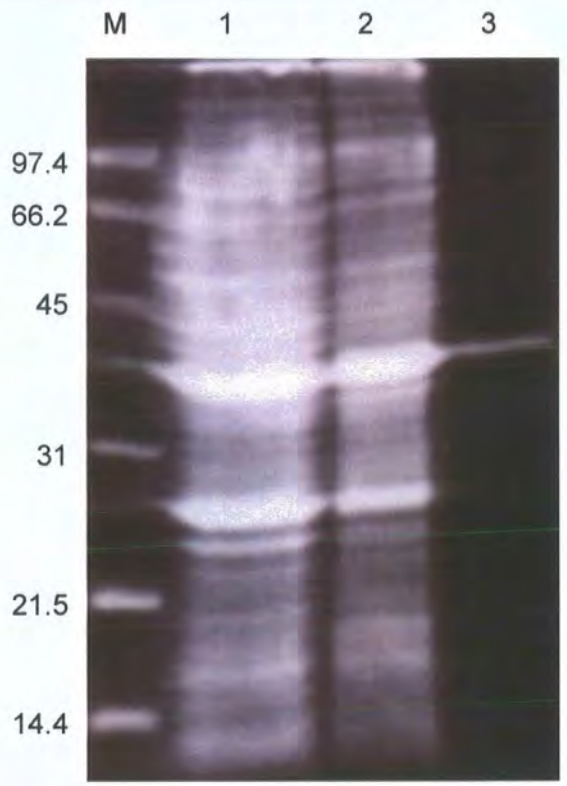

Figure 5.5: Fluorescence image of a Cypro Ruby stained gel showing purified recombinant AtCXE12.
M: size markers (Mw indicated in kDa), 1: insoluble protein, 2: soluble protein, 3: pure AtCXE12.

The purified protein showed very high activities toward both 2,4-D methyl (1.84 ± 0.45μkat/mg) and *p*-nitrophenyl acetate (6.23 ± 0.32μkat/mg). Kinetic studies

for AtCXE12 with *p*-nitrophenyl acetate showed low affinity binding (K_m = 2.4 ± 0.4 mM) with the enzyme having a V_{max} of 20.13 ± 2.3 ukat/mg pure protein corresponding to a turnover number of 720 s^{-1}. The pH optimum for catalysis was determined in 0.1 M potassium phosphate buffer between pH 5.8 and pH 8: the esterase showed the greatest activity at pH 7.4. The purified recombinant AtCXE12 was relatively stable on ice losing, 6 % of its activity when kept on ice overnight (~16 hours).

CHAPTER 6: INVESTIGATION OF A T-DNA INSERTION LINE OF ARABIDOPSIS DEFICIENT IN ATCXE12

6.1 Introduction

Chapter 4 described the purification of AtCXE12, a carboxylesterase that showed high activities toward 2,4-D methyl. Cloning and expression of AtCXE12 confirmed its activities *in vitro* (Chapter 5). For a full characterisation of the role AtCXE12 plays in the arabidopsis xenome, its activity *in vivo* needed to be investigated. If it had the same activity *in vivo* that was observed *in vitro*, then plants deficient in AtCXE12 should hydrolyse, and hence bioactivate, 2,4-D-methyl at a slower rate than wild-type plants. To test this, a SAIL T-DNA insertion line deficient in AtCXE12 expression was identified, characterised and then tested for modified susceptibility to 2,4-D-methyl. To confirm the absence of AtCXE12 in the SAIL plants, a variation on FP-biotin was used to visualise serine hydrolases in wild-type and insertion lines. A description of this probe is given below.

Tri-functional Fluorophosphono Probe (TriFFP)

In a development of FP-biotin (see section 4.1), a rhodamine moiety was added to the biotin and FP functionalities (Adam *et al.* 2002), making a trifunctional FP probe (TriFPP, Figure 6.1). The primary advantage of the addition of a fluorescent group was that it allowed the in-gel detection of labelled peptides.

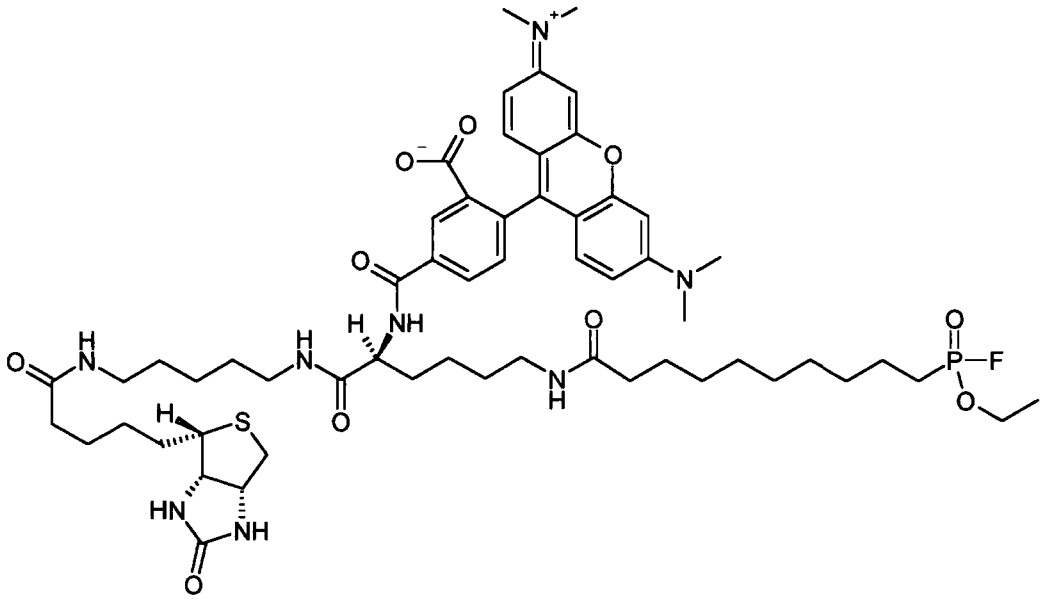

Figure 6.1: Trifunctional probe with fluorophosphono functinoality (TriFFP).

TriFFP is used in this chapter to label serine hydrolases from wild-type arabidopsis and a T-DNA insertion line to examine differences in serine hydrolase expression.

6.2 Results and Discussion

6.2.1 Selection of an AtCXE12-deficient T-DNA insertion line and characterisation of the T-DNA insertion site

T-DNA Express (http://signal.salk.edu/cgi-bin/tdnaexpress) was used to identify T-DNA insertion sites which would be expected to disrupt AtCXE12 expression. The SAIL T-DNA (Sessions *et al.* 2002) insertion line SAIL_445_GO3 was identified and obtained from the Nottingham Arabidopsis Stock Centre (NASC: Nottingham, UK). Homozygous lines were then selected using the diagnostic PCR reaction described on the SIGnAL website (http://signal.salk.edu/tdnaprimers.2.html). Using this method, wild type plants

should be characterised by a PCR product of 1000 bp, formed from the so-called left product (LP) and right product (RP) primers, which are designed to genomic DNA approximately 500bp up and downstream of the expected insertion site. However, when a T-DNA insert is present, this 1kbp product is not produced due to the insertion event between the LP and RP annealing sites. Instead, a product between RP and a primer designed to the left border to the T-DNA insert (LB) is formed, which is between 400 and 600 bp.

Unexpectedly, in the characterisation of SAIL_445_G03 it was found that while the wild type plants produced the 1 Kbp product, the plants that were presumed to be homozygous produced two different products of approximately 400 and 600 bp, with the putative heterozygotes producing all three products (see Figure 6.2).

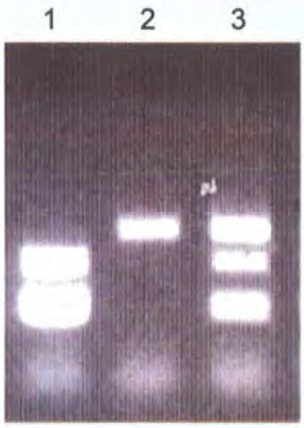

Figure 6.2: Products from diagnostic PCR of SAIL_445_G03 seedlings. 1: homozygote, 2: wild-type, 3: heterozygote.

The primers necessary for the formation of each product were determined. As expected, the left and right product primers (LP and RP) were responsible for the formation of the 1 kbp wild-type product. The 600 bp product was produced by

the T-DNA left border primer (LB) and RP. The 400 bp product was the unexpected product of LB and LP. These results indicated a back-to-back insertion of at least two T-DNAs, which would allow the LB primer to produce PCR products with both the RP and the LP primers. To test this hypothesis, the 400 and 600 bp products were sequenced. The sequence data confirmed the hypothesis of back-to-back insertions and established the exact position of the T-DNA insertion. Additionally, a minor deletion and a substitution in the area of the T-DNA insert were discovered. The position of the T-DNA insert and the nature of the substitution and deletion events are detailed in Figure 6.3.

Figure 6.3: The T-DNA insertion site and associated modifications to the genomic sequence in SAIL_445_GO3. The beginning of the longest AtCXE12 EST is marked *. The beginning of the AtCXE12 coding sequence is indicated: the ATG shown is the start codon.

As may be seen in Figure 6.3, the multiple T-DNA insertion in SAIL_445_GO3 with its corresponding 63bp deletion of genomic DNA is upstream of the AtCXE12 start codon. The longest AtCXE12 EST in the public databases starts at base-pair 18049310, in the middle of the 63bp deletion. This shows that the AtCXE12 transcription start site is either deleted by the T-DNA insertion, or is

possibly upstream of the insertion site. In either case, this would suggest that *AtCXE12* transcription is disrupted in SAIL_445_GO3.

6.2.2 Confirmation of disrupted of AtCXE12 expression

Protein extracts from Col 0 and homozygous SAIL_445_G03 plants were treated with TriFFP and separated using SDS-PAGE. The gel was visualised for rhodamine fluorescence (Figure 6.4).

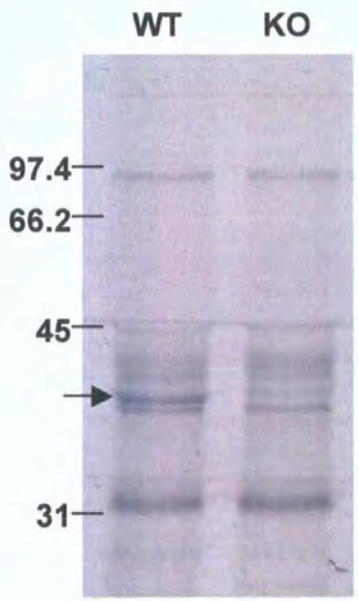

Figure 6.4: Confirmation of knockout of AtCXE12 expression in SAIL_445_G03. Protein extracts of arabidopsis Col0 (**WT**) and homozygous SAIL_445_G03 (**KO**) were labelled with TriFFP, separated by SDS-PAGE then imaged for rhodamine fluorescence. Mw as indicated in kDa, AtCXE12 is arrowed.

The fluorescent image of the labelled serine hydrolases in wild-type and SAIL_445_G03 plants confirmed that AtCXE12 expression was disrupted in the latter.

6.2.3 In vitro investigation of esterase activity in *atcxe12* plants

AtCXE12 shows good activity toward *p*-nitrophenyl acetate and 2,4-D methyl. Correspondingly, it would be expected that the activity toward these substrates would be lower in *atcxe12* knockout plants compared to wild-type. To test this hypothesis, three biological replicates of both knockout and wild type plants were each assayed in triplicate. Compared with wild-type plants, the knock-out plants showed less than a quarter of the activity toward 2,4-D, namely 120 ± 40 pkat/mg protein compared with 510 ± 120 pkat/mg. The hydrolysis of *p*-nitrophenyl acetate was less affected, with the *atcxe12* plants showing three quarters of the wild-type activity (450 ± 40 pkat/mg protein compared to 600 ± 60 pkat/mg). Figures quoted are averages of three biological replicates assayed in triplicate plus and minus the standard deviation.

6.2.4 Investigation into the effects of 2,4-D methyl on *atcxe12* and wild type plants

Since 2,4-D-methyl is significantly less phytotoxic than 2,4-D acid, plants with a reduced rate of hydrolysis of the ester *in planta* should have greater resistance than wild-type plants. To test whether this is the case with *atcxe12* plants, wild type and *atcxe12* seeds were germinated on MS sucrose agar containing from 0 to 100 μM 2,4-D methyl. Both lines of seed germinated on the lower concentrations of herbicide (<20μM). Following germination, they then all

showed symptoms of extreme 2,4-D toxicity: most of the plants eventually transformed to undifferentiated callus. The two lines showed very little overall difference in their response to the treatment. However, at the very lowest treatment rates with 2,4-D-methyl, there was some evidence that the knockout plants were showing greater tolerance to the proherbicide four weeks after the study was initiated. Thus, *atcxe12* plants growing on 0.5 µM and 10 µM 2,4-D-methyl retained greater differentiation than their wild type counterparts (see Figure 6.3). However, as the differences were only observed at one specific time-point, at very low 2,4-D-methyl concentrations, the results could not be considered an adequate demonstration of increased 2,4-D methyl tolerance due to the knockout of AtCXE12.

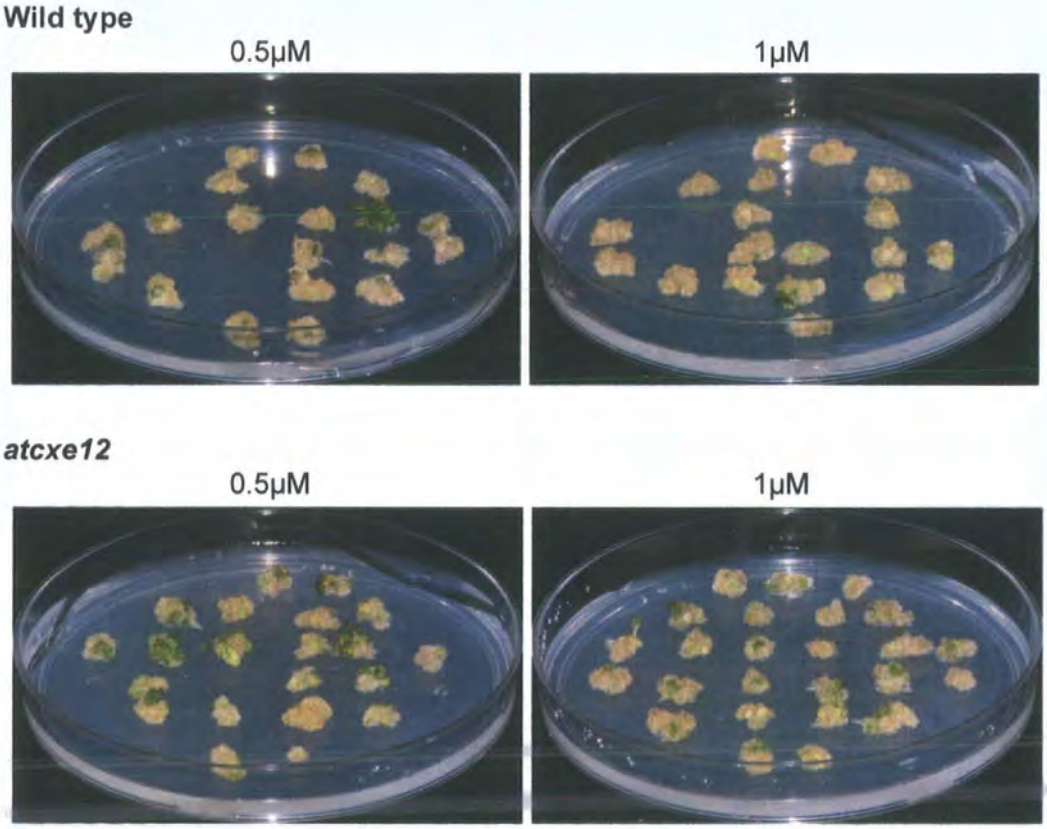

Figure 6.5: Results from the initial toxicity study. Knockout plants show greater retention of differentiation than the wild-type, which are almost entirely callus.

Figures above each image indicate the concentration of 2,4-D methyl in the agar.

A further experiment involving the spray-treatment of arabidopsis seedlings was devised, with the rationale that an acute exposure of plants to 2,4-D methyl may reveal a difference in resistance which the constant uptake of herbicide from the growth medium may have masked. Seedlings of both wild type and knockout plants were grown individually in compost. Four week old plants were sprayed with 0, 7.2, 18 and 36 g/Ha 2,4-D and 2,4-D-methyl formulated in aqueous 0.1 % Tween 20. After 96 hours, the effects of the herbicide treatments were assessed, and the plants were scored for 2,4-D toxicity using the scheme detailed in Table 6.1.

Score	Example	Description
10		Plants look the same as control plants: leaves are straight, bolt straight if present, no evidence of impeded leaf growth.
8		Leaves show some curling, rosette is flattened to soil due to curvature at leaf base, bolt thickened and stunted if present, no evidence of impeded leaf growth.
6		Leaves show pronounced curling, centre of rosette protruding slightly due to curvature at leaf base, bolt absent, apparent leaf area significantly smaller than control plants.
4		Some leaves curled to the point of inversion, rosette centre shows pronounced protrusion, bolt absent, apparent leaf area significantly smaller than control plants.
2		Many leaves curled to the point of inversion, rosette completely distorted, bolt absent, apparent leaf area significantly smaller than control plants.

Table 6.1: Scoring scheme use to assess 2,4-D toxicity

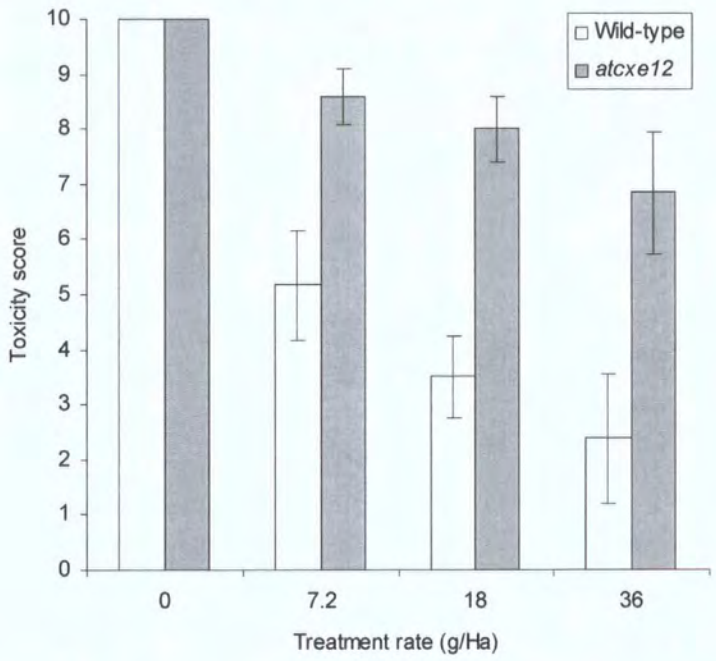

Figure 6.6: Toxicity of 2,4-D methyl to four-week-old wild-type and *atcxe12* plants at four different rates of herbicide treatment.

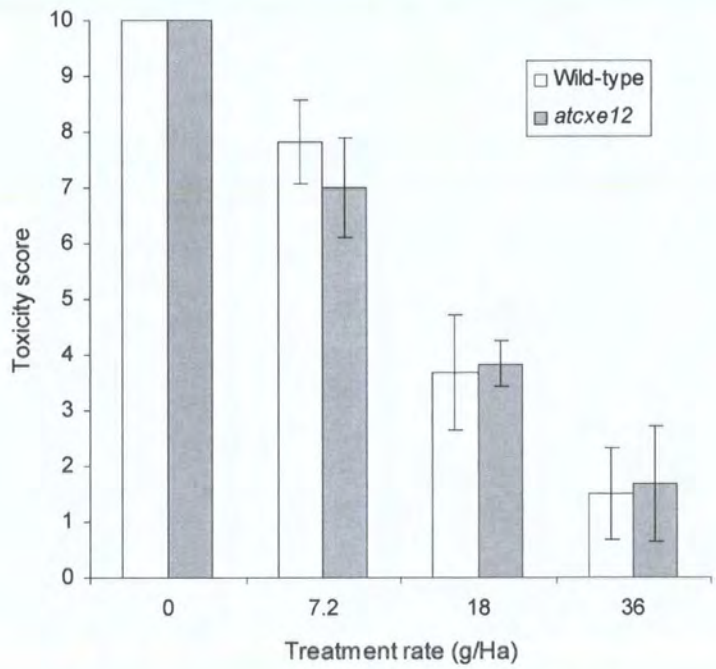

Figure 6.7: Toxicity of 2,4-D to four-week-old wild-type and *atcxe12* plants at four different rates of herbicide treatment.

The toxicity of 2,4-D to both lines was identical, with both sets of plants showing the same dose dependencies to herbicide treatment. The toxicity of 2,4-D-methyl to wild type plants followed a similar pattern to the acid over the same range of treatment rates. This suggests that the ester is hydrolysed very rapidly inside the plant, as is the case with other herbicide esters whose metabolism has been described in previous studies (Roberts, 1998). The knockout plants, by contrast were considerably more tolerant of 2,4-D -methyl (see Figures 6.6 and 6.8).

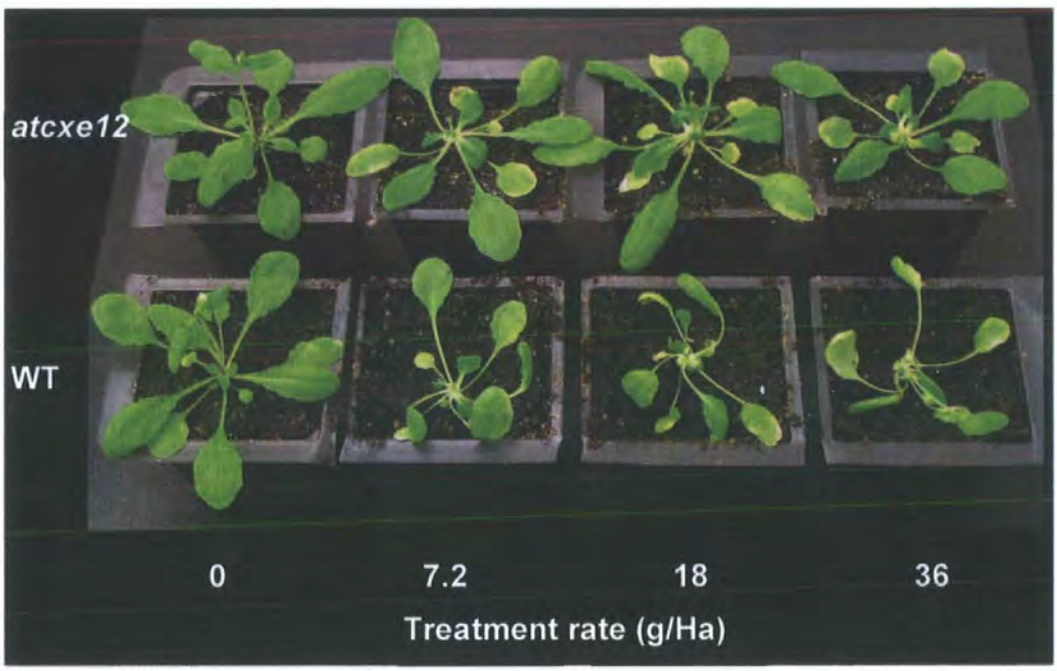

Figure 6.8: Differential toxicity of 2,4-D methyl to wild-type and *atcxe12* plants.

The toxicity study therefore clearly shows the imporance of AtCXE12 in determining the bioactivation of 2,4-D methyl in arabidopsis. This is highly significant in that it has not previously been demonstrated that a change in esterase activity alone is sufficient to increase tolerance to a carboxylic ester proherbicide.

However, it should be noted that a subsequent experiment carried out at Syngenta found that this effect was lost when higher treatment rates of herbicide (50 to 1600 g/Ha) were used on mature plants. This is not entirely unexpected, as there is a residual rate of 2,4-D methyl hydrolysis in *atcxe12* plants. Therefore if herbicide is applied at sufficiently high rates, the residual rate is likely to be sufficient to allow sufficient amounts to be activated so that normal levels of toxicity are observed. It is also possible that the age of the plants has an effect on how quickly the proherbicide is activated.

For a comprehensive assessment of the effect that knocking out AtCXE12 has on 2,4-D methyl metabolism, further studies are required that investigate the effects of 2,4-D methyl on *atcxe12* plants at different times in their development. Additionally, metabolism studies using radiolabelled 2,4-D methyl would allow quantitative data to be generated on the exact difference in the rates of 2,4-D methyl hydrolysis in wild-type and knockout plants.

The study carried out at Syngenta shows that the difference in rates of pro-herbicide activation is not sufficient to protect the knockout plants from the quantities of herbicide that would be used in agricultural applications. However, this does not rule out the possibility of much higher levels of herbicide resistance being generated in other plant species through the knockout of a carboxylesterase: if the esterase is more exclusively responsible for the hydrolysis of the chosen herbicide ester than AtCXE12 is for 2,4-D methyl in *Arabidopsis*, then the levels of resistance generated could conceivably be significantly higher. This raises the possibility of breeding crops with the

intention of deliberately knock out herbicide bioactivating carboxylesterases in order to increase tolerance. The disadvantage of such an approach is that such CXE knockout plants may suffer disadvantages related to the endogenous role of the disrupted enzyme. The *atcxe12* plants described in this chapter showed no visible phenotype until they were sprayed with 2,4-D-methyl, giving no indications of the endogenous role of AtCXE12. However, in light of the roles of plant carboxylesterases elucidated to date, it is possible that AtCXE12 is involved in a response to biotic or abiotic stress, in which case a phenotype is only likely to occur when *atcxe12* plants are subjected to the appropriate stressful conditions.

CHAPTER 7: USE OF CHEMICAL PROBES TO INVESTIGATE PLANT SERINE HYDROLASES

7.1 Introduction

As was discussed in Chapter 1, there is a wide diversity of plant esterases reported in the scientific literature. These have a range of reported biological functions including roles in secondary metabolism, development and response to stress and disease. The work presented in this chapter is an investigation to assess the potential of fluorophosphono (FP) probes to aid the investigation of serine hydrolases in future, building on the earlier use of FP-biotin to aid the purification of carboxylesterases from arabidopsis cell suspension culture (Chapter 4). Of primary importance was to confirm the potential of chemical probes to purify sufficient quantities of serine hydrolases from crude protein extracts to allow their identification with proteomic methods. An additional benefit of carrying out such a study was that the range of enzymes that may be labelled with FP-probes could be investigated, and additional serine hydrolases that are expressed in plants could be proteomically identified.

In the work presented below, TriFPP is used to investigate the range of serine hydrolases found in different arabidopsis tissues. In addition, fenchlorim-treated tissue was also investigated, to determine how application of safeners affects serine hydrolase expression and activity.

7.2 Results and Discussion

7.2.1 Profiling serine hydrolases in foliage, root culture and suspension culture.

Protein extracts from arabidopsis suspension culture, leaves and root culture (± safener treatment) were treated with TriFFP. After excess probe had been removed using gel-filtration, the labelled proteins were purified using streptavidin sepharose then separated using SDS-PAGE. The labelled proteins were visualised for rhodamine fluorescence (Figure 7.1). Relative levels of serine hydrolase were determined through quantification of rhodamine fluorescence.

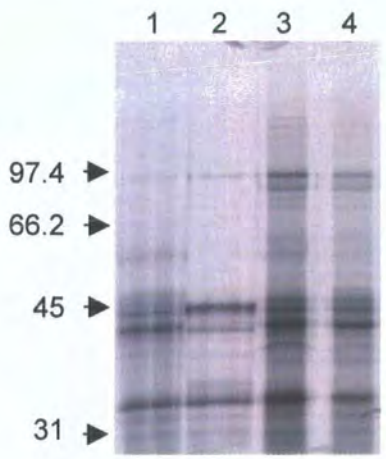

Figure 7.1: Fluorescence image of FP-TFP-labelled proteins, affinity purified from arabidopsis plants and cultures using streptavidin sepharose. Lane 1: foliage, 2: suspension culture, 3: root culture, 4: safener treated root culture. Migration of molecular mass markers is indicated (values in kDa).

The amount of serine hydrolase purified per milligram of starting protein was much lower in leaf and cell culture extracts. Much of the total protein content in leaf material is accounted for by photosynthetically-involved proteins, which would effectively reduce the relative concentration of all other proteins, including the serine hydrolases. This cannot be the case with the cell culture extracts however, as they are grown in the dark and do not exhibit large amounts of photosynthesis-related proteins. Therefore the lower levels of protein visible in the cell culture sample may reflect lower relative concentrations of serine hydrolases. However, this does not correlate with the carboxylesterase specific activities determined for suspension cultures, roots and foliage (see Chapter 3) where suspension culture showed greater specific activities toward many of the substrates tested. This implies that the labelling and purification method used in this study may not give reliable quantification between samples, possibly due to loss of streptavidin sepharose during washing steps.

Some contaminating, non-labelled protein was evident when the gel had been blue-stained to visualise the total protein present (data not shown). However, for the most part, the labelled proteins had been effectively purified away from the rest of the proteome. The rhodamine fluorescence from each lane was quantified, resulting in the data represented in the graphs in Figure 7.2. The data were normalised to the total amount of fluorescence present in each lane to allow comparison of the relative levels of expression of each enzyme within each sample. This normalisation was carried out because the method of affinity purifictaion used (see section 2.2.6) did not allow for the determination of protein concentrations prior to loading of the gel. Therefore the protein loadings could not be standardised relative to each other. The normalisation of the data obtained

from the gel was to allow similar comparisons to be made to those that would have been possible if the protein loadings could have been standardised.

Figure 7.2 shows quantitatively what is also evident from the gel image: root culture and plant tissue contain similar profiles of labelled proteins whilst cell culture shows a very different pattern of expression. One protein in particular, of 45 kDa is much more highly expressed in cell suspension cultures compared to the other labelled proteins, while the protein at 43 kDa was present at much lower levels.

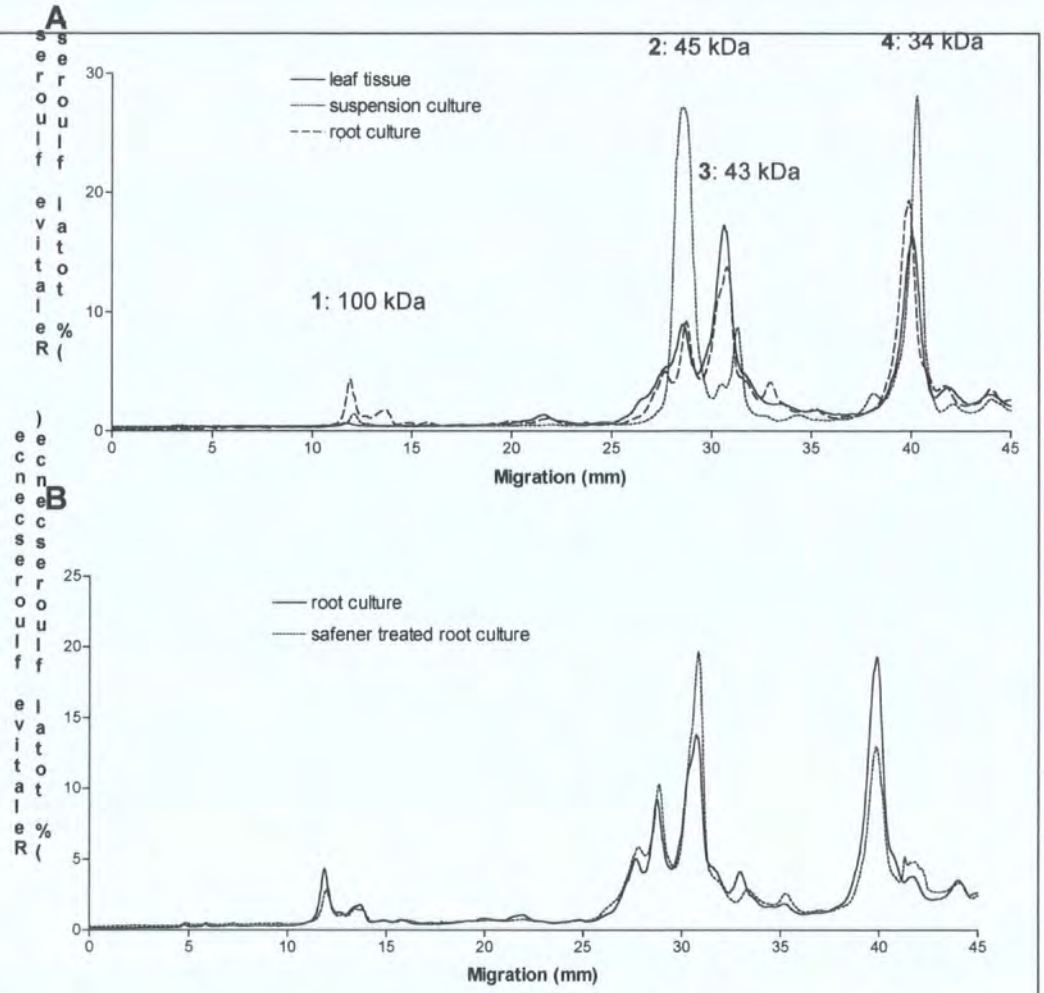

Figure 7.2: Quantification of rhodamine fluorescence from the serine hydrolase purifications. **A**: comparison of TriFPP-reactive proteins from foliage, root culture and cell suspension culture. **B**: TriFPP-reactive proteins from root culture plus and minus safener treatment. Data is normalised to the total fluorescence in each sample to allow for comparison of relative levels of enzyme expression. The four major polypeptides are numbered and approximate masses given.

In the comparison between safener-treated and non-treated root culture, there is a possible change in the levels of the 43 kDa and 34 kDa enzymes, however, it is a relatively small change which would need to be confirmed with further replication of the experiment.

The major fluorescently-labelled polypeptides were excised from the gel and submitted for identification by MALDI-TOF mass spectrometry (Table 7.1). The identities were all determined with $p < 0.05$.

Band	Protein identification	Structural superfamily	Carboxylesterase family	Predicted mass (Da)	TAIR accession
1	prolyl oligopeptidase	α/β	N/A	90317	At1g76140
2	GDS hydrolase	GDS	II	44056	At3g26430
3	AtCXE12	α/β	IV	35759	At3g48690
4	Lysophosholipase-like carboxylesterase	α/β	VI	26996	At5g20060

Table 7.1: The identities of the four major serine hydrolases in arabidopsis.

The MALDI analysis confirmed that the same major polypeptides were expressed in each tissue. Three of the enzymes identified were potential carboxylic ester hydrolases: AtCXE12, a GDS hydrolase and a lysophospholipase-like carboxylesterase. Prolyl oligopeptidase was also identified, showing that TriFPP can label serine hydrolases involved in the cleavage of amide bonds. Three of the enzymes identified belong to the α/β hydrolase fold superfamily, while the other is a GDS hydrolase, so all the enzymes contain a catalytic triad of serine-histidine-aspartate. The structures of the enzymes identified, as well as bioinformatic analyses of their respective enzyme families in arabidopsis are detailed in the following section.

7.2.2 Bioinformatic analysis of serine hydrolases in arabidopsis

This study is the first time that the enzymes identified have been determined in arabidopsis (except for AtCXE12 in Chapter 4). In particular, while several GDS hydrolases have been characterised in other plants (see section 1.5.3.2), the family in arabidopsis has not been described as expressed proteins.

This section will present a bioinformatic analysis of the serine hydrolase sequences that were identified using proteomics. The primary bioinformatic tools utilised to obtain the data presented were iterative BLAST searches to identify homologues of the proteins identified by proteomics, and then MPSS data (massively parallel signature sequencing: http://mpss.udel.edu/at/) were also referred to, to examine levels and locations of expression of the enzymes identified. Additionally, the cellular location of the proteins was predicted using TargetP (http://www.cbs.dtu.dk/services/TargetP/). Finally, the Agrikola website (http://www.agrikola.org/index.php?o=/agrikola/main, Hilson *et al.* 2004) was searched for the phenotypic effects of knocking out each gene. Agrikola is a European project that is endeavouring to knock out every gene in arabidopsis using RNAi. Full genomic coverage has not yet been achieved, but all phenotypes observed so far in the project are detailed in the online database.

7.2.2.1 Nomenclature

There is not an established nomenclature for carboxylesterases: one family of plant carboxylesterases was named by Marshall *et al.* 2003, but the nomenclature proposed (AtCXE1 to 20) is insufficient for the diversity of carboxylesterases that have been identified in plants, which are members of several distinct enzyme families. Additionally, to call enzymes carboxylesterases based solely on sequence homology is misleading: as

discussed in Chapter 1, even relatively closely related enzymes may have quite diverse activities. It therefore seems very unlikely that an entire enzyme family will be found to show activity toward xenobiotic carboxylic esters, which is what is strictly meant by the term carboxylesterase. An alternative could be to call the different families serine hydrolases. This would be accurate, but the term is more broad than it needs to be: most of the enzymes in the families described in Chapter 1 have activities toward carboxylic ester bonds, even if they are not carboxylesterases, so these families will be referred to as carboxylic ester hydrolases. This way, lipases and other enzymes with endogenous substrates are included, as well as carboxylesterases. For the discussion of carboxylic ester hydrolase families in the following sections, each esterase will be referred to in the following format: AbCEHX-Y, where A and b are the initial letters of the genus and species from which the enzyme is derived, X refers to the CEH family number (following the classification detailed by Arpigny and Jaeger (1999)), and Y is to allow differentiation between members of the same family. The numbering of family IV CEHs established by Marshall will be kept, so AtCXE12, for example becomes AtCEH4-12. The enzymes that have confirmed carboxylesterase activity (AtCXE12, AtCXE5 and AtCXE20, see Chapter 4), will still be refered to as CXEs, and their numbers kept as they are to avoid confusion.

7.2.2.2 Family II carboxylic ester hydrolases (CEH2s)

As discussed in Chapter 1, the GDS hydrolases are the only family of CEHs that has a structure not based on the α/β-hydrolase fold. GDS hydrolases have by far the most genes in arabidopsis of any of the CEH families: 103 separate arabidopsis genes were identified by PSI-BLAST using the GDS hydrolase identified by proteomics (AtCEH2-1). Of note is the high level of similarity of many of the genes (up to 95 % sequence identity), showing that the numbers of GDS hydrolases have proliferated in recent evolutionary history. Figure 7.3 shows a tree of all the arabidopsis GDS hydrolases, along with several enzymes from other species that have been described in the literature.

The arabidopsis GDS hydrolase identified by proteomics is in clade IV, along with lanatoside 15'-O-acetylesterase from *Digitalis lanata* (DlLAE), early nodulation factor from *Medicago sativa* (MsENOD8) and *Zm*AChE, acetylcholinesterase from *Zea mays*. Analysis of MPSS data for the CEH2s shows a wide diversity in levels and locations of expression (see Table 7.2). Most CEH2s showed at least low levels of expression, with 27 genes showing no detectable expression in the MPSS database. AtCEH2-1 (band 2 identified by proteomics, see section 7.2.1) had high levels of expression overall, showing greatest expression in callus. This correlates with the TriFFP quantification, where greatest expression was in cell culture, which is generated from callus and is composed of undifferentiated cells. The MPSS data also showed expression of AtCEH2-1 in all other tissues. This is in contrast to many other CEH2s, whose expression was highly localised to one tissue type. Of particular note was the large number of genes with high expression specifically in inflorescence tissue. The number of genes expressed in the flowers may be a little surprising, but

CEHs have been noted in plant reproductive tissues in the past: MC3 from *Pinus radiata* was identified in male pine cones (Walden *et al.* 1999), and serine hydrolases have been shown to be important in pollen tube penetration of the stigma in *Brassica napus* (Hiscock *et al.* 2002). There were also several genes that only showed expression in root tissue and three that showed large levels of expression in germinating seedlings, but no significant expression otherwise. As has been found before with GDS hydrolases, almost all of the enzymes were predicted to be secreted into the apoplast (TargetP, http://www.cbs.dtu.dk/services/).

Most CEH2 genes were present in the Agricola RNAi line database, however only seven had phenotypes documented (see Table 7.3). These were primarily growth phenotypes and were associated with genes that showed high and mainly tissue-specific expression in the MPSS data. Two of the inflorescence-specific gene knockouts showed particularly severe phenotypes, including chlorosis (AtCEH2-26) and sterility (AtCEH2-68). The lines where only growth phenotypes were observed showed high overall expression (AtCEH2-36), or high expression specifically in the leaves (AtCEH2-93) or roots (AtCEH2-40). AtCEH2-1 knockout lines do not show a phenotype according to the database. This is the same result that was observed with *atcxe12* plants, and may be due to similar reasons as those postulated in Chapter 6: both genes may be involved in stress responses, so knockout plants will only show phenotypes when subjected to stressful conditions. An alternative hypothesis is that when a particular CEH is knocked out, other CEHs are upregulated to compensate, masking any phenotype that may otherwise have occured.

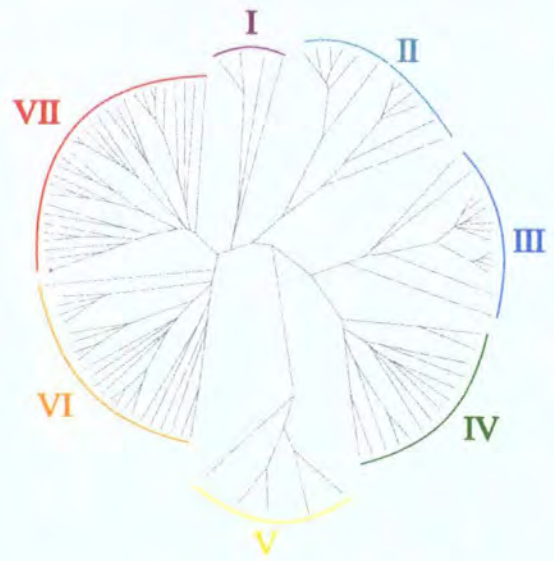

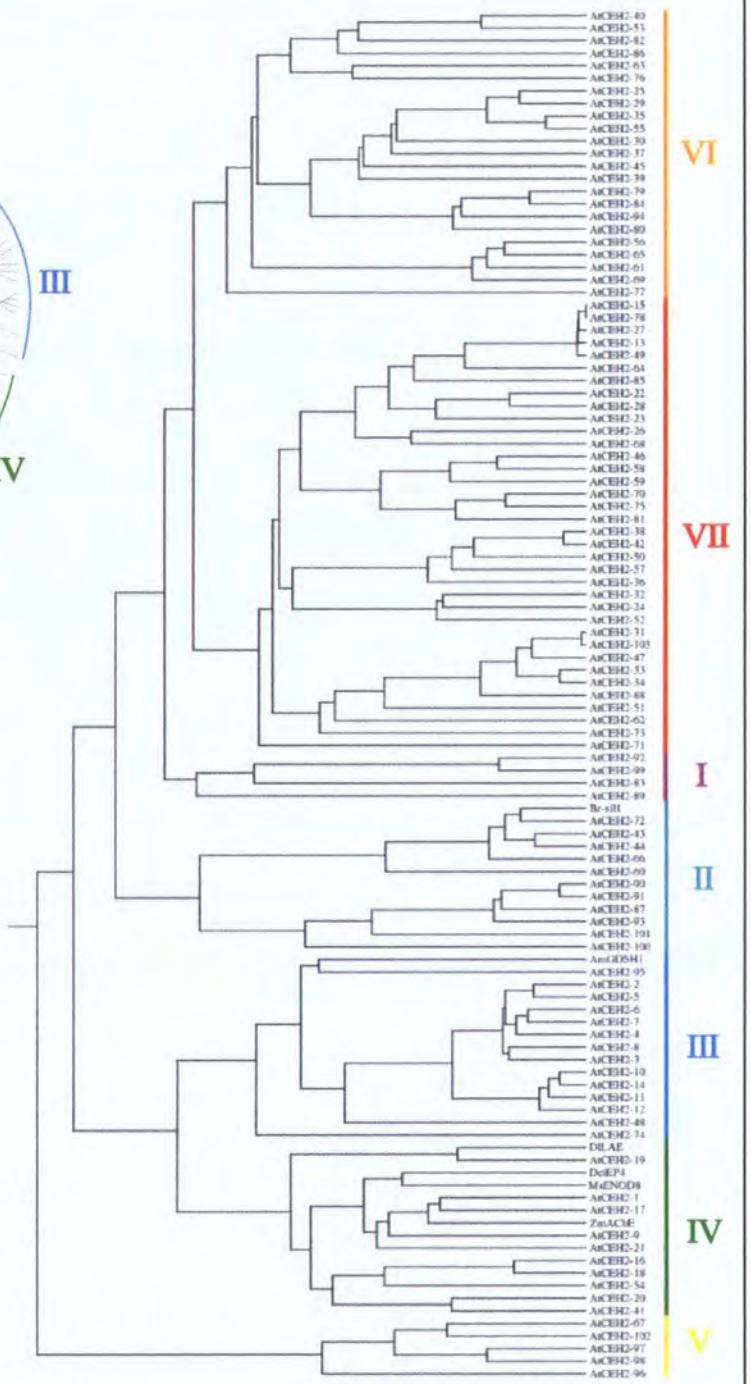

Figure 7.3: Tree (**A**) and cladogram (**B**) of arabidopsis family II CEHs. Clades identified using **A** were numbered to aid identification in **B**. Both diagrams were produced with 100 bootstrapped replicates. Consensus values for the major clades are given in **B**. DILAE: *Digitalis lanata* lanatoside 15'-O-acetylesterase, ZmAChE: *Zea mays* acetylcholinesterase, AmGDSH1: *Alopecurus myosuroides* GDS hydrolase 1, MsENOD8: *Medicago sativa* early nodulation factor, DciEP4: *Daucus carota* elicitor-induced CEH.

Table 7.2 (next page): AtCEH2s. The TAIR accession number for each enzyme is given, along with MPSS expression data and cellular location prediction. * V. high, high, med or low refer to overall levels of expression (v. high: >2000 tpm (transcripts per million) in at least one tissue source, high: >100 tpm, med: > 20 tpm, low: < 20 tpm, - : no expression detected); root, leaf, inf (inflorescence), germ (germinating seedlings) or sil (silique) shows that the specified tissue had substantially more expression than the other tissues. ** Loc: predicted location: S: secreted, cyt: cytosolic, M: mitochondrial.

Name	TAIR	MPSS*	Loc**
AtCEH2-1	At3g26430	high	S
AtCEH2-2	At1g28580	high	S
AtCEH2-3	At1g28600	med	S
AtCEH2-4	At1g28590	-	S
AtCEH2-5	At1g28570	med	S
AtCEH2-6	At1g28610	-	S
AtCEH2-7	At2g27360	med	S
AtCEH2-8	At1g31550	low	S
AtCEH2-9	At5g14450	low	S
AtCEH2-10	At1g28670	med	S
AtCEH2-11	At1g28640	-	S
AtCEH2-12	At1g28650	-	S
AtCEH2-13	At3g43550	-	S
AtCEH2-14	At1g28660	high germ	S
AtCEH2-15	At1g59406	low	S
AtCEH2-16	At1g09390	med	S
AtCEH2-17	At1g67830	med	S
AtCEH2-18	At1g56670	low	S
AtCEH2-19	At4g01130	low	S
AtCEH2-20	At1g54790	low	S
AtCEH2-21	At3g27950	med root	S
AtCEH2-22	At1g75880	high inf	S
AtCEH2-23	At1g75900	low	S
AtCEH2-24	At2g04570	high inf	S
AtCEH2-25	At1g29670	med sil	S
AtCEH2-26	At1g20120	high inf	S
AtCEH2-27	At1g58480	med sil	S
AtCEH2-28	At1g75890	med	S
AtCEH2-29	At1g29660	med leaf sil	S
AtCEH2-30	At1g33810	low	S
AtCEH2-31	At2g31540	low	S
AtCEH2-32	At2g42990	low	S
AtCEH2-33	At2g30310	low root	S
AtCEH2-34	At2g30220	low root	S
AtCEH2-35	At5g45670	low	S
AtCEH2-36	At3g16370	high	S
AtCEH2-37	At1g71691	med sil	S
AtCEH2-38	At5g03810	-	S
AtCEH2-39	At5g15720	-	S
AtCEH2-40	At2g23540	high root	S
AtCEH2-41	At3g05180	high	S
AtCEH2-42	At5g03820	-	S
AtCEH2-43	At1g53940	root	S
AtCEH2-44	At5g40990	low	S
AtCEH2-45	At1g71250	-	S
AtCEH2-46	At1g23500	low	S
AtCEH2-47	At1g58430	inf sil	S
AtCEH2-48	At5g45910	low inf	S
AtCEH2-49	At3g43570	med sil	S
AtCEH2-50	At5g22810	-	S
AtCEH2-51	At1g06990	med inf	S
AtCEH2-52	At4g26790	sil inf	S
AtCEH2-53	At3g50400	-	S

Name	TAIR	MPSS *	Loc **
AtCEH2-54	At3g62280	med root call	S
AtCEH2-55	At4g18970	high not root	S
AtCEH2-56	At5g33370	v. high inf	S
AtCEH2-57	At3g53100	med	S
AtCEH2-58	At1g73610	low sil	S
AtCEH2-59	At5g63170	-	S
AtCEH2-60	At1g53920	low	S
AtCEH2-61	At5g18430	low	M
AtCEH2-62	At2g40250	-	S
AtCEH2-63	At5g37690	high root	S
AtCEH2-64	At3g14820	-	cyt
AtCEH2-65	At3g04290	v. high inf	S
AtCEH2-66	At3g14225	low	S
AtCEH2-67	At5g03590	-	cyt
AtCEH2-68	At1g20130	high inf	M
AtCEH2-69	At4g28780	high inf	S
AtCEH2-70	At1g75910	high inf	S
AtCEH2-71	At5g45950	high inf	S
AtCEH2-72	At1g53990	low	S
AtCEH2-73	At5g45960	high inf	S
AtCEH2-74	At3g48460	high sil	S
AtCEH2-75	At1g75920	high inf	S
AtCEH2-76	At1g74460	high root	S
AtCEH2-77	At4g10950	-	S
AtCEH2-78	At1g58725	med sil	cyt
AtCEH2-79	At2g19060	-	S
AtCEH2-80	At2g19010	-	S
AtCEH2-81	At1g75930	high inf	S
AtCEH2-82	At5g41890	med sil	cyt
AtCEH2-83	At5g55050	low	S
AtCEH2-84	At2g19050	-	S
AtCEH2-85	At5g42170	-	S
AtCEH2-86	At4g16230	low	S
AtCEH2-87	At1g54020	low inf	S
AtCEH2-88	At2g24560	-	S
AtCEH2-89	At1g71120	-	S
AtCEH2-90	At1g54010	high germ	S
AtCEH2-91	At1g54000	high germ	S
AtCEH2-92	At2g04020	-	S
AtCEH2-93	At3g14210	high leaf	S
AtCEH2-94	At4g30140	med root	S
AtCEH2-95	At5g03980	-	S
AtCEH2-96	At2g36330	-	S
AtCEH2-97	At5g03610	high	S
AtCEH2-98	At3g09930	-	S
AtCEH2-99	At2g03980	med	S
AtCEH2-100	At1g54030	high	S
AtCEH2-101	At3g14220	high	S
AtCEH2-102	At5g03600	med inf	M
AtCEH2-103	At2g31550	-	cyt

Name	Agrikola phenotype	MPSS*
AtCEH2-26	Growth, Leaf shape, Chlorosis	high inf
AtCEH2-36	Growth	high
AtCEH2-40	Growth	high root
AtCEH2-64	Silique	-
AtCEH2-68	Growth, Leaf shape, Sterile	high inf
AtCEH2-93	Growth	high leaf

Table 7.3: CEH2s with their Agrikola RNAi knockout phenotypes. MPSS data are also repeated from Table 7.2 to allow comparison. * high: >100 tpm, inf (inflorescence), leaf, root: expression predominantly in specified tissue, - : no detected expression.

7.2.2.3 Family IV carboxylic ester hydrolases (CEH4s)

The CEH4s include all of the enzymes with confirmed carboxylesterase activity identified in the work presented in Chapter 4. The gene family has previously been characterised, and the abundance of transcripts for each gene quantified using RT-PCR (Marshall *et al.* 2003). When compared with MPSS data, the RT-PCR results correlate well overall, although sometimes show expression where the MPSS data would suggest none. This may indicate that MPSS can occasionally give false negative results. None of the RNAi lines in the Agrikola database for family IV enzymes had recorded phenotypes.

7.2.2.4 Family VI carboxylic ester hydrolases (CEH6s)

The fourth band identified by proteomics (AtCEH6-1) belongs to the 6th family of carboxylic ester hydrolases, and is the first plant member of this family to be identified. Iterative BLAST revealed two homologues in arabidopsis and several more in rice and mammalian systems (Figure 7.4). Interestingly the human homologue is an acyl-protein thioesterase. This enzyme is responsible for the removal of palmatoyl modifications from G-protein α subunits (Devedjiev *et al.* 2000). Palmatoylation is an essential factor in the localisation of G-protein subunits to the plasma membrane. Therefore removal of the lipid attachment through action of the thioesterase has an effect on G-protein mediated signal transduction. It is possible that AtCEH-1 has a similar role *in planta*, and if so, is another example of an esterase involved in the propagation of signals in plants.

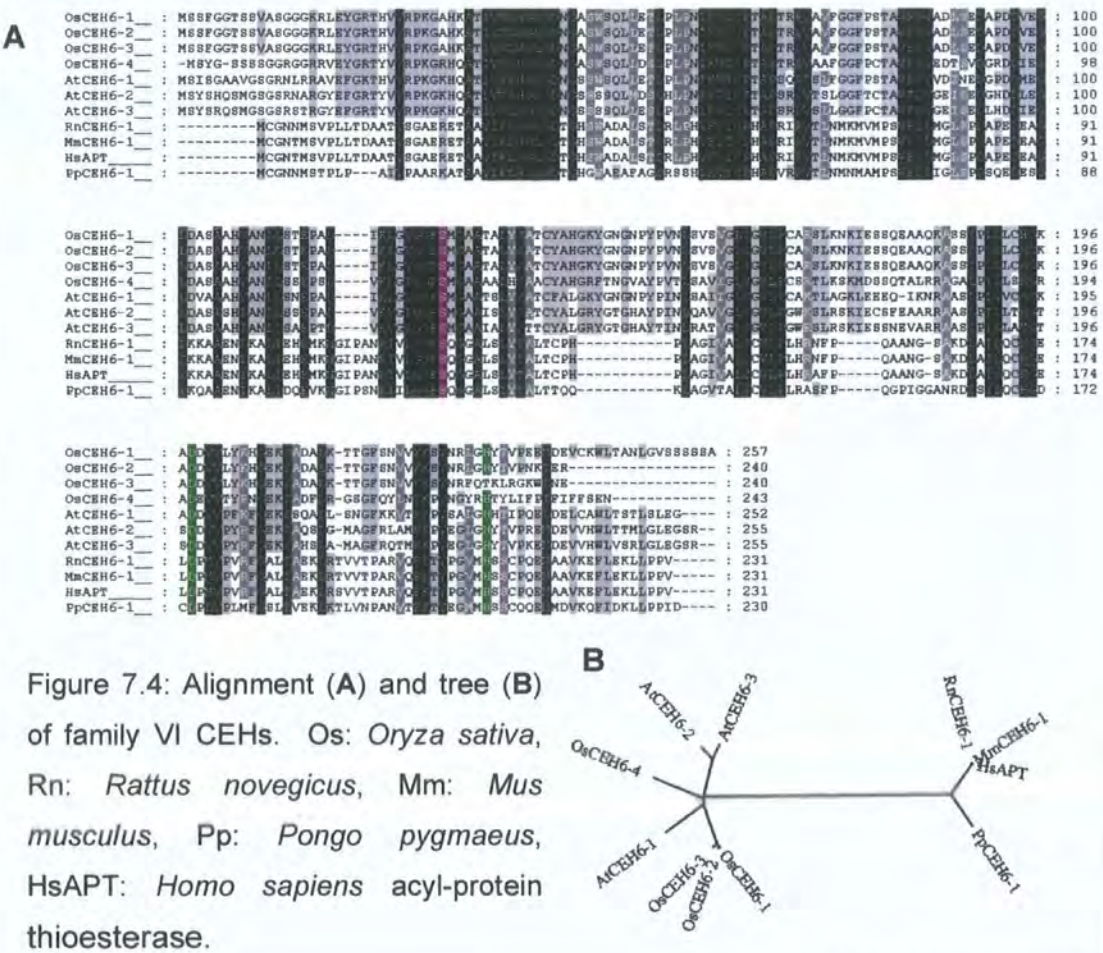

Figure 7.4: Alignment (**A**) and tree (**B**) of family VI CEHs. Os: *Oryza sativa*, Rn: *Rattus novegicus*, Mm: *Mus musculus*, Pp: *Pongo pygmaeus*, HsAPT: *Homo sapiens* acyl-protein thioesterase.

Name	TAIR	MPSS*
AtCEH6-1	AT5G20060	med
AtCEH6-2	AT1G52700	-
AtCEH6-3	AT3G15650	med

Table 7.4: AtCEH6s. The TAIR accession number for each enzyme is given, along with the MPSS expression data. * med: > 20 tpm, - : no expression detected.

The MPSS data indicated that the expression of AtCEH6-1 and AtCEH6-3 is spread amongst all tissues, with no marked localisation. There was no evidence to show AtCEH6-2 is expressed. The Agrikola lines for AtCEH6-1 and AtCEH6-2 were not available at the time of writing, and there was no recorded phenotype for the AtCEH6-3 knockout line.

7.2.2.5 Prolyl endopeptidase

As the name implies, prolyl endopeptidase (also known as prolyl oligopeptidase) cleaves proteins adjacent to proline residues, a role that requires a specialised enzyme due to the kink in the protein backbone cause by the presence of a proline residue.

In contrast to the other serine hydrolases identified in this study, prolyl endopeptidase (PEP) is not part of a family of enzymes in Arabidopsis, with no related Arabidopsis sequences apparent using PSI-BLAST. Similarily, rice only has one PEP sequence. PEP sequences from different species are closely conserved, so that mammalian and plant enzymes share >50 % sequence identity (Figure 7.5). Again, this is in contrast to the other serine hydrolase families

investigated here. It implies that PEP has a well-defined and vital role in organisms throughout nature, as opposed to the disparate roles to which carboxylic ester hydrolases have been recruited throughout evolution.

PEP is significantly larger than the carboxylic ester hydrolases labelled by TriFFP. It is another example of an α/β hydrolase, but possesses a very large N-terminal domain in the form of a β-propeller, which is positioned over the active site and regulates the enzyme's activity (see Figure 7.6). There is a very small entrance to the active site, and it is remarkable that the TriFFP was able to label the active site serine. That PEP was labelled in sufficient quantities to allow its proteomic identification speaks for the effectiveness of the probe, and shows that it may be used to study the expression and activities of a wide range of disparate serine hydrolases.

A

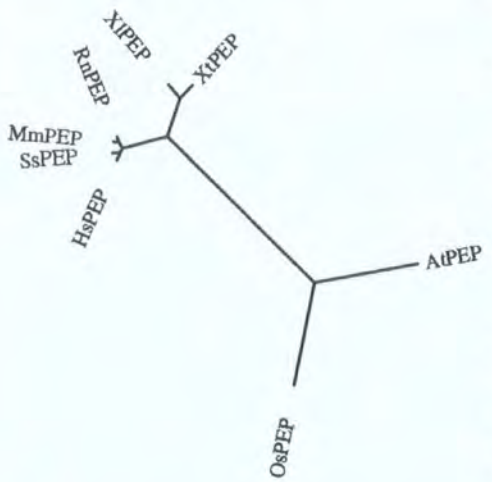

Figure 7.5: Prolyl endopeptidase sequence comparison. **A**: phylogenetic tree and **B**: sequence alignment. Species abbreviations: At: *Arabidopsis thaliana*, Os: *Oryza sativa*, Hs: *Homo sapiens*, Ss: *Sus scrofa* (pig), Mm: *Mus musculus*, Rn: *Rattus norvegicus*, Xl: *Xenopus laevis*, Xt: *Xenopus tropicalis*. Active site residues are in purple (serine) and green (aspartate and histidine).

B

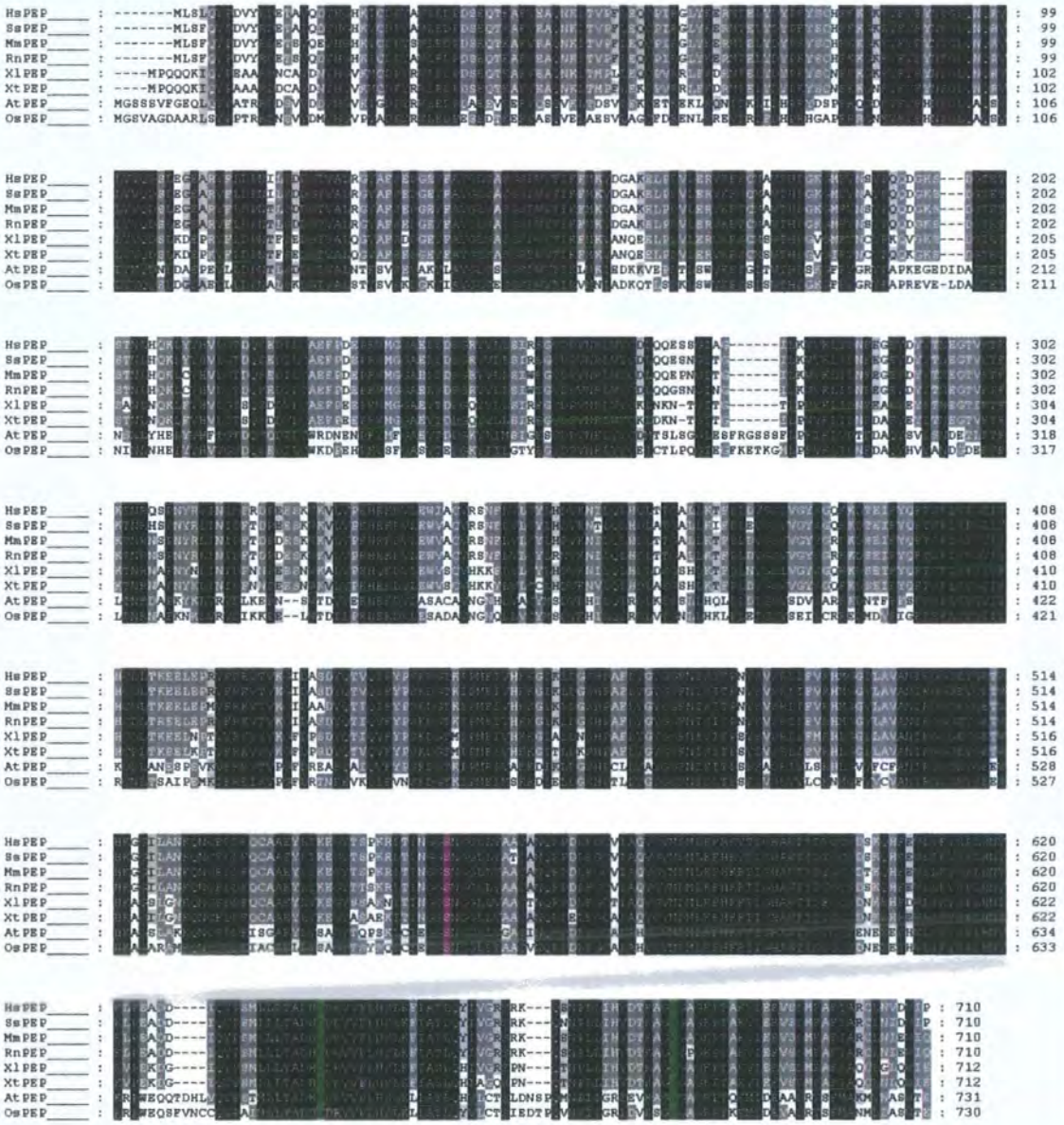

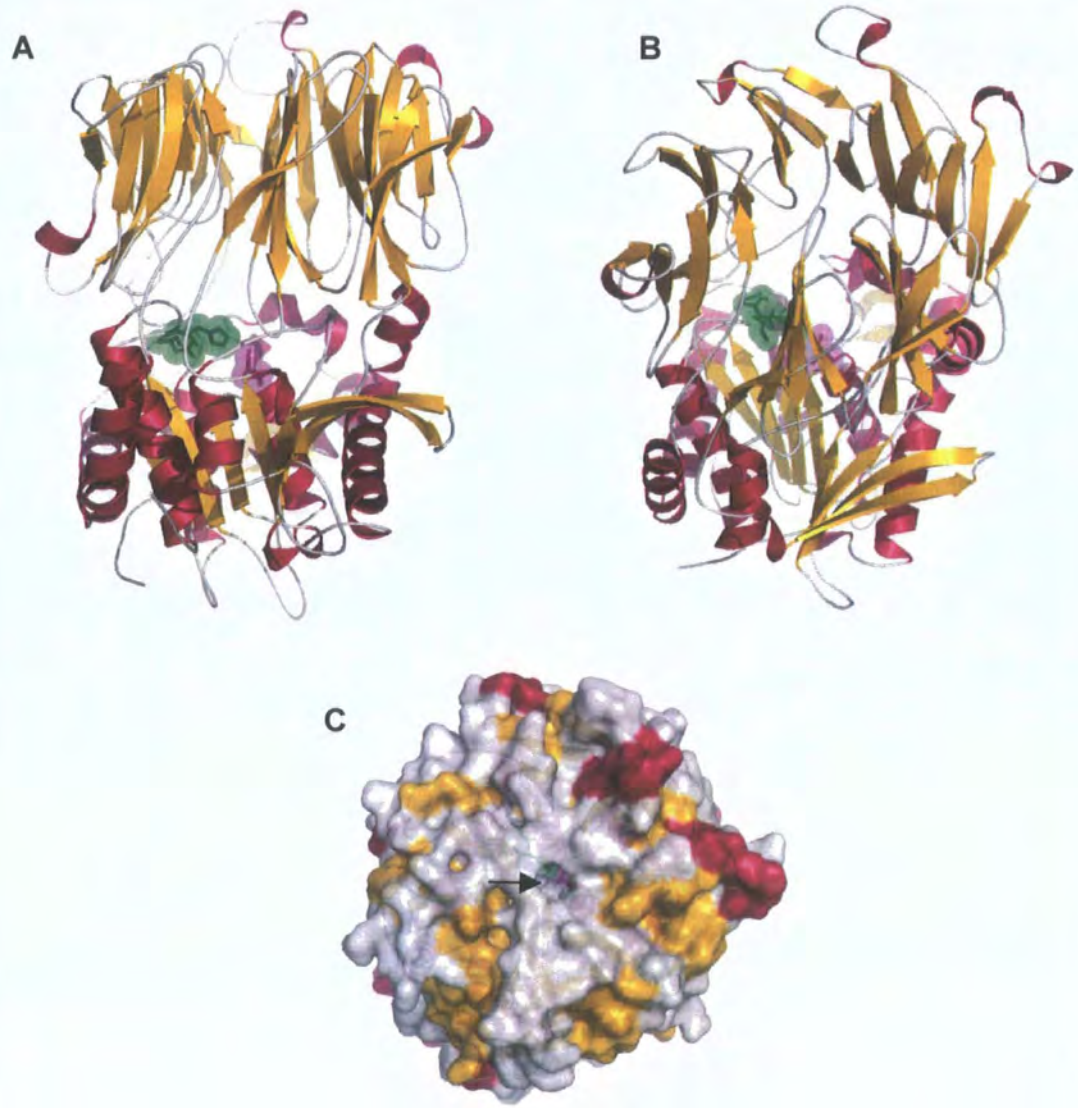

Figure 7.6: The crystal structure of porcine prolyl endopeptidase. **A**: the α/β hydrolase fold domain may be clearly seen in the lower half of the molecule. The upper half is a β-propeller domain, the radial nature of which can be more clearly seen in the tilted orientation of the molecule shown in **B**. **C** is a view of the top of the enzyme, with the surface of the protein shown. The very small entrance to the active site is arrowed. α-helices are shown in red, β-sheets in yellow and active site residues in green and purple.

7.3 Conclusion

Four major arabidopsis serine hydrolases have been identified using TriFFP. None of the enzymes have been identified before in arabidopsis outside of the work in this thesis. The versatility of TriFFP has been demonstrated in that it inhibited a range of enzymes including a peptidase with a restricted active site entrance. With the exception of the prolyl endopeptidase, the enzymes identified are members of families of CEHs in arabidopsis. The families vary dramatically in size: there are just three enzymes in the case of the AtCEH6s, while there are 103 family II enzymes. Bioinformatic studies of the families has revealed a diversity of expression levels and in many cases defined localisations within the plant.

In total, there is a very large number of CEHs in arabidopsis: in addition to those described in this chapter and the family IV members detailed in Marshall *et al.* (2003), there are 14 arabidopsis genes belonging to CEH family I, making a total of 140 arabidopsis CEH genes in total. One clear limitation of the initial proteomic study presented in this chapter is that it only identified four serine hydrolases. The primary reason for this is a lack of resolution in the SDS-PAGE gel. A primary priority in future work of this sort has to be to refine the method used to produce a protein sample suitable for running on a 2-D gel, which would provide much greater resolution.

Arabidopsis is clearly an ideal system for studying the roles of plant carboxylesterases in future, and TriFFP has the potential to aid that study considerably. In order that the full diversity of serine hydrolases in arabidopsis

may be analysed using chemical probes in future, however, a method that allows the greater resolution of the labelled serine hydrolases must be established.

CHAPTER 8: DISCUSSION

This project has made significant progress in the study of plant carboxylesterases. Carboxylesterase activities been profiled in a large number of agronomically important crops and weeds, and *Arabidopsis thaliana* has been established as an ideal model system for the enzymes' investigation. The major arabidopsis carboxylesterase with activity toward 2,4-D methyl (AtCXE12) was isolated, identified, cloned, expressed and characterised. Knock-out plants incapable of producing AtCXE12 were used to show definitively for the first time that differential esterase activity alone is sufficient to alter the toxicity of proherbicide treatment. Finally, trifunctional chemical probes were used to further investigate the plant carboxylesterase proteome, identifying the major serine hydrolases in arabidopsis.

The work has also opened many opportunities for further research, which are discussed in the following sections.

8.1 Exploiting esterases: manipulating rates of agrochemical metabolism.

Chapter 3 revealed that the acyl moiety of an ester is likely to play a significant role in determining the rate of the ester's hydrolysis by plant carboxylesterases. Additionally, it has been established, both in previous work (Jeffcoat and Harries 1975) and in Chapter 6, that differential rates of herbicide bioactivation through carboxylesterase-mediated hydrolysis can lead to herbicide selectivity. This presents the possibility that herbicide selectivity could be created or improved for a given herbicide by esterification of hydroxyl groups with acyl groups designed

to reduce the rate of bioactivation in crop plants. An approach like this would require the extensive mapping of carboxylesterase activities in crops and target weeds in order to identify acyl groups that are poorly hydrolysed by crop carboxylesterases, but are more rapidly metabolised in weeds. The approach as a whole is attractive, as such mapping could be relatively easily carried out with convenient colourimetic substrates such as *p*-nitrophenyl esters, allowing a large number of substrates and plants to be assayed in mass screens in order to identify acyl groups with the required properties. An additional advantage of the strategy is that it does not require the production of new phytotoxic moieties, instead relying on ester modification of existing herbicides in order to alter their potency in selected plant species.

As well as modification of the herbicides applied, there is the potential to alter the levels and activities of the esterases present in the plants being treated. The most obvious, and probably most elegant, method by which crop plant esterase activity could be altered would be through the used of genetic modification. Not only could this alter the way that xenobiotics are metabolised in the crop, but it also has the proven potential to confer resistance to pathogens: an esterase from *Pantoea dispersa* which is capable of detoxifying the phytotoxic metabolite albicidin was engineered into sugarcane. The sugarcane was subsequently resistant to *Xanthomonas albilineans*, which produces the toxin and normally causes a disease known as leaf scald (Zhang and Birch, 1997). In addition, due to the role that esterases undoubtedly play in many plant stress responses, the overexpression of selected esterases could conceivably increase resistance to abiotic stresses as well. However, due to the current hostile public perception of genetic modification as a technology, these strategies are possibly untenable in

the present climate. However, genetic modification of esterase expression is not the only means by which esterase activity could be manipulated. Biochemical treatments could be applied to plants in order to inhibit esterase activity, and the resulting change in the carboxylesterase part of the xenome could be exploited with the use of proherbicide esters like those discussed above. Existing organophosphate inhibitors would be an obvious initial choice, but more selective inhibitors could also be developed. There is also the potential for upregulating certain carboxylesterases using biochemical treatment: the close association of some carboxylesterases with signalling pathways within the plant presents the possibility of increasing production of those enzymes in selected plants by treating plants with a signalling compound such as salicylic acid. Such an approach could conceivably be used to promote increased detoxification of herbicides that are inactivated through hydrolysis. Admittedly, an application of a signalling compound to a field would alter the xenome of all plants in the field, crops and weeds alike. However, the wide diversity of plant carboxylesterases suggests that the enzymes upregulated in each species would be likely to have very different activities, so an application may result in a differential alteration of the xenome of each species treated.

However, for approaches like those outlined above to be directed properly and exploited to their full potential, plant carboxylesterases would need to be characterised to a much higher level than has currently been achieved. A full characterisation of carboxylesterases would also undoubtedly benefit many other areas of plant biology, since carboxylesterases and related enzymes have been shown to be involved in many extremely important processes *in planta*, particularly in responses to biotic and abiotic stress. The next section addresses

methods by which the plant carboxylesterase proteome could be effectively investigated.

8.2 Using fluorophosphono (FP) chemical probes to map carboxylesterase expression and regulation

The work described in Chapters 4 and 7 has illustrated the effectiveness of using chemical probes to profile plant enzymes that exhibit a particular active site chemistry. The primary advantage of using such probes is that they enable the simplification of the proteome down to a much smaller, clearly defined subset of proteins. Instead of trying to deal with thousands of different proteins, chemical probes allow the analysis of a specific group of (for example) tens of proteins, which have been enriched dramatically from their concentrations in crude protein extract, allowing the identification of enzymes with levels of expression that dictate that they would normally be overlooked entirely. The potential ways in which FP probes could be utilised in order to investigate plant carboxylesterases are outlined in the following sections.

8.2.1 Analysis of carboxyesterase expression and regulation

A proteomic approach to the investigation of carboxylesterase expression and regulation is particularly desirable due to the indications in Chapter 4 that some may be regulated through post-translational modification. Use of a trifunctional FP probe would enable levels of serine hydrolase expression in plants to be established, and if used in conjunction with two-dimensional gel electrophoresis, phosphorylation events would be immediately apparent due to the change in a protein's pI that accompanies phosphorylation events. If used post stress-

treatment, purification of serine hydrolases using FP-probes would be a rapid way of identifying those carboxylesterases upregulated in response to the stress.

8.2.2 Increasing the specificity of FP-probe-based investigations

As has been shown in Chapters 4 and 7, FP-probes label multiple serine hydrolases in *Arabidopsis*. However, there is potential to increase the specificity of labelling and differentiate between different parts of the serine hydrolase proteome. For example with the use of competing inhibitors such as eserine when labelling with FP-probes, the serine hydrolase part of the proteome could be differentiated into cholinesterases and other enzymes. Alternatively, if a substrate of interest was added during inhibition, those enzymes that metabolised the substrate would be at least partially protected from the probe, so could be identified when the products of such an inhibition were analysed alongside the labelled proteins from an inhibition carried out without substrate. Other methods of improving the FP probe's specificity would be to alter the structure of the probe itself. Making the probe more bulky adjacent to the FP moiety or including hydrophilic functional groups would alter which enzymes are inhibited. Creating a library of different probes with various moieties next to the FP reactive group would allow the profiling of multiple carboxylesterase binding sites simultaneously, by investigating which probes bind to which enzymes.. Porcine liver esterase is an example of where binding site mapping of this sort has been extensively carried out by investigating the esterase's activities to a range of differently sized substrates (see Figure 8.1). The mapping of the active site has enabled porcine liver esterase to be used for specific applications in chemical synthesis (Ottolina and Carrea, 2002). Mapping using FP-probe

variants could be used in conjunction with the biochemical studies discussed in section 8.1 to aid the design of herbicide esters.

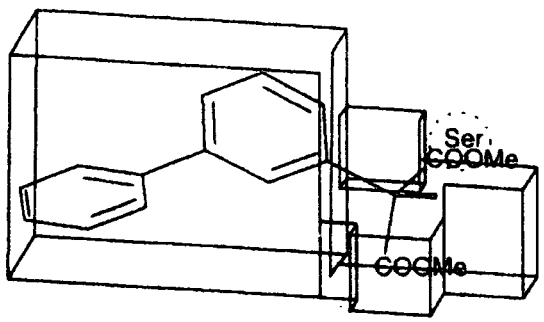

Figure 8.1: The active site of porcine liver esterase, as mapped using a range of structurally constrained ester substrates (taken from Ottolina and Carrea, 2002).

8.2.3 Histochemistry using FP-probes

Staining for carboxylesterase activity in sections of tissue has been carried out in the past using naphthyl esters in the same way that esterase activities may be stained in isoelectric focussing gels (Xia and Steeves, 1999). The method could be adapted with the use of an FP-probe, so that all serine hydrolases could be visualised. The method could be refined by using two probes with different fluorophors: an initial probe with fluorophor 1 could be used to inhibit in the presence of a competing reversible inhibitor or substrate, then a second inhibition using the second fluorophor-linked probe would be carried out which would label those enzymes which had been protected from the first inhibitor. When the section of tissue was imaged for the presence of the two fluorophors, the localisation of esterases that have activity toward a given substrate, or are inhibited by a certain inhibitor would be revealed. Alternatively, structural

variants of the probe like those discussed in section 8.2.2 could be used to determine the localisation of specific esterases.

8.2.4 Identifying carboxylesterase-associated proteins

It has been demonstrated in chapter 4 how FP-probes can dramatically simplify the purification of individual carboxylesterases. Once a single labelled enzyme is immobilised on streptavidin beads, the beads could be incubated with crude protein preparations, washed with low levels of salt to remove non-specifically bound proteins, then specifically bound proteins could be eluted and visualised.

8.2.4 Regeneration of carboxylesterase activity

The primary disadvantage of using FP-probes is that the end result is in the form of inactive protein. Whilst this is immaterial if the only goal is to identify the proteins purified, it prevents any further biochemical characterisation beyond what can be deduced from the inhibition itself, or achieved prior to inhibition. An ideal situation would be if the inhibition could be reversed post-purification, leading to pure active protein. A potential way of achieving reactivation is thorough the use of oxime compounds (Figure 8.2). Oximes have been found to reactivate organophosphate-inhibited mammalian acetylcholinesterase, although the mechanism by which they do this is unknown (Luo *et al.* 1999).

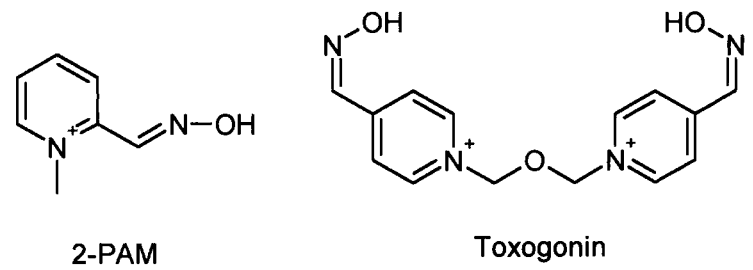

2-PAM Toxogonin

Figure 8.2: Oxime compounds, which can regenerate organophosphate-inhibited acetylcholinesterase.

It has been found that in the presence of quaternatery ligands such as edrophonium (Figure 8.3), over 90 % of original acetylesterase activity can be restored with 1mM oxime (Luo *et al.* 1998).

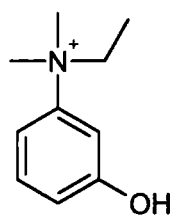

Figure 8.3: Edrophonium

However, in the same paper it is also stated that reactivation rates may vary dramatically depending on the inhibiting organophosphate and the enzyme that is inhibited. In spite of this, even if a large percentage of activity was lost overall, purification of active esterase via an FP-probe inhibition could provide a rapid and convenient method for isolating active serine hydrolases from crude protein extract.

8.3 Possible roles of carboxylesterases *in planta*

8.3.1 Endogenous roles of carboxylic ester hydrolases

This thesis has described the presence of a very large number of arabidopsis genes that may code for carboxylesterases. However the endogenous role of the proteins they encode is currently unknown. As many of the plant esterases described in Chapter 1 are involved in signalling pathways common to all plants, it seems likely that homologues for each of these will be found in arabidopsis. The esterases involved in secondary metabolism like LAE and PNAE are likely to be more species specific. Nevertheless, there is a high probability that esterases involved in secondary metabolism will be identified in arabidopsis. Indications of possible reactions may be mediated by arabidopsis esterases may be found using AraCyc, part of The Arabidopsis Information Resource (TAIR, www.arabidopsis.org). AraCyc aims to detail all of *Arabidopsis* metabolism, and specify the enzymes involved with each reaction. It also supplies a list of all the reactions that are included in the database but do not have an enzyme assigned to them. Included in this list is one reaction in particular that is obviously esterase-mediated: the hydrolysis of O-sinapoylcholine (sinapine, see Figure 8.4).

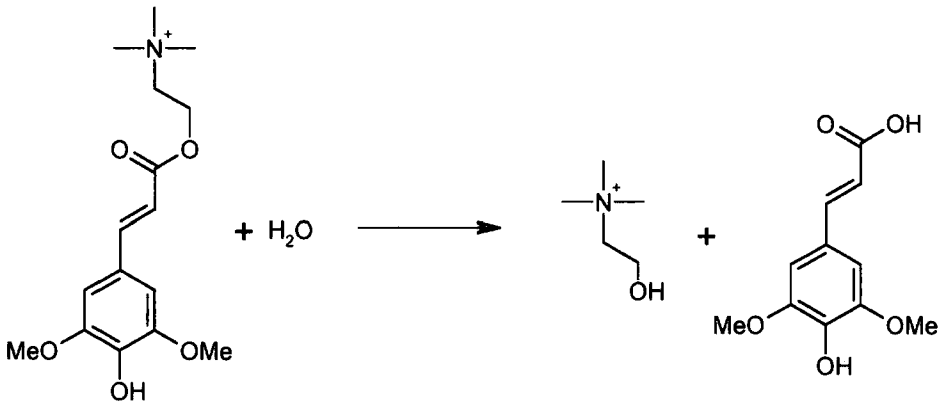

Figure 8.4 Hydrolysis of sinapine into sinapate and choline.

An examination of the literature reveals a number of additional phenylpropanoid cholinesters in plants (Figure 8.5), for which hydrolytic activity has been found in radish (*Raphanus sativus*), but the enzymes responsible have not been identified (Strack *et al.* 1980).

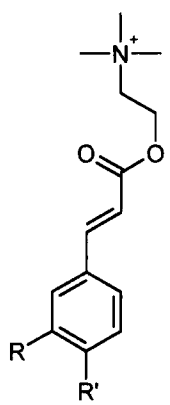

Compound	R	R'
cinnamoylcholine	H	H
coumaroylcholine	H	OH
caffeoylcholine	OH	OH
feruloylcholine	OMe	OH

Figure 8.5: Phenylpropanoid cholinesters that are hydrolysed in *Raphanus sativus* (Strack *et al.* 1980).

Another area in which it is clear that carboxylic ester hydrolases are involved is in the metabolism of esters of plant signalling compounds. CEHs are already implicated in methyl jasmonate and methyl salicylate hydrolysis. Intriguingly,

several other signalling compounds, including auxins and gibberellins are carboxylic acids, presenting the possibility that they also exist as esters whose levels are mediated by CEH activities.

8.3.2 Endogenous roles of carboxylesterases

The question of what role carboxylesterases fulfil in plants is less straightforward: why have plants evolved the capability of hydrolysing a wide range of xenobiotic esters? It is immediately apparent why animals have the capability to detoxify exogenous compounds, since animals, especially herbivores, constantly encounter potentially dangerous compounds in their food. However, as autotrophs, plants have no need of enzymes to detoxify antifeedant compounds. However, there is significant natural source of phytotoxins which plants must be able to detoxify in order to survive: this section will argue that much of the xenobiotic ester hydrolysing capability present in the plant xenome has evolved primarily to aid detoxification of phytotoxins produced by plant pathogens. Plants are subject to attack from a wide diversity of pathogenic microorganisms, both bacterial and fungal. These pathogens produce a wide array of phytotoxic compounds, which include esters and lactones such as those in Figure 8.6.

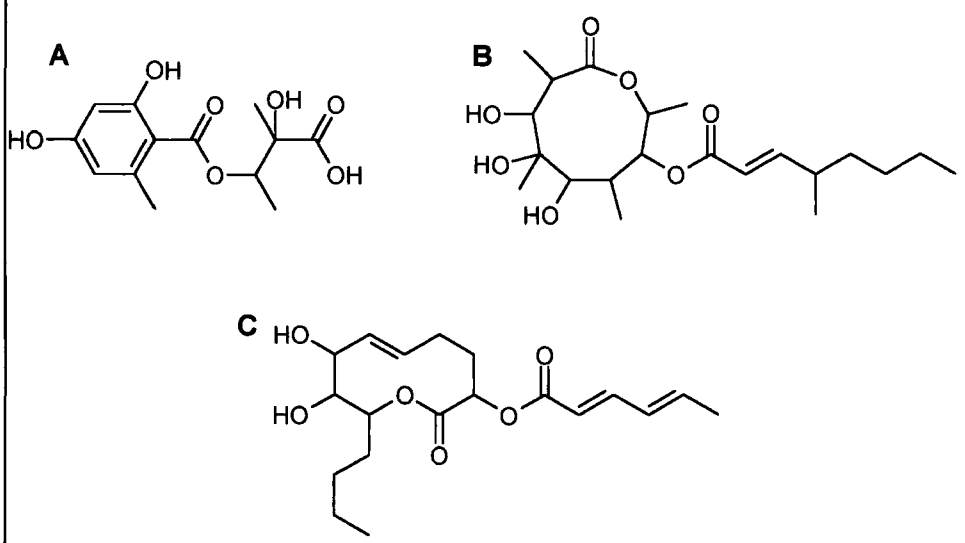

Figure 8.6: Phytotoxic fungal and bacterial esters and lactones (Cutler, 1995). **A:** Phomozin (from *Phomopsis helianthi*), **B:** Botcinolide (*Botrytis cinerea*) **C:** Pinolidoxin (*Ascochyta pinodes*).

Also produced by plant pathogens are compounds that mimic plant growth factors. Of special interest in the context of the work presented in this thesis is 2,5'-dihydroxy-3'-nitrophenylacetic acid methyl ester (Figure 8.7), a compound produced by *Pseudomonas syringae* pv. *papulans*, which causes blister spot disease in apples and pears (Cutler, 1995). The compound acts as an auxin mimic, in a very similar way to 2,4-D-methyl. This presents the possibility that AtCXE12 is expressed in plants to help with the detoxification of such compounds. Alternatively, it could be that pathogens producing such compounds are exploiting the presence of enzymes like AtCXE12 in plants so that their toxins are bioactivated *in planta* in the same way herbicide esters are. This presents the possibility that *atcxe12* plants may be expected to be either less or more resistant to fungal pathogens that produce such compounds than wild-type plants, depending on which hypothesis is correct.

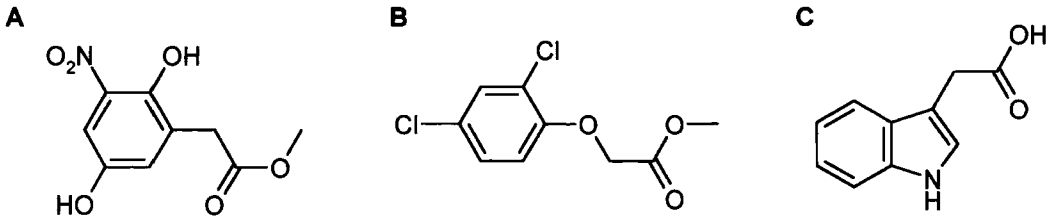

Figure 8.7: 2,5'-dihydroxy-3'-nitrophenylacetic acid methyl ester (**A**). 2,4-D-methyl (**B**) and indole acetic acid (**C**) are also shown for comparison.

There is other, circumstantial evidence that CXEs exist for the purpose of detoxifying toxic compounds produced by pathogens. The hypothesis may explain why there is such a proliferation of CEH genes in the arabidopsis genome (see Chapter 7): the evolution of such a large number of genes may well have been in response to an equally rapid evolution of pathogen-produced toxins. The toxins in Figure 8.6 are quite curious in one respect: all of them have side groups neighbouring the ester bond, making the bond less accessible. This observation would also fit in with the "arms race" hypothesis: maybe the reason these compounds are still toxic to plants is that they have evolved so as not to be easily hydrolysed by the plants' defensive carboxylesterases.

Additionally, it is possibly no coincidence that the largest CEH gene family codes for enzymes that are predominantly extracellular: it would be a considerable advantage to the plant to be able to cleave esters before they entered the cell, as the hydrolysis products would be likely to be more hydrophilic than the ester, making them less able to cross the plasma membrane.

Finally however, the strongest argument is a general evolutionary one: plant pathogens produce phytotoxic compounds, so plants without detoxification mechanisms would be killed.

There is a strong evolutionary pressure on plants to produce effective detoxification mechanisms, and carboxylesterases are part of those detoxification systems.

8.4 Conclusion

This thesis has characterised a carboxylesterase from arabidopsis important in xenobiotic metabolism. Additionally, it has employed functional chemical probes as tools in the investigation of serine hydrolases and has demonstrated the effectiveness of such an approach. The opportunities for future research are considerable, to exploit plant carboxylesterases in plant metabolism of agrochemicals and also to carry out more fundamental research, which is needed to elucidate the diverse functions of carboxylic ester hydrolases in plants.

REFERENCES

Adam GC, Sorensen EJ, Cravatt BF (2002): Trifunctional chemical probes for the consolidated detection and identification of enzyme activities from complex proteomes. Molecular & Cellular Proteomics 1 (10): 828-835

Akoh CC, Lee GC, Liaw YC, Huang TH, Shaw JF (2004): GDSL family of serine esterases/lipases. Progress In Lipid Research 43 (6): 534-552

Aldridge WN (1953): Serum esterases .1. 2 types of esterase (A and B) hydrolysing para-nitrophenyl acetate, propionate and butyrate, and a method for their determination. Biochemical Journal 53 (1): 110-117

Arpigny JL, Jaeger KE (1999): Bacterial lipolytic enzymes: classification and properties. Biochemical Journal 343: 177-183

Bowles D, Isayenkova J, Lim EK, Poppenberger B (2005): Glycosyltransferases: managers of small molecules. Current Opinion In Plant Biology 8 (3): 254-263

Baudouin E, Charpenteau M, Roby D Marco Y, Ranjeva R, Ranty B (1997): Functional expression of a tobacco gene related to the serine hydrolase family. Eur. J. Biochem. 248: 700-706

Blom N, Gammeltoft S, Brunak S (1999): Sequence and structure-based prediction of eukaryotic protein phosphorylation sites. Journal of Molecular Biology 294 (5): 1351-1362

Bornscheuer UT (2002): Microbial carboxyl esterases: classification, properties and application in biocatalysis. FEMS Microbiology Reviews 26 (1): 73-81

Brenner S, Johnson M, Bridgham J, Golda G, Lloyd DH, Johnson D, Luo S, McCurdy S, Foy M, Ewan M, Roth R, George D, Eletr S, Albrecht G, Vermaas E, Williams SR, Moon K, Burcham T, Pallas M, DuBridge RB, Kirchner J, Fearon K, Mao J, and Corcoran K (2000): Gene expression analysis by massively parallel signature sequencing (MPSS) on microbead arrays. Nature Biotechnology 18, 630-634.

Brick DJ, Brumlik MJ, Buckley JT, Cao JX, Davies PC, Misra S, Tranbarger TJ, Upton C (1995): A new family of lipolytic plant enzymes with members in rice, arabidopsis and maize. Febs Letters 377 (3): 475-480

Bujnicki JM, Elofsson A, Fischer D, Rychlewski L (2001): LiveBench-2: Large-scale automated evaluation of protein structure prediction servers. Proteins-Structure Function and Genetics 184-191

Carino LA, Montgomery MW (1968): Identification of some soluble esterases of carrot (*Daucus carota* L). Phytochemistry 7 (9): 1483

Cheng J, Randall AZ, Sweredoski MJ, Baldi P (2005): SCRATCH: a protein structure and structural feature prediction server. Nucleic Acids Research 33: W72-W76

Cherry JP, Katterman FRH (1971): Nonspecific esterase isozyme polymorphism in natuarl populations of *Gossypium thurberi*. Phytochemistry 10: 141-145

Chigrin VV, Morgunova EA, Sautich MA, Skazhennik MA, Evseev VM (1976): Changes of Esterase Activity in Wheat Leaves During Infection with Stem Rust. Soviet Plant Physiology 23(3) 490-494

Clifford DR, Hislop EC, Shellis C (1977): Factors affecting activity of nitrophenol fungicides .5. Effects of fungal and plant esterases on fungicidal activity of nitrophenyl esters. Pesticide Science 8 (1): 13-22

Cubadda R, Quattrucci E (1974): Separation by gel electrofocusing and characterization of wheat esterases. Journal of the Science of Food and Agriculture 25 (4): 417-422

Cummins I, Burnet M, Edwards R (2001): Biochemical charaterisation of esterases active in hydrolysing xenobiotics in wheat and competing weeds. Physiologia Plantarum 113 477-485

Cummins I, Edwards R (2004): Purification and cloning of an esterase from the weed black-grass (*Alopecurus myosuroides*), which bioactivates aryloxyphenoxypropionate herbicides. Plant Journal 39 (6): 894-904

Cutler HG (1995): Microbial natural-products that affect plants, phytopathogens, and certain other microorganisms. Critical Reviews In Plant Sciences 14 (5): 413-444

De Carvalho VM, Marques RM, Lapenta AS, Machado MDPS (2003): Functional classification of esterases from leaves of *Aspidosperma polyneuron* M. Arg. (Apocynaceae). Genetics and Molecular Biology 26(2): 195-198

De Simone G, Galdiero S, Manco G, Lang D, Rossi M, Pedone C (2000): A snapshot of a transition state analogue of a novel thermophilic esterase belonging to the subfamily of mammalian hormone-sensitive lipase. Journal of Molecular Biology 303 (5): 761-771

Dodson G, Wlodawer A (1998): Catalytic triads and their relatives. Trends In Biochemical Sciences 23 (9): 347-352

Dogru E, Warzecha H, Seibel F, Haebel S, Lottspeich F, Stockigt J (2000): The gene encoding polyneuridine aldehyde esterase of monoterpenoid indole alkaloid biosynthesis in plants is an ortholog of the α/β hydrolase super family. European Journal of Biochemistry 267 1397-1406

Edwards R, Dixon DP, Walbot V (2000): Plant glutathione S-transferases: enzymes with multiple functions in sickness and in health. Trends In Plant Science 5 (5): 193-198

Edwards R, Del Buono D, Fordham M, Skipsey M, Brazier M, Dixon DP, Cummins I(2005): Differential induction of glutathione transferases and glucosyltransferases in wheat, maize and *Arabidopsis thaliana* by herbicide safeners. Zeitschrift Für Naturforschung C-A Journal of Biosciences 60 (3-4): 307-316

Emanuelsson O, Nielsen H, Brunak S, von Heijne G (2000): Predicting subcellular localization of proteins based on their N-terminal amino acid sequence. Journal of Molecular Biology 300 (4): 1005-1016

Forouhar F, Yang Y, Kumar D, Chen Y, Fridman E, Park SW, Chiang Y, Acton TB, Montelione GT, Pichersky E, Klessig DF, Tong L (2005): Structural and biochemical studies identify tobacco SABP2 as a methyl salicylate

esterase and implicate it in plant innate immunity. Proceedings of the National Academy of Sciences of the United States of America 102 (5): 1773-1778

Frossard P, Voss G (1978): Hydrolysing esterases in developing *Vicia-faba* L. Zeitschrift für Pflanzenphysiologie 87 (5): 429-434

Frossard P, Voss G (1979): Release of nonspecific esterases from the roots of *Vicia-faba* L. Experientia 35 (4): 459-460

Goodenough PW, Riley TEW (1985): Increase in esterase-activity during maturation of *Malus pumila* fruit. Annals of Applied Biology 107 (2): 349-351

Goullet P, and Picard B (1995): The electrophoretic polymorphism of bacterial esterases. FEMS Microbiology Reviews 16: 7-31

Hanefeld U, Straathof AJJ, Heijnen JJ (1999): Study of the (S)-hydroxynitrile lyase from Hevea brasiliensis: mechanistic implications. Biochimica Et Biophysica Acta-Protein Structure and Molecular Enzymology 1432 (2): 185-193

Haslam R, Raveton M, Cole DJ, Pallett KE, Coleman JOD (2001): The identification and properties of apoplastic carboxylesterases from wheat that catalyse deesterification of herbicides. Pesticide Biochemistry and Physiology 71 (3): 178-189

Hassal KA (1990); The Biochemistry and Uses of Pesticides (2nd edition) VCH

Hasslacher M, Schall M, Hayn M, Griengl H, Kohlwein SD, Schwab H (1996): Molecular cloning of the full length cDNA of (S)-hydroxynitrile lyase from *Hevea brasiliensis*. The Journal of Biological Chemistry, 271(10) 5884-5891

Heikinheimo P, Goldman A, Jeffries C, Ollis DL (1999): Of barn owls and bankers: a lush variety of alpha/beta hydrolases. Structure With Folding & Design 7 (6): R141-R146

Hildmann T, Ebneth M, Penacortes H, Sanchezserrano JJ, Willmitzer L, Prat S (1992): General roles of abscisic and jasmonic acids in gene activation as a result of mechanical wounding. Plant Cell 4 (9): 1157-1170

Hilson P, Allemeersch J, Altmann T, Aubourg S, Avon A, Beynon J, Bhalerao RP, Bitton F, Caboche M, Cannoot B, Chardakov V, Cognet-Holliger C, Colot V, Crowe M, Darimont C, Durinck S, Eickhoff H, Falcon de Longevialle A, Farmer EE, Grant M, Kuiper MTR, Lehrach H, Léon C, Leyva A, Lundeberg J, Lurin C, Moreau Y, Nietfeld W, Paz-Ares J, Reymond P, Rouzé P, Sandberg G, Dolores Segura M, Serizet C, Tabrett A, Taconnat L, Thareau V, Van Hummelen P, Vercruysse S, Vuylsteke M, Weingartner M, Weisbeek P J, Wirta V, Wittink FRA, Zabeau M and Small I (2004): Versatile gene-specific sequence tags for Arabidopsis functional genomics: transcript profiling and reverse genetics applications. Genome Research 14: 2176-2189

Hilton S, Buckley JT (1991): Action of a microbial lipase acyltransferase on phospholipid monolayers. Biochemistry 30 (24): 6070-6074

Hinderer W, Koster J, Barz W (1986): Purification and properties of a specific isoflavone 7-O-glucoside-6''-malonate malonylesterase from the roots of chickpea. Archives of Biochemsitry and Biophysics 248 570-578

Hiscock SJ, Bown D, Gurr SJ, Dickinson HG (2002): Serine esterases are required for pollen tube penetration of the stigma in Brassica. Sexual Plant Reproduction 15 (2): 65-74

Hoagland RE, Graf G (1972): Enzymatic-hydrolysis of herbicides in plants. Weed Science 20 (4): 303

Hoglund A, Donnes P, Blum T, Adolph HW, Kohlbacher OMultiLoc (2006): prediction of protein subcellular localization using N-terminal targeting sequences, sequence motifs and amino acid composition. Bioinformatics 22 (10): 1158-1165

Hotelier T, Renault L, Cousin X, Negre V, Marchot P, Chatonnet A (2004): ESTHER, the database of the alpha/beta-hydrolase fold superfamily of proteins. Nucleic Acids Research 32: D145-D147

Hughes J, Decarvalho JPC, Hughes MA (1994): Purification, characterization, and cloning of alpha-hydroxynitrile lyase from cassava (*Manihot-esculenta* Crantz). Archives of Biochemistry and Biophysics 311 (2): 496-502

Ichinose Y, Hisayasu Y, Sanematsu S, Ishiga Y, Seki H, Toyoda K, Shiraishi T, Yamada T (2001): Molecular cloning and functional analysis of pea cDNA *E86* encoding homologous protein to hypersensitivity related hsr203J. Plant Science 160 997-1006

Jahangir R, McCloskey CB, Mc Clung WG, Labow RS, Brash JL, Santerre JP (2003): The influence of protein adsorption and surface modifying macromolecules on the hydrolytic degradation of a poly(ether-urethane) by cholesterol esterase. Biomaterials 24 (1): 121-130

Jeffcoat B, Harries WN (1975): Selectivity and mode of action of Flamprop-isopropyl, Isopropyl (±)-2-[N-(3-chloro-4-fluorophenyl)benzamido]propionate, in the control of *Avena fatua* in Barley. Pestic. Sci. 6 283-296

Johansson K, El-Ahmad M, Friemanna R, Jornvall H, Markovic O, Eklund H (2002): Crystal structure of plant pectin methylesterase. Febs Letters 514 (2-3): 243-249

Jones DT (1999): Protein secondary structure prediction based on position-specific scoring matrices. Journal Of Molecular Biology 292 (2): 195-202

Kandzia R, Grimm R, Eckerskorn C, Lindemann P, Luckner M (1998): Purification and characterisation of lanatoside 15'-O-acetylesterase from *Digitalis lanata* Ehrh. Planta 204 383-389

Kim JH, Lee J, Oh B, Kimm K, Koh IS (2004): Prediction of phosphorylation sites using SVMs. Bioinformatics 20 (17): 3179-3184

Kim YS, Lee HH, Ko MK, Song CE, Bae CY, Lee YH, Oh BJ (2001): Inhibition of fungal appressorium formation by pepper esterase. MPMI 14(1) 80-85

Kneusel RE, Schiltz E, Matern U (1994): Molecular characterization and cloning of an esterase which inactivates the macrolide toxin brefeldin-A. Journal of Biological Chemistry 269 (5): 3449-3456

Krell HW, Sandermann H (1984): Plant biochemistry of xenobiotics. European Journal of Biochemistry 143(1) 57-62

Kumar D, Klessig DF (2003): High affinity salicylic acid-binding protein 2 is required for plant innate immunity and has salicylic acid-stimulated lipase activity. PNAS 100(26) 16101-16106

Lambert C, Leonard N, De Bolle X, Depiereux E (2002): ESyPred3D: Prediction of proteins 3D structures. Bioinformatics 18 (9): 1250-1256

Lee KA, Cho TJ (2003): Characterisation of a salicylic acid and pathogen induced lipase-like gene in chinese cabbage. Journal of Biochemistry and Molecular Biology 36(5) 433-441

Lee PW, Stearns SM, Powell WR (1988): Metabolic fate of fenvalerate in wheat plants. Journal of Agricultural Food Chemistry 36: 189–193.

Leinweber FJ (1997): Possible physiological roles of carboxylic ester hydrolases. Drug Metabolism Reviews 18 (4): 379-439

Liu YS, Patricelli MP, Cravatt BF (1999): Activity-based protein profiling: The serine hydrolases. Proceedings of the National Academy of Sciences of the United States of America 96 (26): 14694-14699

Luo CY, Ashani Y, Doctor BP (1998): Acceleration of oxime-induced reactivation of organophosphate-inhibited fetal bovine serum acetylcholinesterase by monoquaternary and bisquaternary ligands. Molecular Pharmacology 53 (4): 718-726

Luo CY, Saxena A, Smith M, Garcia G, Radic Z, Taylor P, Doctor BP (1999): Phosphoryl oxime inhibition of acetylcholinesterase during grime reactivation is prevented by edrophonium. Biochemistry 38 (31): 9937-9947

Marco YJ, Ragueh F, Godiard L, Froissard D (1990): Transcriptional activation of 2 classes of genes during the hypersensitive reaction of tobacco leaves infiltrated with an incompatible isolate of the phytopathogenic bacterium *Pseudomonas solanacearum*. Plant Molecular Biology 15: 145-154

Marshall SDG, Putterill JJ, Plummer KM, Newcomb RD (2003): The carboxylesterase gene family from *Arabidopsis thaliana*. Journal of Molecular Evolution 57: 487-500

McMurray (1995): Organic chemistry (4th Edition). Brooks/Cole Publishing Company

Merino MT, Humanes L, Roldan JM, Diez J, LopezRuiz A (1996): Production of limonoate A-ring lactone by immobilized limonin D-ring lactone hydrolase. Biotechnology Letters 18 (10): 1175-1180

Molgaard A, Kauppinen S, Larsen S (2000): Rhamnogalacturonan acetylesterase elucidates the structure and function of a new family of hydrolases. Structure With Folding & Design 8 (4): 373-383

Momonoki YS (1997): Asymmetric distribution of acetylcholinesterase in gravistimulated maize seedlings. Plant Physiology 114 (1): 47-53

Morris PC (2001): MAP kinase signal transduction pathways in plants. New Phytologist 151 (1): 67-89

Muarlidharan J, John E, Channamma L, Theerthaprasad D (1995): Changes in esterases in response to blast infection in fingermillet seedlings. Phytochemistry 43 (6): 1151-1155

Norgaard MJ, Montgomery MW (1968): Some esterases of pea (*Pisum sativum*). Biochimica et Biophysica Acta 151 (3): 587

Oakeshott JG, Claudianos C, Russell RJ, Robin GC (1999): Carboxyl/cholinesterases: a case study of the evolution of a successful multigene family. Bioessays 21 (12): 1031-1042

Obenauer JC, Cantley LC, Yaffe MB (2003): Scansite 2.0: Proteome-wide prediction of cell signaling interactions using short sequence motifs. Nucleic Acids Research 31 (13): 3635-3641

Ollis DL, Cheah E, Cygler M, Dijkstra B, Frolow F, Franken SM, Harel M, Remington SJ, Silman I, Schrag J, Sussman JL, Verschueren KHG, Goldman A (1992): The Alpha/Beta-Hydrolase Fold. Protein Engineering 5 (3): 197-211

Ottolina and Carrea (2002): Rationalization of enzyme enantioselectivity by active-site cubic-space models. Canadian Journal Of Chemistry 80 (6): 559-564

Ounissi H, Courvalin P (1985): Nucleotide-sequence of the gene EreA encoding the erythromycin esterase in *Escherichia-coli*. Gene 35 (3): 271-278

Owen MDK (2000): Current use of transgenic herbicide-resistant soybean and corn in the USA. Crop Protection 19 (8-10): 765-771

Pontier D, Tronchet M, Rogowsky P, Lam E, Roby D (1998): Activation of hsr203, a plant gene expressed during incompatible plant-pathogen interactions, is correlated with programmed cell death. Molecular Plant-Microbe Interactions 11(6) 544-554

Panda T, Gowrishankar BS (2005): Production and applications of esterases. Applied Microbiology and Biotechnology 67 (2): 160-169

Pereira AJ, Lapenta AS, Vidigal PS, Machado MDPS (2001): Differential esterase expression in leaves of *Manihot esculenta* Crantz infected with *Xanthomonas axonopodis* pv. *manihotis*. Biochemical Genetics 39 (9-10): 289-296

Pringle D, Dickstein R (2004): Purification of ENOD8 proteins from *Medicago sativa* root nodules and their characterisation as esterases. Plant Physiology and Biochemistry 42: 73-79

Redinbo MR, Potter PM (2005): Mammalian carboxylesterases: from drug targets to protein therapeutics. Drug Discovery Today 10 (5): 313-

Ro HS, Hong HP, Kho BH, Kim S, Chung BH (2004): Genome-wide cloning and characterization of microbial esterases. FEMS Microbiology Letters 233 (1): 97-105

Roberts MR, Foster GD, Blundell RP, Robinson SW, Kumar A, Draper J, Scott R (1993): Gametophytic and sporophytic expression of an anther-specific *Arabidopsis-thaliana* gene. Plant Journal 3 (1): 111-120

Roberts TR (ed.) (1998): Metabolic pathways of agrochemicals. Part 1, Herbicides and plant growth regulators. Cambridge: Royal Society of Chemistry

Rudolph K, Stahmann MA (1965): Multiple hydrolases in bean leaves and the effect of the halo blight disease caused by *Pseudomonas phaseolicola* (Burkh.) Dowson. Plant Physiology 41 389-394

Ruppert M, Woll J, Giritch A, Genady E, Ma XY, Stockigt J (2005): Functional expression of an ajmaline pathway-specific esterase from *Rauvolfia* in a novel plant-virus expression system. Planta 222 (5): 888-898

Sagane Y, Nakagawa T, Yamamoto K, Michikawa S, Oguri S, Momonoki YS (2005): Molecular characterization of maize acetylcholinesterase. A novel enzyme family in the plant kingdom. Plant Physiology 138 (3): 1359-1371

Satoh T, Hosokawa M (1998): The mammalian carboxylesterases: From molecules to functions. Annual Review Of Pharmacology And Toxicology 38: 257-288

Schrattenholz A, Godovaczimmermann J, Schafer HJ, Albuquerque EX, Maelicke A (1993): Photoaffinity-labeling of torpedo acetylcholine-receptor by physostigmine. European Journal Of Biochemistry 216 (2): 671-677

Schwartz HM, Biedron SI, Vonholdt MM, Rehm S (1964): A study of some plant esterases. Phytochemistry 3: 189-200

Sessions A, Burke E, Presting G, Aux G, McElver J, Patton D, Dietrich B, Ho P, Bacwaden J, Ko C, Clarke JD, Cotton D, Bullis D, Snell J, Miguel T, Hutchison D, Kimmerly B, Mitzel T, Katagiri F, Glazebrook J, Law M, Goff SA (2002): A high-throughput arabidopsis reverse genetics system. Plant Cell 14 (12): 2985-2994

Strack D, Nurmann G, Sachs G (1980): Sinapine esterase .2. specificity and change of sinapine esterase-activity during germination of *Raphanus-sativus*. Zeitschrift Fur Naturforschung C-A Journal of Biosciences 35 (11-1): 963-966

Stuhlfelder C, Lottspeich F, Mueller MJ (2002), Purification and partial amino acid sequences of an esterase from tomato. Phytochemistry 60 233-240

Stuhlfelder C, Mueller MJ, Warzecha H (2004): Cloning and expression of a tomato cDNA encoding a methyl jasmonate cleaving esterase. European Journal of Biochemistry 271 2976-2983

Taipalensuu J, Falk A, Rask L (1996): A wound- and methyl jasmonate-inducible transcript coding for a myrosinase-associated protein with similarities to an early nodulin. Plant Physiology 110 (2): 483-491

Taylor EJ, Gloster TM, Turkenburg JP, Vincent F, Brzozowski AM, Dupont C, Shareck F, Centeno MSJ, Prates JAM, Puchart V, Ferreira LMA, Fontes CMGA, Biely P, Davies GJ (2006): Structure and activity of two metal ion-dependent acetylxylan esterases involved in plant cell wall degradation reveals a close similarity to peptidoglycan deacetylases. Journal of Biological Chemistry 281 (16): 10968-10975

Upton C, Buckley JT (1995): A new family of lipolytic enzymes. Trends In Biochemical Sciences 20 (5): 178-179

Veerabhadrappa PS, Montgomery MW (1971): purification and characterisation of carboxylesterases of green beans. Phytochemisty 10 1175-1182

Walden AR, Walter C, Gardner RC (1999): Genes expressed in *Pinus radiata* male cones include homologs to anther-specific and pathogenesis response genes. Plant Physiology 121 (4): 1103-1116

Wäspi U, Misteli B, Hasslacher M, Jandrositz A, Kohlwein SD, Schwab H, Dudler R (1998): A defense-related rice gene Pir7B encodes an α/β hydrolase fold protein exhibiting esterase activity towards naphthol AS esters. Eur. J. Biochem. 254 32-37

Wei YY, Schottel JL, Derewenda U, Swenson L, Patkar S, Derewenda ZS (1995): A novel variant of the catalytic triad in the *Streptomyces scabies* esterase. Nature Structural Biology 2 (3): 218-223

Wei YY, Contreras JA, Sheffield P, Osterlund T, Derewenda U, Kneusel RE, Matern U, Holm C, Derewenda ZS (1999): Crystal structure of brefeldin A esterase, a bacterial homolog of the mammalian hormone-sensitive lipase. Nature Structural Biology 6 (4): 340-345

Wright GD (2005): Bacterial resistance to antibiotics: Enzymatic degradation and modification. Advanced Drug Delivery Reviews 57: 1451-1470

Xia Q, Steeves TA (1999): Initial differentiation of vascular tissue in the shoot apex of carrot (*Daucus carota* L.). Annals of Botany 83 (2): 157-166

Zhong GY, Goren R, Riov J, Sisler EC, Holland D (2001): Characterization of an ethylene-induced esterase gene isolated from Citrus sinensis by competitive hybridization. Physiologia Plantarum 113 (2): 267-274